Gut microbiome alterations at acute myeloid leukemia diagnosis are associated with muscle weakness and anorexia

Sarah A. Pötgens,[1] Violaine Havelange,[2,3] Sophie Lecop,[1] Fuyong Li,[4,5] Audrey M. Neyrinck,[1] Florence Bindels,[6] Nathalie Neveux,[7] Jean-Baptiste Demoulin,[3] Ine Moors,[8] Tessa Kerre,[8] Johan Maertens,[9,10] Jens Walter,[11] Hélène Schoemans,[9,12] Nathalie M. Delzenne[1] and Laure B. Bindels[1,13]

[1]Metabolism and Nutrition Research Group, Louvain Drug Research Institute, UCLouvain, Université catholique de Louvain, Brussels, Belgium; [2]Department of Hematology, Cliniques Universitaires Saint-Luc, UCLouvain, Université catholique de Louvain, Brussels, Belgium; [3]Experimental Medicine Unit, De Duve Institute, UCLouvain, Université catholique de Louvain, Brussels, Belgium; [4]Department of Infectious Diseases and Public Health, Jockey Club College of Veterinary Medicine and Life Sciences, City University of Hong Kong, Kowloon, Hong Kong SAR, China; [5]Department of Agricultural, Food and Nutritional Science, University of Alberta, Edmonton, Alberta, Canada; [6]Maison Médicale de Grez-Doiceau, Grez-Doiceau, Belgium; [7]Clinical Chemistry Department, Cochin Hospital, Paris Centre University Hospitals, Paris, France; [8]Department of Hematology, Ghent University Hospital, Ghent University, Ghent, Belgium; [9]Department of Hematology, University Hospitals Leuven, Leuven, Belgium; [10]Department of Microbiology, Immunology and Transplantation, KU Leuven, Leuven, Belgium; [11]Department of Medicine, School of Microbiology, APC Microbiome Ireland, University College Cork, Cork, Ireland; [12]Department of Public Health and Primary Care, ACCENT VV, KU Leuven, Leuven, Belgium and [13]Welbio Department, WEL Research Institute, Wavre, Belgium

Correspondence: L.B. Bindels
laure.bindels@uclouvain.be

Received: August 25, 2023.
Accepted: March 19, 2024.
Early view: March 28, 2024.

https://doi.org/10.3324/haematol.2023.284138

Gut microbiome alterations at acute myeloid leukemia diagnosis are associated with muscle weakness and anorexia

Sarah A. Pötgens[1], Violaine Havelange[2,3], Sophie Lecop[1], Fuyong Li[4,5], Audrey M. Neyrinck[1], Florence Bindels[6], Nathalie Neveux[7], Jean-Baptiste Demoulin[3], Ine Moors[8], Tessa Kerre[8], Johan Maertens[9,10], Jens Walter[11], Hélène Schoemans[9,12], Nathalie M. Delzenne[1], Laure B. Bindels[1,13]

[1]Metabolism and Nutrition Research Group, Louvain Drug Research Institute, UCLouvain, Université catholique de Louvain, Brussels, Belgium.

[2]Department of Hematology, Cliniques Universitaires Saint-Luc, UCLouvain, Université catholique de Louvain, Brussels, Belgium.

[3]Experimental Medicine Unit, De Duve Institute, UCLouvain, Université catholique de Louvain, Brussels, Belgium.

[4]Department of Infectious Diseases and Public Health, Jockey Club College of Veterinary Medicine and Life Sciences, City University of Hong Kong, Kowloon, Hong Kong SAR, China.

[5]Department of Agricultural, Food and Nutritional Science, University of Alberta, Edmonton, Alberta, Canada.

[6]Maison Médicale de Grez-Doiceau, Grez-Doiceau, Belgium.

[7]Clinical Chemistry Department, Cochin Hospital, Paris Centre University Hospitals, Paris, France

[8]Department of Hematology, Ghent University Hospital, Ghent University, Ghent, Belgium.

[9]Department of Hematology, University Hospitals Leuven, Leuven, Belgium.

[10]Department of Microbiology, Immunology and Transplantation, KU Leuven, Leuven, Belgium

[11]Department of Medicine, School of Microbiology, APC Microbiome Ireland, University College Cork, Cork, Ireland.

[12]Department of Public Health and Primary Care, ACCENT VV, KU Leuven, Leuven, Belgium

[13]Welbio Department, WEL Research Institute, Wavre, Belgium

Supplementary Materials and Methods

Study objectives

This cohort study aims to investigate the composition and activity of the gut microbiota of patients newly diagnosed for acute myeloid leukaemia (AML), in relationship with their food habits and cachectic hallmarks. The recruitment for this study took place with the help of clinicians, nurses and data managers at the Saint-Luc clinics, University Hospital Leuven (Campus Gasthuisberg) and University Hospital Gent.

The primary objective was to assess the composition and activity of the gut microbiota in patients with acute myeloid leukaemia (AML) compared to matched control subjects.

Secondary objectives were the following ones: (i) to investigate correlations between the gut microbiota, cachectic hallmarks and gut microbiota-related markers in the blood (gut permeability markers, microbial compounds, microbial metabolites); (ii) to characterize the changes in the gut microbial ecosystem that are induced by chemotherapy and associated with colitis; (iii) to assess whether the composition of the gut microbiota can predict the severity of chemotherapy-related colitis. Only the first secondary outcome is presented in the current manuscript.

The study was registered at ClinicalTrials.gov (NCT03881826).

Study design

Thirty patients newly diagnosed with AML were recruited between December 2015 and December 2019 from three Belgian University hospitals (Saint-Luc Brussels (n = 13), UZ Leuven (n = 15), and UZ Gent (n = 2)). This is an academic multi-centric prospective study. Patients were included before any chemotherapy. Biological samples (urine, faeces, blood) were collected, alongside information on nutritional habits, appetite and medical records. Muscle strength and body composition were also measured. Only patients receiving a standard chemotherapy were followed after the start of the chemotherapy. For these patients, biological samples were collected and body composition, muscle strength and appetite were evaluated at 2 different time points, namely at the end of the chemotherapy and at discharge. Control (CT) subjects from the general population were recruited between December 2017 and January 2020 based on the same inclusion/exclusion criteria, except for the AML diagnosis. They were matched (1:1) for several factors known to impact GM, such as age[1], sex[2-4], BMI[5], and smoking status[6]. Whole-group analyses were applied

on these matched cohorts as previously advised[7]. When we initiated the project in 2015, sample size could not be calculated as the effect size and the inter-individual variability were unknown. This study was considered as exploratory and expected to provide information concerning the effect size[8]. The number of patients was therefore chosen based on similar studies[9-13]. Retrospectively, we estimated the power of the MicroAML study using information collected in a previous study performed in a cohort of 24 healthy volunteers[10, 14]. In the Food4Gut healthy cohort, we found an average standard deviation of 12% for the Shannon index of alpha-diversity[10], a measurement of the microbial diversity. Using PASS 14.0.7, we found a power of 89% to detect with 30 subjects/group at a threshold p-value (alpha) of 0.05 a minimal 10% change in this alpha-diversity index, supposing a similar standard deviation of 12%. This calculation indicates that the MicroAML study is adequately powered to detect such changes in the gut microbiota of leukemic patients *vs* healthy volunteers.

Inclusion Criteria for AML patients

Patients with

- A diagnosis of AML and related precursor neoplasms according to WHO 2008 classification (excluding acute promyelocytic leukaemia) including secondary AML (after an antecedent haematological disease (e.g. MDS) and therapy-related AML) OR acute leukaemia's of ambiguous lineage according to WHO 2008 OR a diagnosis of refractory anaemia with excess of blasts (MDS REAB) 2 and IPSS (International Prognostic Scoring System)-R score > 2.
- World Health Organization performance status 0, 1 or 2
- Sampled bone marrow and/ blood cells at diagnosis with molecular analysis.
- Written informed consent
- Good command of the French or Dutch language

Inclusion Criteria for CT subjects

- For each enrolled patient, a healthy control was recruited and matched for age, sex, BMI and smoking habits (except one).
- Written informed consent
- Good command of the French or Dutch language

Exclusion Criteria for AML patients and CT subjects

- Age < 18 years
- Age > 75 years
- Pregnancy
- Antibiotics consumption during the last 30 days before inclusion
- Recent chemotherapy (< 3 months), with exclusion of hydroxyurea
- BMI >30
- Any history of chronic intestinal affections (Crohn disease, inflammatory bowel disease, gluten intolerance)
- Gastric bypass
- Current treatment with antidiabetic or hypoglycaemic drugs

Data collection

All biological sampling and data collection were performed at the time of diagnosis before the beginning of the chemotherapy treatment and the administration of any antibiotics.

Biological sampling

Faeces and urine were collected and were immediately (< 15 min) frozen at -20°C for a maximum of one week and then stored at -80°C. Blood samples were kept on ice, centrifuged at 4°C within 30 min and plasma aliquots were stored at -80°C. Fasting status was reported.

Case report form

Case report forms were collected to document medical history, drug records including consumption of pre- and probiotics, antibiotics in the last 90 days, as well as lab assessment of haemoglobin, white blood cell count, C-reactive protein, albumin, and glycaemia levels.

Body composition and muscle strength

Body composition was assessed using bioimpedancemetry (Body composition analyser, Tanita BC-420MA/SMA). Muscle strength was measured using a Jamar hand dynamometer in the dominant hand (3 measures, separated by 15 s). Patients were asked for weight loss during the last six months.

Dietary and other assessments

The overall quality of patients' dietary habits was evaluated by a food frequency questionnaire (FFQ) validated in the Belgian population[15]. The analysis of the FFQ gives an overall dietary score and several sub-scores: dietary quality score, dietary diversity score, dietary equilibrium score (adequacy and moderation scores). Patients also filled questionnaires to evaluate their alcohol intake on a weekly basis. The short tobacco test was used to evaluate tobacco dependence and consumption[16]. Appetite was assessed using the simplified nutritional assessment questionnaire (SNAQ)[17]. A score ≤ 14 reflects a risk of weight loss in the next six months.

Measurement of cytokines, GDF15, FGF21, LBP, insulin and citrulline

Plasma cytokines (IL6, IL8, IL10, MCP1, TNFα, TGFβ1, GDF15), FGF21 and insulin (in fasted state) were measured using a customized U-plex kit and a Meso Scale Discovery microplate reader (Meso Scale Discovery, Rockville, MD, USA). LBP levels were assessed using an ELISA kit (HycultBiotech, PA, USA). Citrulline was measured in plasma (EDTA) using ion exchange chromatography. Combining fasted glycaemia and insulin, we calculated the HOMA-IR2 index[18] for 19 patients in each group.

Gut microbiome analyses

DNA extraction and total bacteria quantification

DNA was extracted from faecal samples following the protocol Q described by Costea et al[19]. This protocol uses the QIAamp DNA Stool Mini Kit (Qiagen, Germany) and includes a bead-beating step. Treatment with RNAse A was performed (10 mg/ml, Thermo Fisher Scientific, USA). DNA concentration was determined, and purity (A260/A280) was checked using a NanoDrop 2000 (Thermo Fisher Scientific, USA).

Absolute quantification of the total bacterial load was performed by quantitative polymerase chain reaction (qPCR) using the primers Bacteria Universal P338F (ACTCCTACGGGAGGCAGCAG) and P518r (ATTACCGCGGCTGCTGG)[20]. Real-time PCR was performed with a QuantStudio3 (Applied Biosystems, The Netherlands) using SYBR Green (GoTaq® qPCR mix, Promega, USA) for detection. All samples (0.1ng/µl) were run in duplicate in a single 96-well reaction plate. Final concentrations were as follow: cDNA 2 µl/25 µl, primers 300 nM, and SyberGreen mix 1X (MeteorTaq DNA polymerase, dNTP, RT buffer, $MgCl_2$ 4 mM, SYBR® Green I, ROX passive reference and stabilizers, as provided by the manufacturer). Thermocycling

conditions were as follow: initiation step at 95°C 2 min; cycling stage at 95°C 30 s, 60°C 30 s, 72°C 30 s, 40 cycles; melt curve stage at 95°C 1 s, 65°C 20 s, increment of 0.1°C every 1 s until reaching 95°C. Threshold was manually adjusted to reach the linear range of the log-fluorescent curves and CT values were determined using the QuantStudio Software (Version 1.4.3, Applied Biosystems, The Netherlands). Absolute quantification was achieved through the inclusion of a standard curve (performed in duplicate) on each plate generated by diluting DNA from pure culture of *L. acidophilus* NCFM (five-fold serial dilution). Cell counts were determined by plating and expressed as "colony-forming unit" (CFU) before DNA isolation.

16S rRNA gene sequencing - data generation

Sequencing of 16S rRNA gene is a well-established technique allowing taxonomical assessment of the gut microbiota. This method uses primers that target a specific region of the 16S rRNA gene. Indeed, this gene has the advantage to have highly variable regions flanked by highly conserved regions in all bacteria. The sequencing of these variable regions allows microbial phylogenies determination. In this study, amplicon sequencing of the microbiome was done at the University of Minnesota Genomics Centre. Briefly, the V5-V6 region of the 16S rRNA gene was PCR-enriched using the primer pair V5F_Nextera (TCGTCGGCAGCGTCAGATGTGTATAAGAGACAGRGGATTAGATACCC) and V6R_Nextera (GTCTCGTGGGCTCGGAGATGTGTATAAGAGACAGCGACRRCCATGCANCACCT) in a 25 µl PCR reaction containing 5 µl of template DNA, 5 µl of 2X HotStar PCR master mix, 500 nM of final concentration of primers and 0.025 U/µl of HostStar Taq+ polymerase (QIAGEN). PCR-enrichment reactions were conducted as follow, an initial denaturation step at 95°C for 5 min followed by 25 cycles of denaturation (20 s at 98°C), annealing (15 s at 55°C), and elongation (1 min at 72°C), and a final elongation step (5 min at 72°C). Next, the PCR-enriched samples were diluted 1:100 in water for input into library tailing PCR. The PCR reaction was analogous to the one conducted for enrichment except with a KAPA HiFi Hot Start Polymerase concentration of 0.25 U/µl, while the cycling conditions used were as follows: initial denaturation at 95°C for 5 min followed by 10 cycles of denaturation (20 s at 98°C), annealing (15 s at 55°C), and elongation (1 min at 72°C), and a final elongation step (5 min at 72°C). The primers used for tailing are the following: F-indexing primer AATGATACGGCGACCACCGAGATCTACAC[i5]TCGTCGGCAGCGTC and R-indexing

primer CAAGCAGAAGACGGCATACGAGAT[i7]GTCTCGTGG GCTCGG, where [i5] and [i7] refer to the index sequence codes used by Illumina. The resulting 10 µl indexing PCR reactions were normalized using a SequalPrep normalization plate according to the manufacturer's instructions (Life Technologies). 20 µl of each normalized sample was pooled into a trough, and a SpeedVac was used to concentrate the sample pool down to 100 µl. The pool was then cleaned using 1X AMPureXP beads and eluted in 25 µl of nuclease-free water. The final pool was quantitated by QUBIT (Life Technologies) and checked on a Bioanalyzer High-Sensitivity DNA Chip (Agilent Technologies) to ensure correct amplicon size. The final pool was then normalized to 2 nM, denatured with NaOH, diluted to 8 pM in Illumina's HT1 buffer, spiked with 20% PhiX, and heat denatured at 96°C for 2 min immediately prior to loading. A MiSeq 600 cycle v3 kit was used to sequence the pool. Raw sequences can be found in the SRA database (project ID: PRJNA813705).

16S rRNA gene sequencing - bioinformatics

Subsequent bioinformatics analyses were performed *in-house* as previously described[21]. Initial quality filtering of the reads was performed with the Illumina Software, yielding an average of 84 585 pass-filter reads per sample. Quality scores were visualized with the FastQC software (http://www.bioinformatics.babraham.ac.uk/ publications.html), and reads were trimmed to 220 bp (R1) and 200 bp (R2) with the FASTX-Toolkit (http://hannonlab.cshl.edu/fastx_toolkit/). Next, reads were merged with the merge-illumina-pairs application v1.4.2 (with P = 0.03, enforced Q30 check, perfect matching to primers which are removed by the software, and otherwise default settings including no ambiguous nucleotides allowed)[22]. The UPARSE pipeline implemented in USEARCH v11[23] was used to further process the sequences. Amplicon sequencing variants (ASVs) were identified using UNOISE3[24]. Such method infers the biological sequences in the sample prior to the introduction of amplification and sequencing errors, and distinguishes sequence variants differing by as little as one nucleotide[25]. The analysis allowed the identification of 3968 ASVs. ASVs were identified using the RDP database. Taxonomic prediction was performed using the *nbc_tax* function[26], an implementation of the RDP Naive Bayesian Classifier algorithm[27]. Alpha diversity indexes were calculated using QIIME[28] on the rarefied ASV table. Rarefaction was performed using Mothur 1.32.1[29] by randomly selecting 40 612 sequences for all samples, except two (103: 24 133 sequences and 507: 16 814 sequences).

16S rRNA gene sequencing - biostatistics

Unrarefied data were filtered to select for a minimum abundance of 0.01% and a minimal prevalence of 25% in one group. Principal component analysis (PCA) was performed on CLR-transformed data[30] using the *pca* function in the *mixOmics* R package[31]. The CLR transformation consists in a centered log ratio transformation and allows transforming compositional data into an Euclidian space. A pseudo-count equal to half the minimal value found in the dataset was applied prior the CLR transformation[32]. Significantly impacted phyla, families and genera were identified using a Mann-Whitney U-test in R since normality was not inspected for every phylum/family/genus. The p-value was adjusted to control for the false discovery rate (FDR) for multiple testing according to the Benjamini and Hochberg (BH) procedure[33]. A q-value < 0.1 was considered significant.

Metagenomics sequencing - data generation

Untargeted metagenomics sequencing was performed at the Centre d'expertise et de services Génome Québec. Genomic DNA was quantified using the Quant-iT™ PicoGreen® dsDNA Assay Kit (Life Technologies). Libraries were generated from 50 ng of genomic DNA using the NEBNext Ultra II DNA Library Prep Kit for Illumina (New England BioLabs) as per the manufacturer's recommendations. Adapters and PCR primers were purchased from IDT. Size selection of libraries contained the desired insert size has been performed using SparQ beads (Qiagen). Libraries were quantified using the Kapa Illumina GA with Revised Primers-SYBR Fast Universal kit (Kapa Biosystems). Average size fragment was determined using a LabChip GXII (PerkinElmer) instrument.

The libraries were normalized and pooled and then denatured in 0.05 N NaOH and neutralized using HT1 buffer. The pool was loaded at 225 pM on an Illumina NovaSeq S4 lane using Xp protocol as per the manufacturer's recommendations. The run was performed for 2x150 cycles (paired-end mode). A phiX library was used as a control and mixed with libraries at 1% level. Base calling was performed with RTA v3.4.4 . Program bcl2fastq2 v2.20 was then used to demultiplex samples and generate fastq reads.

Metagenomics sequencing – bioinformatics

Trimmomatic (version 0.39)[34] was used to trim adapters and low-quality reads (average quality scores < 20), and only reads with the length no less than 100 bp remained for the downstream

analysis. Bowtie2 (version 2.3.5.1)[35], with *-N 1* and otherwise default options, was applied to remove reads classified as bacteriophage phiX174 (NCBI accession: NC_001422.1) and filter out human DNA reads based on the human genome reference GRCh38 . MetaPhlAn3 (version 3.0.2) and HUMAanN 3.0 was used to estimate the taxonomic composition and functional profiles of the gut microbiome, with the default settings[36]. Genes were then regrouped in 2373 Level-4 enzyme commission (EC) categories system (*humann_regroup_table --groups uniref90_level4ec*). Both genes and EC enzyme functions were normalized in cpm. The *human_barplot* function was used to explore the contribution of individual species and genera to selected functions. Raw sequences can be found in the SRA database (project ID: PRJNA813705).

Metagenomics sequencing – biostatistics on taxonomical data

Taxa were filtered to select for 320 taxa with a mean average abundance above 0.01% and a mean prevalence of 25% in at least one group of samples. PCA were computed from CLR-transformed data[30] followed by Permutational Multivariate Analysis of Variance (PERMANOVA) using the *adonis* function in the *vegan* R package[37]. Different variables were tested, including AML, BMI, sex, muscle strength, haemoglobin and age. The PERMANOVA allowed to evaluate the explanatory power of each factor individually. Significantly affected taxa were identified using a Mann-Whitney U-test with BH correction. A q-value < 0.1 was considered significant.

As multiple differential abundance methods help to ensure robust biological interpretation[38], we also used alternative differential abundance methods, namely a Mann-Whitney U-test with BH correction applied on CLR-transformed data and ALDEx2[39]. The R scripts used to perform differential abundance analyses are available on GitHub at the following address: https://github.com/laurebindels/MicroAML. Similar results were found using these methods. A list of bacteria of putative interest was gathered for data integration with metabolomics datasets as well as clinical and biochemical data, by selecting bacterial taxa present in the top 20 of each approach. When parent taxa were present in this list and identical/highly similar in terms of abundance values, the lowest taxonomical level was conserved. This approach allowed the selection of a list of 21 taxa referred in the manuscript as “top altered bacteria” and are presented in Table S2.

Bacterial features were estimated as previously described[40]. For each sample, the cumulative relative abundance of taxa that were associated with an obligate anaerobic metabolism or an oral habitat was determined. The level of oral bacteria was computed based on an aggregation at the

species level and the expanded Human oral microbiome database V3[41]. The level of obligate anaerobe bacteria was computed based on an aggregation at the genus level and the oxygen class indicated in the List of Prokaryotes according to their Aerotolerant or Obligate Anaerobic Metabolism (OXYTOL 1.3, Mediterranean institute of infection in Marseille).

The Random Forest algorithm was used to model the bacterial taxonomic signature of the AML status. The AUC or "area under the receiver-operator curve" measures the accuracy of trained forests. The AUC is a widely used estimator of true positive and false positive prediction rates. For this analysis, outcomes were AML or no AML and the dataset, namely the relative abundance of taxa identified in the top altered bacteria, was randomly split in a training and a testing set with a ratio of 0.666 (20 patients in the training dataset and 10 patients in the testing dataset) using the *caTools* R package[42]. Using the *randomForest*[43] and *ROCR*[44] R packages, we trained 300 forests, containing 1001 trees each, with the training dataset, and we selected the model with the highest AUC. The accuracy of this model was predicted using the testing dataset. A trained forest produces a variable importance list based on mean decrease accuracy. For this analysis, the variable importance list is a list of taxa that contributed most to the correct group assignment of every sample and is presented in Figure S5.

Metagenomics sequencing – biostatistics on functional data

Functions were filtered to select for 1465 functions with a mean average abundance above 1 and a mean prevalence of 25% in at least one group of samples. PCA were computed from CLR-transformed data[30] followed by PERMANOVA using the *adonis* function in the *vegan* R package[37]. Twenty-two significantly affected functions were identified using MaAsLin2[36] (LM method, LOG transformation, no normalization). Model validation was achieved for the top 5 functions by visual inspection of the plot of the residuals against the fitted values. The LM method was preferred to the CPLM method based on the distribution of the residues of the models for these top 5 significant features. A q-value < 0.1 was considered significant.

The Random Forest algorithm was used to model the bacterial functional signature of the AML status. For this analysis, outcomes were AML or no AML and the dataset, namely the relative abundance of altered bacterial functions, was randomly split in a training and a testing set with a ratio of 0.666 (20 patients in the training dataset and 10 patients in the testing dataset) using the *caTools* R package[42]. Using the *randomForest*[43] and *ROCR*[44] R packages, we trained 300 forests,

containing 1001 trees each, with the training dataset, and we selected the model with the highest AUC. The accuracy of this model was predicted using the testing dataset. A trained forest produces a variable importance list based on mean decrease accuracy. For this analysis, the variable importance list is a list of that contributed most to the correct group assignment of every sample and is presented in Figure S5.

^{1}H-NMR Metabolomics analyses

Sample preparation

Faecal samples were prepared as follow: 200 mg of faeces were diluted into 1000 µl NMR buffer (H_2O–D_2O (1:1), pH = 7 ($NaHPO_4$-NaH_2PO_4 0.2 M), trimethylsilylpropanoic acid (TSP) 1 mM as standard) and homogenised in a TissueLyser (4 min, 25 Hz). The homogenate was centrifuged (10 min 13 000 g 4°C). The supernatant was then transferred into a 1.5 ml Eppendorf tube for a second centrifugation (3 min 13 000 g 4°C). This last supernatant was transferred into 5 mm diameter NMR tubes.

Plasma samples (Heparin tubes) were prepared as follow: AMICON ultra 0.5 ml – 10 kDa filters tubes were rinsed 5 times with 500 µl of distilled water followed by centrifugation (15 min 14 000 g 4°C). 500 µl of plasma were then filtered (30 min 14 000 g 4°C) followed by 250 µl of phosphate buffer (30 min 14 000 g 4°C) (H_2O–D_2O (1:9), pH = 7 ($NaHPO_4$-NaH_2PO_4 0.2 M). 150 µl of phosphate buffer (D_2O, pH = 7 ($NaHPO_4$-NaH_2PO_4 0.2 M), TSP 4 mM as standard) were directly added to the filtrate. After mixing (5 s vortex) 600 µl were transferred into 5 mm NMR tubes.

Urine samples were prepared as follow: urine samples were thawed overnight at 4°C, mixed (5 s vortex) and centrifuged (5 min 3 500 g 4°C). 630 µl of the supernatant were then mixed (5 s vortex) with 70 µl of NMR buffer (D_2O, pH = 7.1 ($KHPO_4$-K_2HPO_4 1.5 M), TSP 2.9 mM, NaN_3 0.2%) and then centrifuged (5 min 3 500 g 4°C). 600 µl were transferred into 5 mm NMR tubes. pH was measured to check that all samples ranged between 6.8 and 7.1.

Note that samples were randomly allocated to four groups that were analysed on four consecutive days, so that each sample spectrum was acquired within 12 hours of its preparation. Quality controls were included in each set of samples (one per day) to ensure the reproducibility and homogeneity of the obtained data. For faeces and plasma analyses, quality controls consisted in extra aliquots of

faces/plasma of a volunteer. For urine analyses, quality controls consisted in an aliquot of a pool (four different individuals) of AML and CT urine extra samples.

Data collection

NMR data were acquired on a Bruker Avance 600 MHz NMR spectrometer equipped with a cryoprobe. During acquisition, sample temperature was maintained at 300 K. Spectra were collected with a 1D NOESY pulse sequence for the plasma and urine samples and with a 1D CPMG pulse sequence for faecal samples. The 1D NOESY pulse sequence covered 21 ppm. Spectra were digitized in 65K data points during a 2.6 s acquisition time. The mixing time was set to 10 ms, and the relaxation delay between scans was set to 4 s. The 1D CPMG pulse sequence covered 20 ppm. Spectra were digitized in 65K data points during a 2.7 s acquisition time. The relaxation delay between scans was set to 4 s. Spectra were acquired using 128 scans for faecal and urine samples and 256 scans for plasma samples. To confirm metabolite identification, 2D ^{1}H-^{1}H NMR spectra, such as J-RES and TOCSY, as well as ^{1}H-^{13}C HSQC, were acquired for selected samples.

Data processing

The data were processed using MestReNova (v14.2). The spectra were zero filled with a factor of two. They were submitted to apodization using a 0.3 Hz decaying exponential function and fast Fourier transformed. Automated phase correction and second-order polynomial baseline correction were applied to all samples. All spectra were aligned on TSP. Spectral quality control was performed and some spectra were re-run. After re-run, all spectra passed the quality control and were included in further analyses. Only the region from 0.12 to 10 ppm was conserved. Water signal was removed from all spectra before statistical analyses. Considering the contaminations due to the filtering step, regions 3.36-3.37, 3.55-3.58 and 3.64-3.68 ppm were excluded from the analyses for plasma samples. Probabilistic quotient normalisation was performed. Intelligent bucketing was realised using the Matlab software (v9.2)[45]. Metabolites were assigned using the Chenomx NMR Suite (v8.43), the Bruker B-BIOREFCODE database (Amix software v3.9.15), the HMDB[46] and additional 2D NMR experiments on selected representative samples. The Chenomx NMR Suite was used to perform a relative quantification of the identified metabolite concentrations. TSP was used as a chemical shift and quantification reference for all spectra. Quantitative fitting of each spectrum was carried out in batch mode, followed by manual adjustment.

Statistical analyses

The tables of metabolite concentrations for each compartment were analysed in R. When missing data did not exceed 40% in both groups (CT and AML), a left-censored missing data imputation method was applied using the *impute.QRILC* function implemented in the *imputeLCMD* R package[47]. This was possible for all metabolites presented in this paper except for 3-phenylpropionate and maleate. For these two metabolites, no imputation was performed and the difference between both groups was tested by a Fisher's Exact Test in R. Significantly affected metabolites were identified by a Mann–Whitney U test since normality was not tested for each metabolite. The p-value was adjusted to control for the FDR. Q-values inferior to 0.1 were kept. The bubbleplot was generated using an *in-house* script including the *tidyverse* R package[48]. PCA with scaling to unit variance and partial least square discriminant analysis (PLS-DA) were respectively performed using the functions *pca* and *plsda* of the *mixOmics* R package[31].

Statistical analyses

General statistical overview

Normality was assessed using d'Agostino and Pearson omnibus normality test. If normality was not respected in one group, the nonparametric Mann–Whitney U test was used. Fisher's exact test was used to check for variance equality between groups. Student's t-test was used when variances were not statistically different. In case of variance inequality, Welch's t-test was used. Coherently, normal variables are presented as mean with standard deviation (SD) whereas non-normal variables are presented as median with interquartile range (IQR). $P < 0.05$ was considered statistically significant. For all *-omics* data, normality was not assessed and Mann-Whitney U-tests were therefore used. When needed, a correction for FDR was applied[33]. In this case, a q-value < 0.1 was considered significant. Statistical analyses were performed using GraphPad Prism 8.0 and R.

Integration analyses

Correlations between the top altered bacteria and (i) faecal, blood and urine metabolites and (ii) clinical, dietary, inflammatory, and metabolic parameters were performed in R using Spearman correlations. When adjusting for potential covariates such as age, partial Spearman rank-based correlations were computed using the *pcor* function (http://www.yilab.gatech.edu/pcor). FDR correction was applied. Metabolites/parameters with at least one correlation with one of the bacteria with a p-value < 0.05 were kept for inclusion in the heatmap. P-value < 0.05 were marked with a

‘+’ and q-value < 0.1 were marked with a ‘*’. The same method was applied for the correlations between the top bacterial functions and faecal, blood and urine metabolites.

Supplementary Results and Discussion

AML patients with hyperinsulinemia or hyperglycaemia display specific GM alterations

When looking at the glycaemia, insulin and HOMA-IR2 results presented in Figure 2C, it appears that some AML patients present much higher level of these parameters compared to the rest of the cohort. The four patients that are very different to the rest of the AML group for insulin levels and HOMA-IR2 are the same. Among those four patients, only one of them has also a higher glycaemia than the rest of the patients. The other two patients that have higher glycaemia levels do not have insulin levels and HOMA-IR2 that differ from the rest of the AML group.

The analysis of the microbiota stratifying the individuals by insulinemia and glycaemia were performed separately. Individuals were stratified in three groups, namely CT_low, AML_low and AML_high. For the analysis stratifying by insulinemia, the four patients with higher insulin levels than the rest of the cohort were allocated to the AML_high group, the rest of the AML patients were allocated to the AML_low group and the healthy individuals were included in the CT_low group. For the analysis stratifying by glycaemia, the three patients with high glycaemia levels (defined as glycaemia above 120mg/dl) were included in the AML_high group, the rest of the AML patients were allocated to the AML_low group and the healthy individuals were included in the CT_low group.

PCA at the species level stratified by insulinemia did not show a clear clustering of the AML_high group (new Figure S7A) since all three groups were superimposed. Moreover, insulinemia class did not explain a significant part of the variance in the dataset according to the PERMANOVA analysis. Interestingly, four species were significantly different between individuals with low versus high insulin levels (p-value < 0.05, q-value ns) (Figure S7B). *Phascolarctobacterium faecium*, *Bacteroides caccae* and *Bacteroides fragilis* were more abundant in the AML_high group whereas *Eubacterium eligens* was decreased in AML_high individuals. Similarly, PCA at the species level stratified by glycaemia did not show a clear clustering of the AML_high group (Figure S8A) and the PERMANOVA analysis was not significant either. However, six species were significantly different between individuals with low versus high glycaemia (p-value < 0.05, q-value ns) (Figure S8B). *Intestinibacter bartlettii*, *Bacteroides ovatus* and *Fusicatenibacter*

saccharivorans were decreased in the AML_high group whereas *Clostridium sp CAG 242*, *Firmicutes bacterium CAG 94* and *Streptococcus oralis* were decreased in those same individuals compared to the rest of the cohort.

Different databases, namely Disbiome[49], gutMDisorder[50], and Pubmed, were screened to investigate whether these bacteria of interest were previously associated with diseases or syndromes characterized by high blood levels of insulin and glucose, such as type I and II diabetes, obesity and metabolic syndrome. A compilation of the results is presented in Table S5.

The increase of *Phascolarctobacterium faecium*, *Bacteroides caccae* and *Streptococcus oralis* found in the AML_high group is in line with its increased abundance in individuals with type I or II diabetes. In the same manner, the decrease of *Eubacterium eligens* and *Intestinibacter bartlettii* is in accordance with its decreased abundance in individuals with type I diabetes among other diseases. Interestingly, *Intestinibacter bartlettii* was found to be correlated with markers for insulin resistance in 53 postmenopausal women with obesity[51]. In contrast, the increase of *Bacteroides fragilis* and *Bacteroides ovatus* observed in the AML_high group is in line with the results found in some studies but not others. *Bacteroides fragilis* was found to be increased in children with type I diabetes in one study[52] and in children with obesity in another study[53]. However, *Bacteroides fragilis* was also found to be decreased in a study with children with type I diabetes[54]. The results found concerning *Bacteroides ovatus* were also contradictory. In our study, *Bacteroides ovatus* was significantly decreased in AML patients with higher glycaemia levels, such as in children with obesity[55]. However, *B. ovatus* was increased in two studies of children with type I diabetes[52, 54]. Unfortunately, no information was found concerning the abundance of *Fusicatenibacter saccharivorans*, *Clostridium sp CAG 242* and *Firmicutes bacterium CAG 94* in diseases and syndromes characterized by high insulinemia and glycaemia.

To conclude, although the results presented above should be interpreted with caution given the very limited number of patients in the AML patients with high insulinemia/glycaemia, hence the lack of significance after correction for multiple testing, the bacterial species that vary significantly appear to be consistent with the information present in the literature.

Blood glutamine levels correlate with skeletal muscle mass and function

The plasma metabolomic signature of AML patients revealed signs of purine nucleotide metabolism deficiency and metabolic stress (e.g., increased hypoxanthine, reduction in TCA cycle intermediates, decreased glutamine alongside increased glutamate). Whether this stress may contribute to muscle alterations was explored through an additional set of correlations (Figure S22). Among these metabolites, only glutamine significantly correlated with lean mass, lean weight, and muscle strength (Figure S22). This correlation could reflect a deleterious impact of glutamine depletion driven by AML cells on the muscle as the skeletal muscle is the main storage site and endogenous source for glutamine.

Additional discussion on the potential of FMT in AML treatment and cachexia

Patients with AML usually receive induction chemotherapy coupled with antibiotic treatment. Those patients experience an alteration of the gut microbiota[56, 57] that remains after the end of the treatment[58, 59].

Fecal microbiota transplant represents an actionable measure to counteract the effect of treatment on the microbiota and cachexia. As stated in the introduction, Malard and colleagues[60] investigated the safety and diversity-enhancing ability of autologous fecal microbiota transfer (FMT) in patients with AML receiving intensive chemotherapy and antibiotics. Fecal material collected at the time of diagnosis was used for fecal microbiota transfer. This transfer appeared to be safe and could restore microbial richness and diversity based on α-diversity indices. However, autologous FMT with an intact microbiota is not always possible since patients have often already received antibiotic treatment by the time of diagnosis. Third-party FMT are thus an alternative. A randomized double-blind placebo-controlled trial on allogeneic hematopoietic cell transplantation recipients and patients with AML evaluated the ability of third-party oral FMT to decrease infection rates[61]. Third-party FMT did not reduce infection rates but was safe and ameliorated intestinal dysbiosis by restoring α-diversity index (and even exceeding baseline values), by restoring commensal bacteria (such as *Collinsella*) and by reducing the abundance of pathobionts (such as *Enterococcus* and *Dialister*). Therefore, both autologous and third-party FMT seem to be safe for AML patients undergoing chemotherapy. In this context, even when a fecal collection at diagnosis before any

antibiotics consumption is possible, the microbial quality of such sample that would be used for autologous FMT remains questionable. Indeed, our work reveals important alterations in the gut microbiota composition and function of AML patients already at diagnosis, which can be linked to metabolic and inflammatory dysregulations in those patients. Our findings call therefore for caution when using autologous fecal material transfer during the therapeutic care of AML patients and goes in favor of heterologous transfer to increase the gut microbiota diversity and richness in these patients.

To our knowledge, no study has been made on FMT and cachexia in AML patients. De Clercq and colleagues[62] performed a double-blind randomized placebo-controlled trial on 24 cachectic patients with metastatic HER2-negative gastroesophageal cancer which received autologous FMT or third-party FMT from a healthy obese donor. Allogenic FMT did not improve any of the cachexia outcomes (such as satiety and caloric intake) but increased disease control rate and showed a tendency of increased overall survival median and progression-free survival. Further research evaluating the impact of FMT on cachexia and its efficacy to tackle it has still to be performed.

References

1. Ghosh TS, Shanahan F, O'Toole PW. The gut microbiome as a modulator of healthy ageing. Nat Rev Gastroenterol Hepatol. 2022;19(9):565-584.
2. Falony G, Joossens M, Vieira-Silva S, et al. Population-level analysis of gut microbiome variation. Science. 2016;352(6285):560-564.
3. Zhang X, Zhong H, Li Y, et al. Sex- and age-related trajectories of the adult human gut microbiota shared across populations of different ethnicities. Nat Aging. 2021;1(1):87-100.
4. Zhernakova A, Kurilshikov A, Bonder MJ, et al. Population-based metagenomics analysis reveals markers for gut microbiome composition and diversity. Science. 2016;352(6285):565-569.
5. Crovesy L, Masterson D, Rosado EL. Profile of the gut microbiota of adults with obesity: a systematic review. Eur J Clin Nutr. 2020;74(9):1251-1262.
6. Antinozzi M, Giffi M, Sini N, et al. Cigarette Smoking and Human Gut Microbiota in Healthy Adults: A Systematic Review. Biomedicines. 2022;10(2):
7. Stuart EA. Matching methods for causal inference: A review and a look forward. Stat Sci. 2010;25(1):1-21.
8. . Guidelines for the Care and Use of Mammals in Neuroscience and Behavioral Research. Washington (DC), 2003.
9. Chua LL, Rajasuriar R, Azanan MS, et al. Reduced microbial diversity in adult survivors of childhood acute lymphoblastic leukemia and microbial associations with increased immune activation. Microbiome. 2017;5(1):35.
10. Hiel S, Bindels LB, Pachikian BD, et al. Effects of a diet based on inulin-rich vegetables on gut health and nutritional behavior in healthy humans. Am J Clin Nutr. 2019;109(6):1683-1695.
11. Leclercq S, Matamoros S, Cani PD, et al. Intestinal permeability, gut-bacterial dysbiosis, and behavioral markers of alcohol-dependence severity. Proc Natl Acad Sci U S A. 2014;111(42):E4485-4493.
12. Dewulf EM, Cani PD, Claus SP, et al. Insight into the prebiotic concept: lessons from an exploratory, double blind intervention study with inulin-type fructans in obese women. Gut. 2013;62(8):1112-1121.
13. Nicolucci AC, Hume MP, Martinez I, Mayengbam S, Walter J, Reimer RA. Prebiotics Reduce Body Fat and Alter Intestinal Microbiota in Children Who Are Overweight or With Obesity. Gastroenterology. 2017;153(3):711-722.
14. Rodriguez J, Hiel S, Neyrinck AM, et al. Discovery of the gut microbial signature driving the efficacy of prebiotic intervention in obese patients. Gut. 2020;69(11):1975-1987.
15. Hoebeeck LI, Rietzschel ER, Langlois M, et al. The relationship between diet and subclinical atherosclerosis: results from the Asklepios Study. Eur J Clin Nutr. 2011;65(5):606-613.
16. de l'Homme G, Bacque MF, Housset B, Lebeau B. [Tobacco dependence: a short evaluation questionnaire]. Presse Med. 1992;21(13):606-608.
17. Wilson MM, Thomas DR, Rubenstein LZ, et al. Appetite assessment: simple appetite questionnaire predicts weight loss in community-dwelling adults and nursing home residents. Am J Clin Nutr. 2005;82(5):1074-1081.
18. Holman R, Hines G, Kennedy I, Stevens R, Matthews D, Levy J. A calculator for HOMA. Diabetologia. 2004;47(
19. Costea PI, Zeller G, Sunagawa S, et al. Towards standards for human fecal sample processing in metagenomic studies. Nat Biotechnol. 2017;35(11):1069-1076.
20. Ovreas L, Forney L, Daae FL, Torsvik V. Distribution of bacterioplankton in meromictic Lake Saelenvannet, as determined by denaturing gradient gel electrophoresis of PCR-amplified gene fragments coding for 16S rRNA. Appl Environ Microbiol. 1997;63(9):3367-3373.
21. Potgens SA, Thibaut MM, Joudiou N, et al. Multi-compartment metabolomics and metagenomics reveal major hepatic and intestinal disturbances in cancer cachectic mice. J Cachexia Sarcopenia Muscle. 2021;12(2):456-475.

22. Eren AM, Vineis JH, Morrison HG, Sogin ML. A filtering method to generate high quality short reads using illumina paired-end technology. PLoS One. 2013;8(6):e66643.
23. Edgar RC. UPARSE: highly accurate OTU sequences from microbial amplicon reads. Nat Methods. 2013;10(10):996-998.
24. Edgar RC. UNOISE2: improved error-correction for Illumina 16S and ITS amplicon sequencing. bioRxiv. 2016;081257.
25. Callahan BJ, McMurdie PJ, Holmes SP. Exact sequence variants should replace operational taxonomic units in marker-gene data analysis. ISME J. 2017;11(12):2639-2643.
26. Edgar RC. Accuracy of taxonomy prediction for 16S rRNA and fungal ITS sequences. PeerJ. 2018;6(e4652.
27. Wang Q, Garrity GM, Tiedje JM, Cole JR. Naive Bayesian classifier for rapid assignment of rRNA sequences into the new bacterial taxonomy. Appl Environ Microbiol. 2007;73(16):5261-5267.
28. Caporaso JG, Kuczynski J, Stombaugh J, et al. QIIME allows analysis of high-throughput community sequencing data. Nat Methods. 2010;7(5):335-336.
29. Schloss PD, Westcott SL, Ryabin T, et al. Introducing mothur: open-source, platform-independent, community-supported software for describing and comparing microbial communities. Appl Environ Microbiol. 2009;75(23):7537-7541.
30. Gloor GB, Macklaim JM, Pawlowsky-Glahn V, Egozcue JJ. Microbiome Datasets Are Compositional: And This Is Not Optional. Front Microbiol. 2017;8(2224.
31. Rohart F, Gautier B, Singh A, Lê Cao KA. mixOmics: An R package for 'omics feature selection and multiple data integration. PLoS Computational Biology. 2017;13(11):
32. Mallick H, Rahnavard A, McIver LJ, et al. Multivariable association discovery in population-scale meta-omics studies. PLoS Comput Biol. 2021;17(11):e1009442.
33. Benjamini Y, Hochberg Y. Controlling the False Discovery Rate: A Practical and Powerful Approach to Multiple Testing. Journal of the Royal Statistic Society: Series B (Methodological). 1995;57(1):289-300.
34. Bolger AM, Lohse M, Usadel B. Trimmomatic: a flexible trimmer for Illumina sequence data. Bioinformatics. 2014;30(15):2114-2120.
35. Langmead B, Salzberg SL. Fast gapped-read alignment with Bowtie 2. Nat Methods. 2012;9(4):357-359.
36. Beghini F, McIver LJ, Blanco-Miguez A, et al. Integrating taxonomic, functional, and strain-level profiling of diverse microbial communities with bioBakery 3. Elife. 2021;10(
37. Oksanen J, Blanchet GF, Friendly M, et al. vegan: community Ecology. 2.5-7 ed: R package, 2020.
38. Nearing JT, Douglas GM, Hayes MG, et al. Microbiome differential abundance methods produce different results across 38 datasets. Nature Communications. 2022;13(1):342.
39. Fernandes AD, Reid JN, Macklaim JM, McMurrough TA, Edgell DR, Gloor GB. Unifying the analysis of high-throughput sequencing datasets: characterizing RNA-seq, 16S rRNA gene sequencing and selective growth experiments by compositional data analysis. Microbiome. 2014;2(15.
40. Podlesny D, Durdevic M, Paramsothy S, et al. Identification of clinical and ecological determinants of strain engraftment after fecal microbiota transplantation using metagenomics. Cell Rep Med. 2022;3(8):100711.
41. Escapa IF, Chen T, Huang Y, Gajare P, Dewhirst FE, Lemon KP. New Insights into Human Nostril Microbiome from the Expanded Human Oral Microbiome Database (eHOMD): a Resource for the Microbiome of the Human Aerodigestive Tract. mSystems. 2018;3(6):
42. Tuszynski J, Dietze M. Tools: Moving Window Statistics, GIF, Base64, ROC AUC, etc. https://cran.r-project.org/src/contrib/Archive/caTools/, 2005.
43. Liaw A, Wiener M. Classification and Regression by randomForest. R News. 2002;2(3):18-22.
44. Sing T, Sander O, Beerenwinkel N, Lengauer T. ROCR: visualizing classifier performance in R. http://rocr.bioinf.mpi-sb.mpg.de. Bioinformatics. 2005;21(20):

45. Sousa SAA, Magalhães A, Ferreira MMC. Optimized bucketing for NMR spectra: Three case studies. Chemometrics and Intelligent Laboratory Systems. 2013;122(93-102.
46. Wishart DS, Feunang YD, Marcu A, et al. HMDB 4.0: the human metabolome database for 2018. Nucleic Acids Res. 2018;46(D1):D608-D617.
47. Lazar C. imputeLCMD: a collection of methods for left-censored missing data imputation. CRAN, R Package, version 20. 2015;
48. Wickham H, Averick M, Bryan J, et al. Welcome to the Tidyverse. Journal of Open Source Software. 2019;4(1686.
49. Janssens Y, Nielandt J, Bronselaer A, et al. Disbiome database: linking the microbiome to disease. BMC Microbiol. 2018;18(1):50.
50. Qi C, Cai Y, Qian K, et al. gutMDisorder v2.0: a comprehensive database for dysbiosis of gut microbiota in phenotypes and interventions. Nucleic Acids Res. 2023;51(D1):D717-D722.
51. Brahe LK, Le Chatelier E, Prifti E, et al. Specific gut microbiota features and metabolic markers in postmenopausal women with obesity. Nutr Diabetes. 2015;5(6):e159.
52. de Goffau MC, Luopajarvi K, Knip M, et al. Fecal microbiota composition differs between children with beta-cell autoimmunity and those without. Diabetes. 2013;62(4):1238-1244.
53. Ignacio A, Fernandes MR, Rodrigues VA, et al. Correlation between body mass index and faecal microbiota from children. Clin Microbiol Infect. 2016;22(3):258 e251-258.
54. Giongo A, Gano KA, Crabb DB, et al. Toward defining the autoimmune microbiome for type 1 diabetes. ISME J. 2011;5(1):82-91.
55. Maya-Lucas O, Murugesan S, Nirmalkar K, et al. The gut microbiome of Mexican children affected by obesity. Anaerobe. 2019;55(11-23.
56. D'Angelo CR, Sudakaran S, Callander NS. Clinical effects and applications of the gut microbiome in hematologic malignancies. Cancer. 2021;127(5):679-687.
57. Galloway-Pena JR, Smith DP, Sahasrabhojane P, et al. The role of the gastrointestinal microbiome in infectious complications during induction chemotherapy for acute myeloid leukemia. Cancer. 2016;122(14):2186-2196.
58. Rashidi A, Ebadi M, Rehman TU, et al. Lasting shift in the gut microbiota in patients with acute myeloid leukemia. Blood Adv. 2022;6(11):3451-3457.
59. Rattanathammethee T, Tuitemwong P, Thiennimitr P, et al. Gut microbiota profiles of treatment-naive adult acute myeloid leukemia patients with neutropenic fever during intensive chemotherapy. PLoS One. 2020;15(10):e0236460.
60. Malard F, Vekhoff A, Lapusan S, et al. Gut microbiota diversity after autologous fecal microbiota transfer in acute myeloid leukemia patients. Nat Commun. 2021;12(1):3084.
61. Rashidi A, Ebadi M, Rehman TU, et al. Randomized Double-Blind Phase II Trial of Fecal Microbiota Transplantation Versus Placebo in Allogeneic Hematopoietic Cell Transplantation and AML. J Clin Oncol. 2023;41(34):5306-5319.
62. de Clercq NC, van den Ende T, Prodan A, et al. Fecal Microbiota Transplantation from Overweight or Obese Donors in Cachectic Patients with Advanced Gastroesophageal Cancer: A Randomized, Double-blind, Placebo-Controlled, Phase II Study. Clin Cancer Res. 2021;27(13):3784-3792.

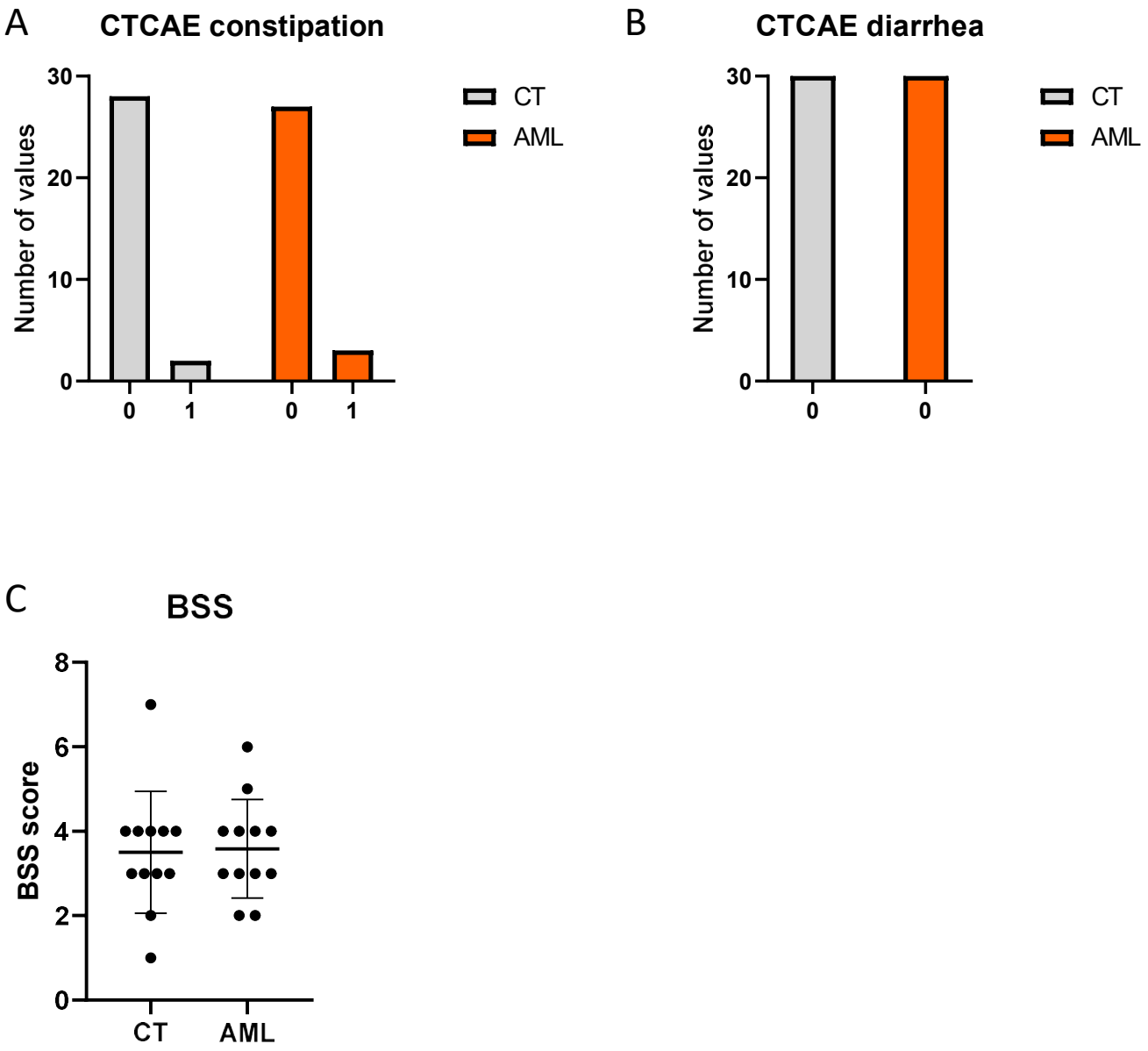

Figure S1. AML patients do not display transit alterations compared to CT subjects.
A) CTCAE constipation scores. B) CTCAE diarrhea scores. C) Bristol stool scale (BSS) scores for 12 matched AML and CT subjects. AML in orange *vs.* CT in grey.

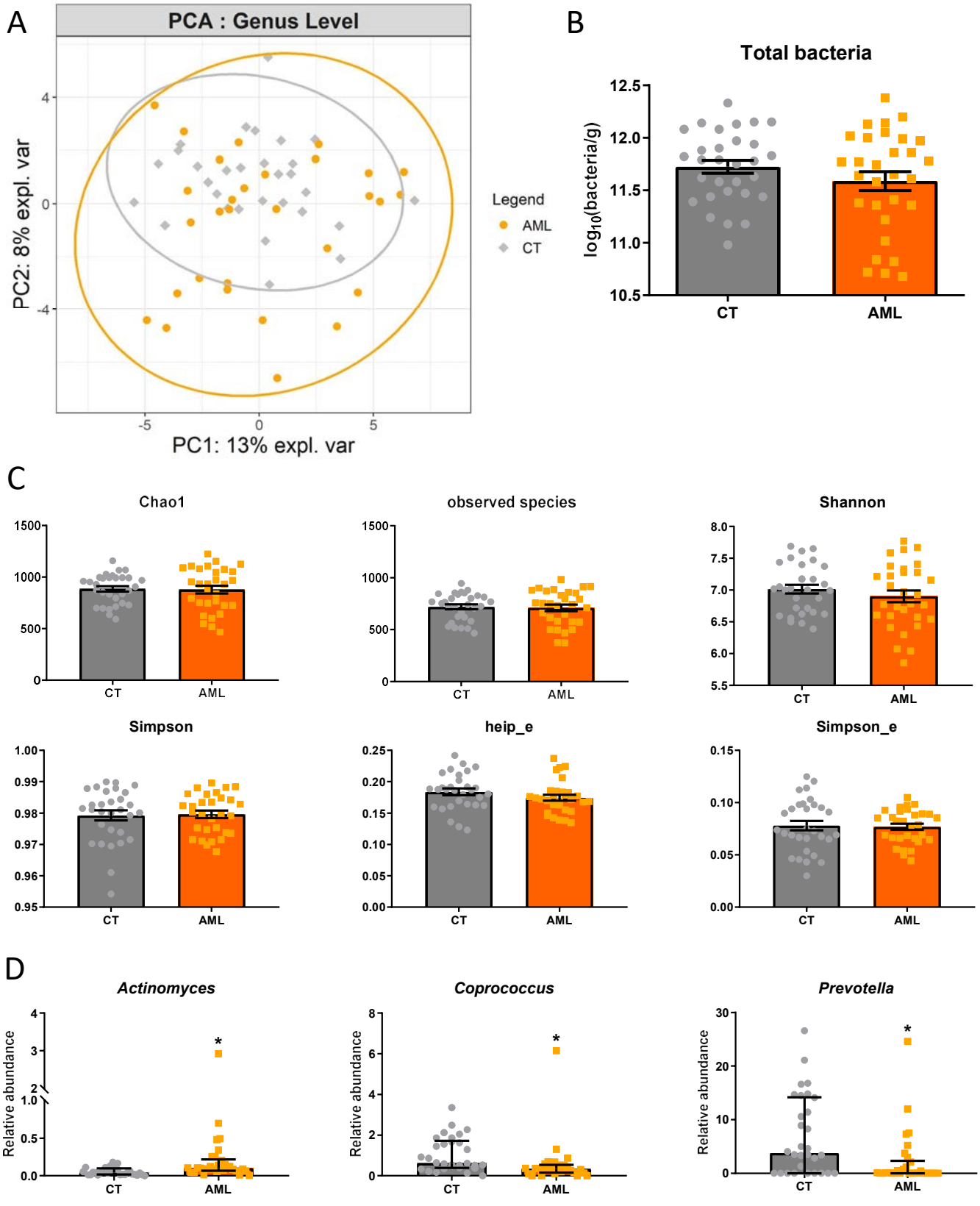

Figure S2. Alterations in the gut microbiota composition in CT subjects and AML patients (results of 16S rRNA gene sequencing).

A) Principal component analysis (PCA) at the genus level. PERMANOVA: R^2 = 2.7% * B) Total bacteria levels measured by qPCR. C) α-diversity indexes. Indexes that are normally distributed are expressed as mean (standard deviation) and are tested using a Student t-test or a Welch's t test. Indexes that are non-normally distributed are expressed as median (interquartile range) and are tested by a Mann-Whitney U-test. D) Significant changes at the lowest taxa level. Mann-Whitney U-tests with an FDR correction were applied. All q-values < 0.1. *n* = 30. AML in orange *vs.* CT in grey. *: p-value < 0.05

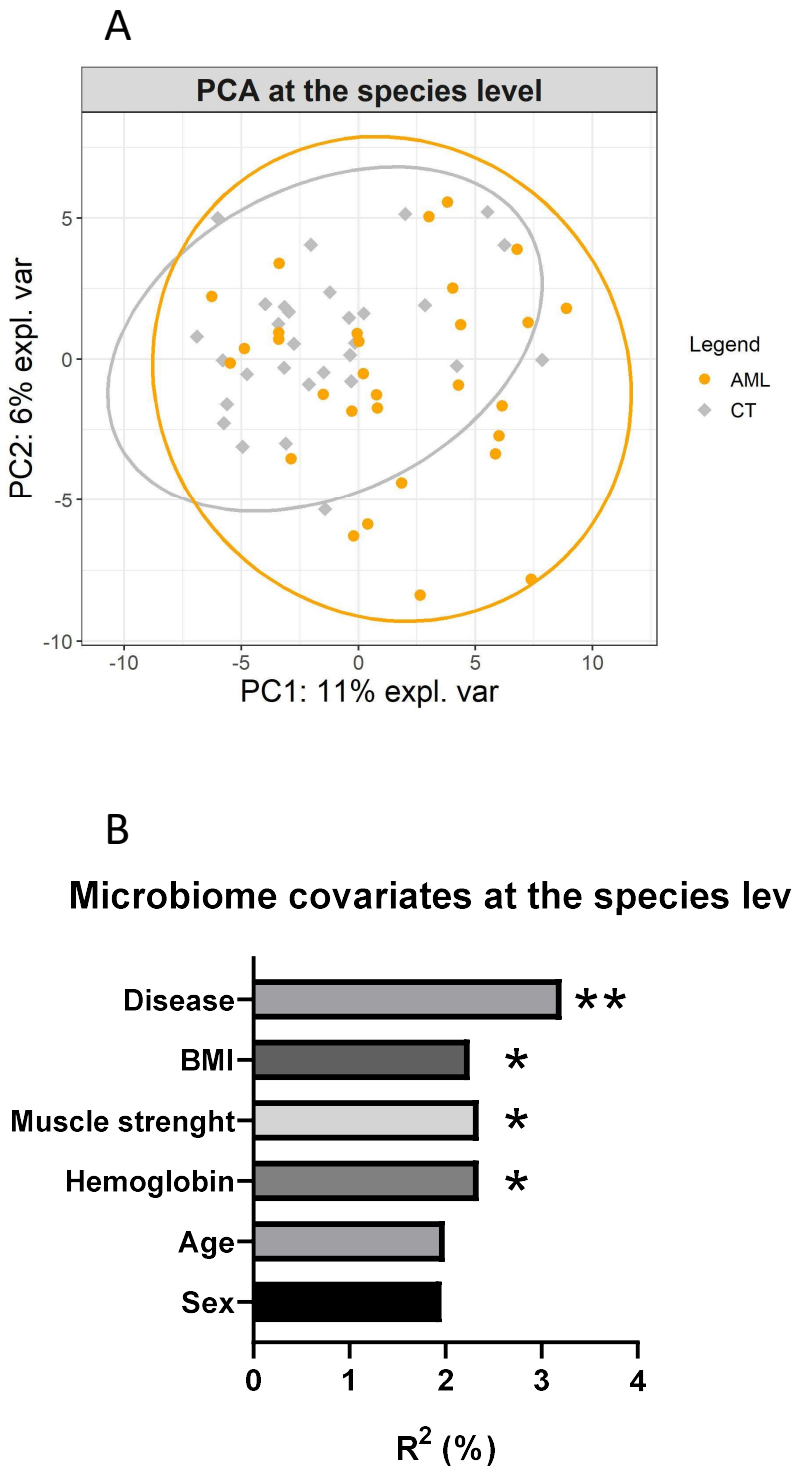

Figure S3. Alterations in the gut microbiota composition in CT subjects and AML patients (results of metagenomics sequencing).

A) Principal component analysis (PCA) at the species level. PERMANOVA: R^2 = 3.2% **. B) Contribution of disease, BMI, muscle strength, hemoglobin, age and sex to the variance in the PCA at the species level (PERMANOVA results). **p-value < 0.01; *p-value < 0.05

Figure S4. Bacterial contribution, per genera and per species, to the bacterial functions determined by metagenomics, that are significantly changed between CT (c) and AML (l). The relative abundance of each function is presented in Fig 1. Cpm, count per million. Plots were drawn using the *human_barplot* function in HUMAnN 3.00.

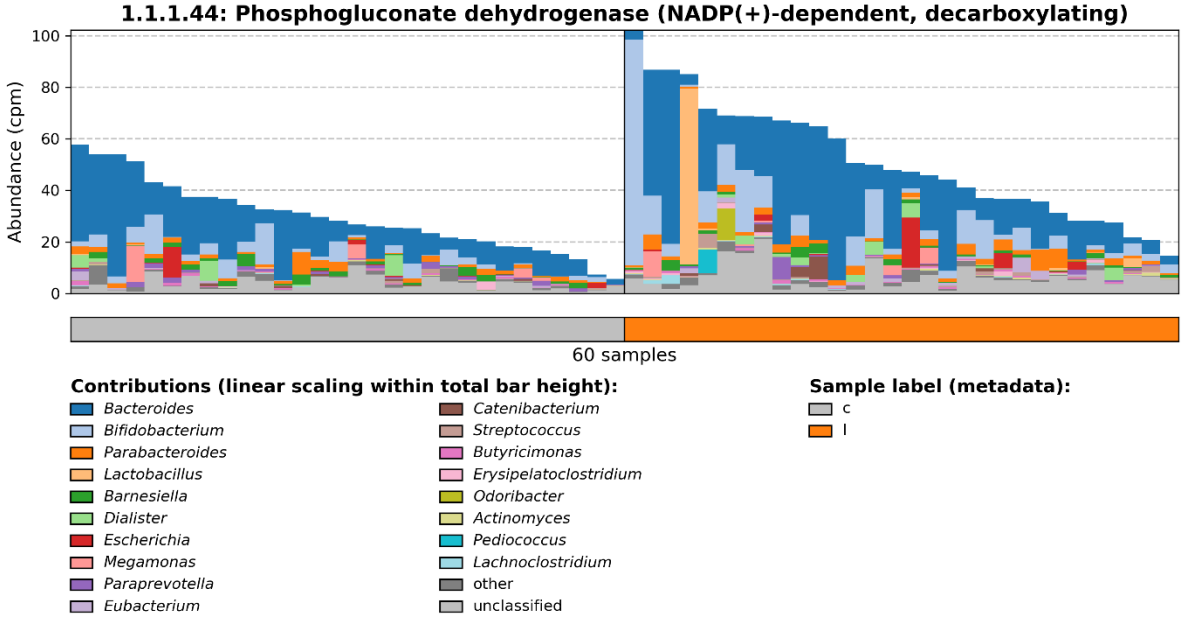

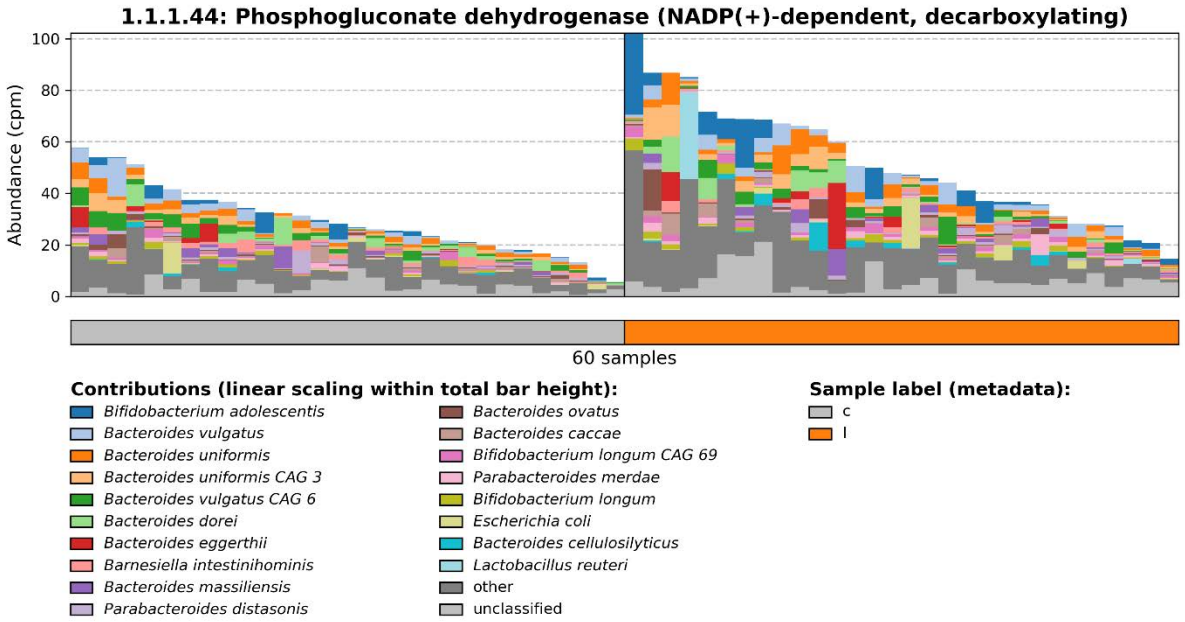

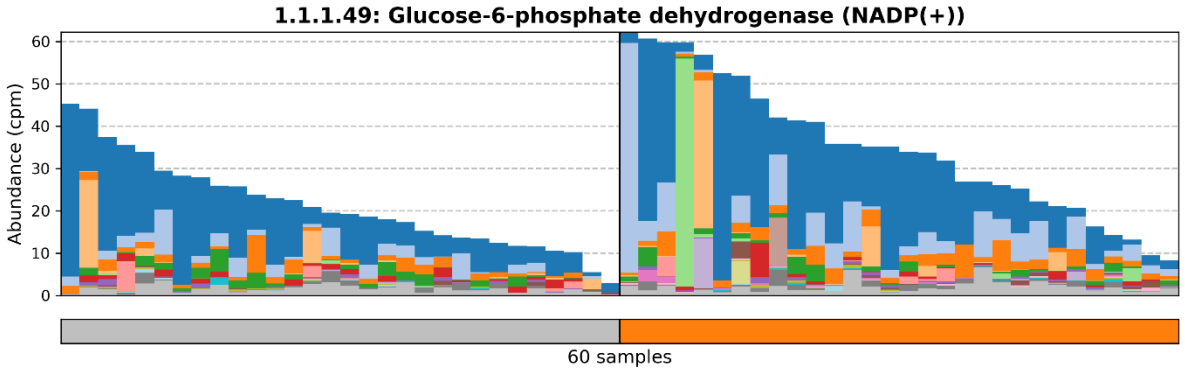

Contributions (linear scaling within total bar height):

- *Bacteroides*
- *Bifidobacterium*
- *Parabacteroides*
- *Escherichia*
- *Barnesiella*
- *Lactobacillus*
- *Paraprevotella*
- *Megamonas*
- *Butyricimonas*
- *Klebsiella*
- *Streptococcus*
- *Odoribacter*
- *Lachnoclostridium*
- *Actinomyces*
- *Coprobacter*
- *Pediococcus*
- *Alistipes*
- *Haemophilus*
- other
- unclassified

Sample label (metadata):

- c
- l

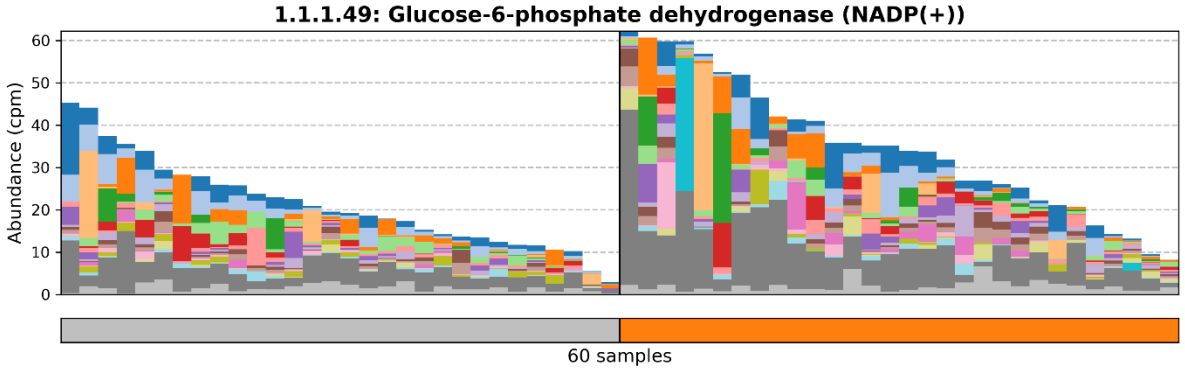

Contributions (linear scaling within total bar height):

- *Bacteroides vulgatus*
- *Bacteroides vulgatus CAG 6*
- *Bacteroides dorei*
- *Escherichia coli*
- *Bacteroides eggerthii*
- *Barnesiella intestinihominis*
- *Bacteroides massiliensis*
- *Parabacteroides distasonis*
- *Bacteroides caccae*
- *Parabacteroides merdae*
- *Bifidobacterium longum*
- *Bifidobacterium longum CAG 69*
- *Bacteroides cellulosilyticus*
- *Bacteroides ovatus*
- *Paraprevotella xylaniphila*
- *Bifidobacterium adolescentis*
- *Lactobacillus reuteri*
- *Bacteroides thetaiotaomicron*
- other
- unclassified

Sample label (metadata):

- c
- l

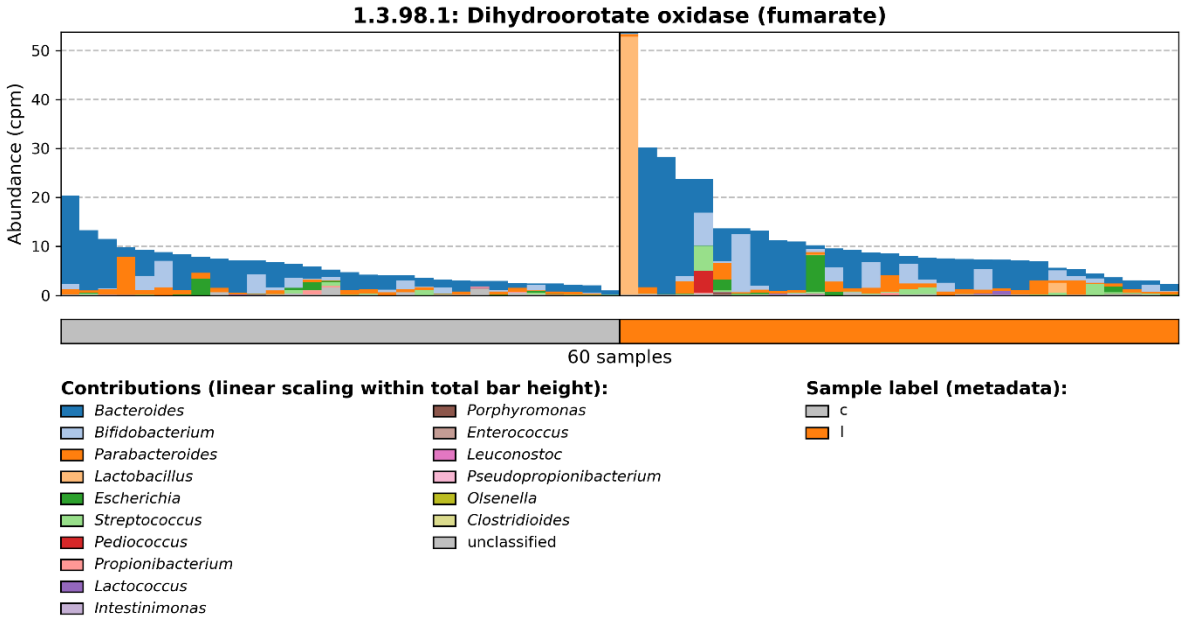
1.3.98.1: Dihydroorotate oxidase (fumarate)
Abundance (cpm)
0
10
20
30
40
50
60 samples
Contributions (linear scaling within total bar height):
Bacteroides
Bifidobacterium
Parabacteroides
Lactobacillus
Escherichia
Streptococcus
Pediococcus
Propionibacterium
Lactococcus
Intestinimonas
Porphyromonas
Enterococcus
Leuconostoc
Pseudopropionibacterium
Olsenella
Clostridioides
unclassified
Sample label (metadata):
c
l

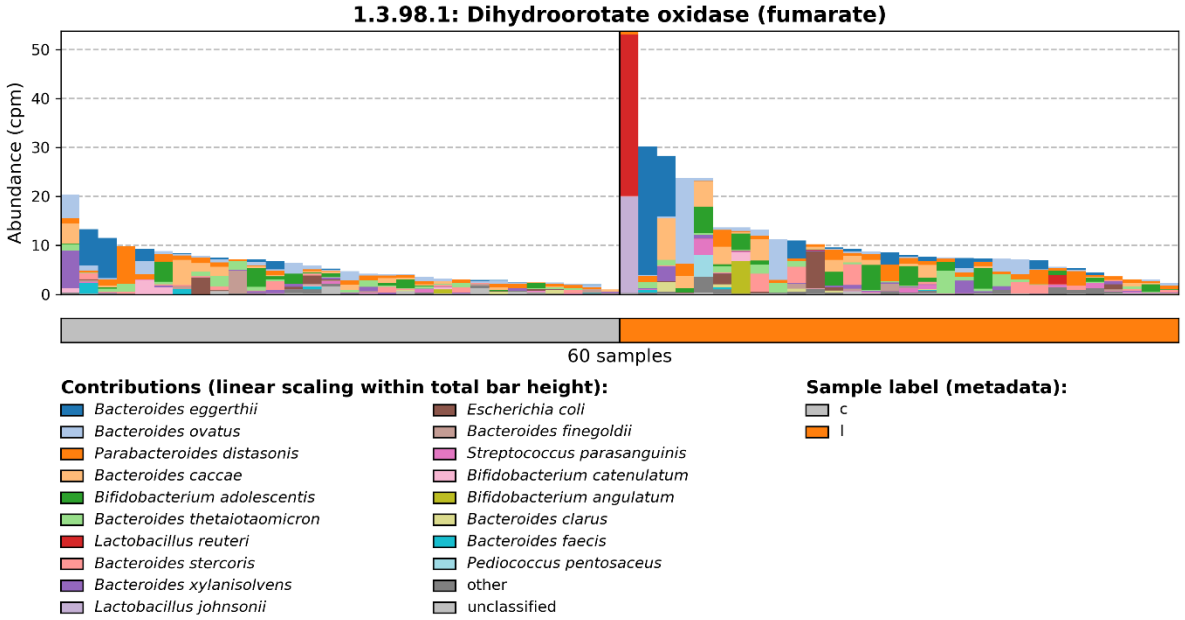
1.3.98.1: Dihydroorotate oxidase (fumarate)
Abundance (cpm)
0
10
20
30
40
50
60 samples
Contributions (linear scaling within total bar height):
Bacteroides eggerthii
Bacteroides ovatus
Parabacteroides distasonis
Bacteroides caccae
Bifidobacterium adolescentis
Bacteroides thetaiotaomicron
Lactobacillus reuteri
Bacteroides stercoris
Bacteroides xylanisolvens
Lactobacillus johnsonii
Escherichia coli
Bacteroides finegoldii
Streptococcus parasanguinis
Bifidobacterium catenulatum
Bifidobacterium angulatum
Bacteroides clarus
Bacteroides faecis
Pediococcus pentosaceus
other
unclassified
Sample label (metadata):
c
l

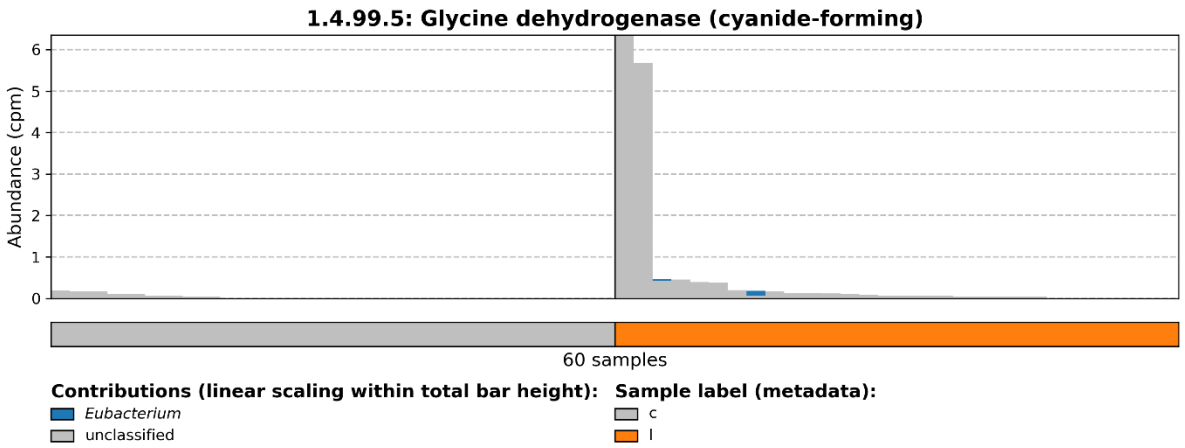
1.4.99.5: Glycine dehydrogenase (cyanide-forming)
Abundance (cpm)
0
1
2
3
4
5
6
60 samples
Contributions (linear scaling within total bar height):
Eubacterium
unclassified
Sample label (metadata):
c
l

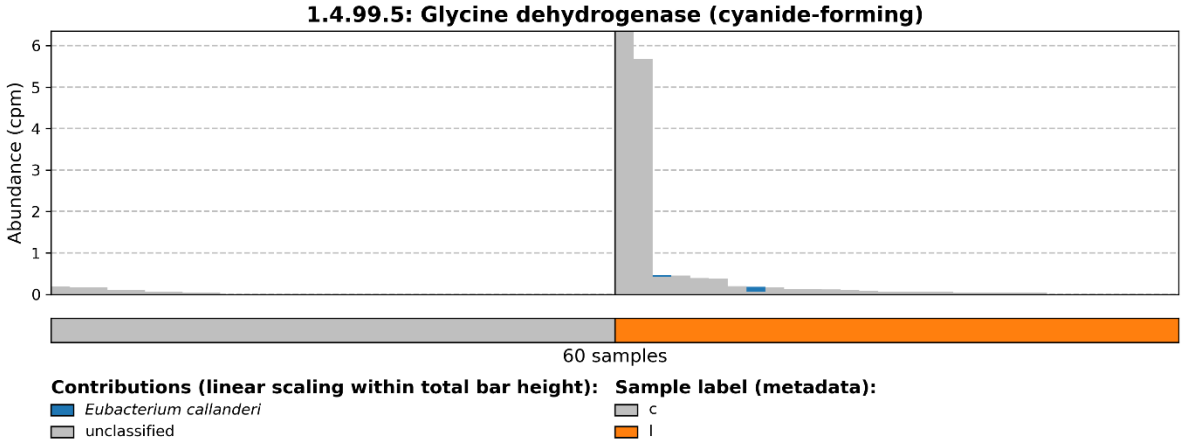
1.4.99.5: Glycine dehydrogenase (cyanide-forming)
Abundance (cpm)
0
1
2
3
4
5
6
60 samples
Contributions (linear scaling within total bar height):
Eubacterium callanderi
unclassified
Sample label (metadata):
c
l

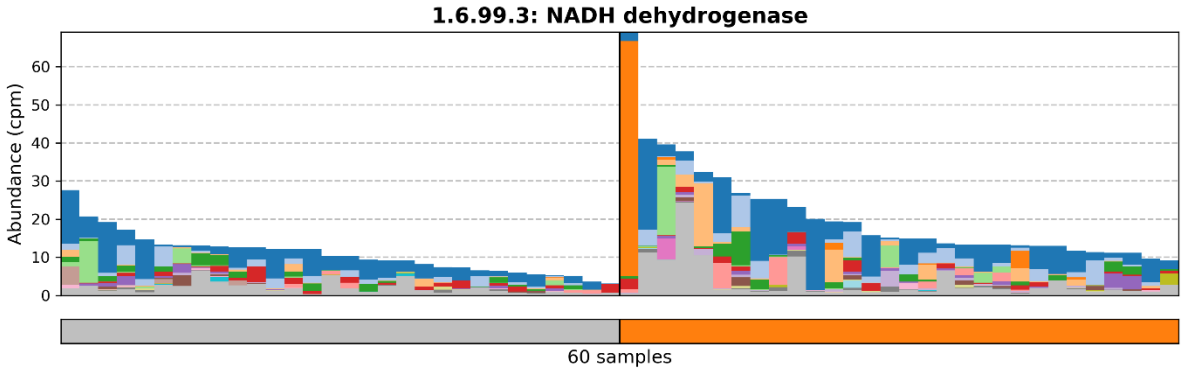

Contributions (linear scaling within total bar height):

- *Bacteroides*
- *Bifidobacterium*
- *Lactobacillus*
- *Streptococcus*
- *Fusicatenibacter*
- *Escherichia*
- *Coprococcus*
- *Catenibacterium*
- *Clostridium*
- *Actinomyces*
- *Romboutsia*
- *Hafnia*
- *Klebsiella*
- *Haemophilus*
- *Lactococcus*
- *Blautia*
- *Enterococcus*
- *Hungatella*
- other
- unclassified

Sample label (metadata):

- c
- l

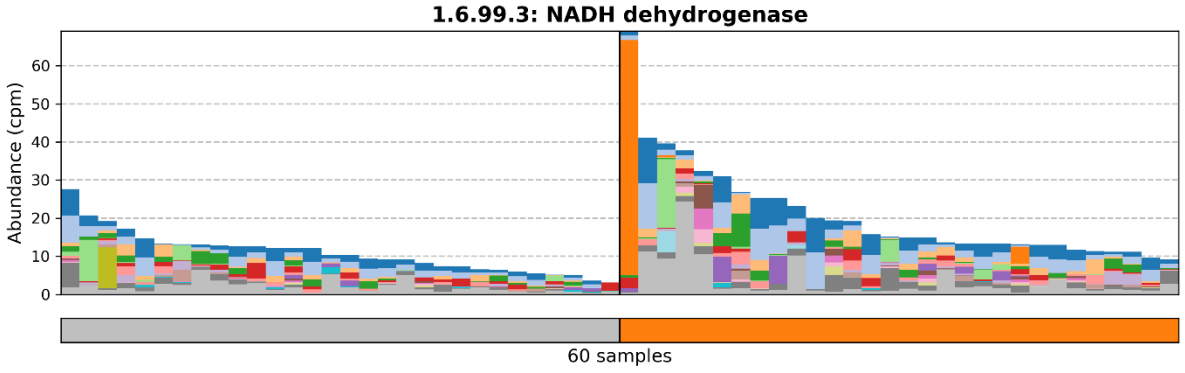

Contributions (linear scaling within total bar height):

- *Bacteroides uniformis*
- *Bacteroides uniformis CAG 3*
- *Lactobacillus reuteri*
- *Bifidobacterium longum CAG 69*
- *Fusicatenibacter saccharivorans*
- *Escherichia coli*
- *Coprococcus comes CAG 19*
- *Bifidobacterium longum*
- *Catenibacterium mitsuokai*
- *Clostridium disporicum*
- *Streptococcus salivarius*
- *Romboutsia ilealis*
- *Streptococcus thermophilus*
- *Streptococcus salivarius CAG 79*
- *Bacteroides xylanisolvens*
- *Streptococcus parasanguinis*
- *Bacteroides finegoldii*
- *Klebsiella pneumoniae*
- other
- unclassified

Sample label (metadata):

- c
- l

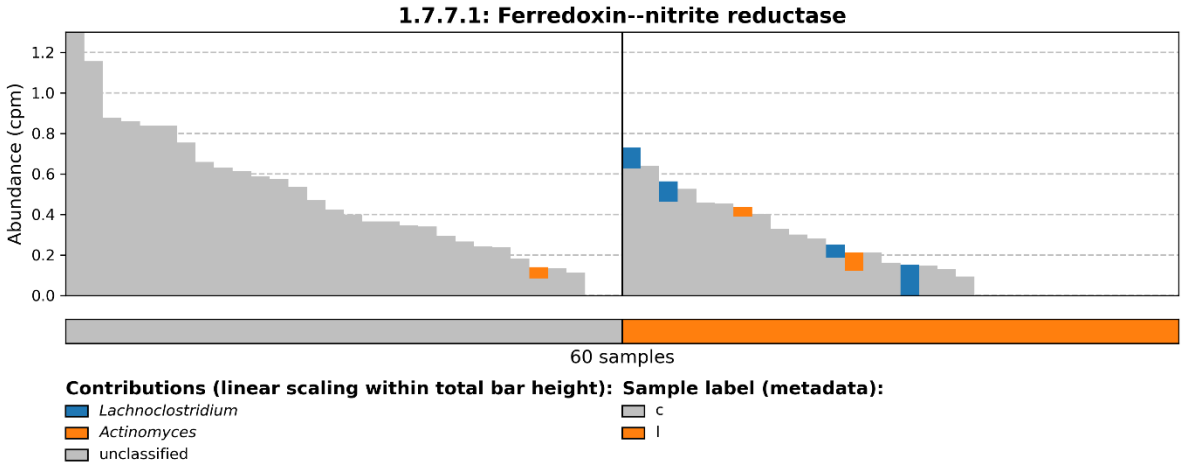
1.7.7.1: Ferredoxin--nitrite reductase
Abundance (cpm)
1.2
1.0
0.8
0.6
0.4
0.2
0.0
60 samples
Contributions (linear scaling within total bar height):
Lachnoclostridium
Actinomyces
unclassified
Sample label (metadata):
c
l

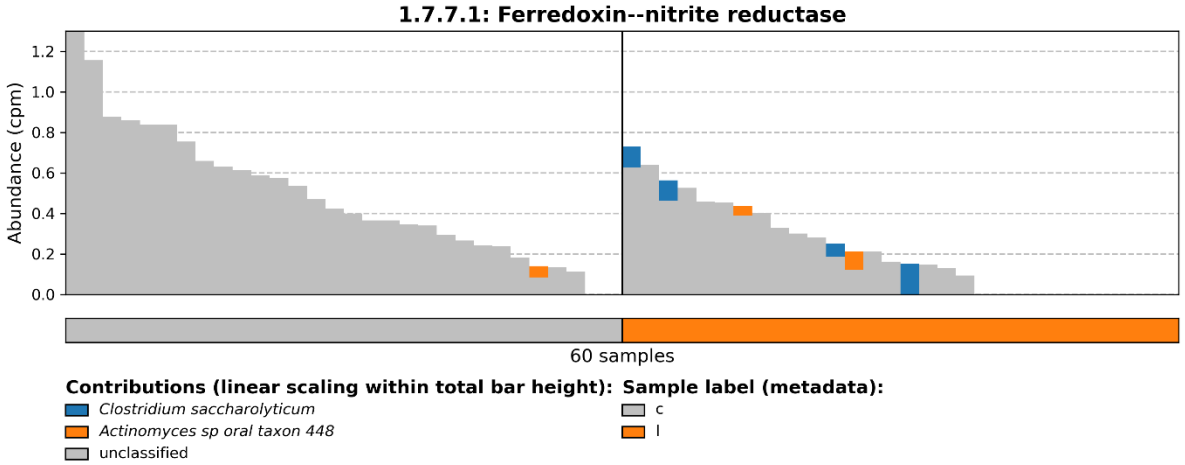
1.7.7.1: Ferredoxin--nitrite reductase
Abundance (cpm)
1.2
1.0
0.8
0.6
0.4
0.2
0.0
60 samples
Contributions (linear scaling within total bar height):
Clostridium saccharolyticum
Actinomyces sp oral taxon 448
unclassified
Sample label (metadata):
c
l

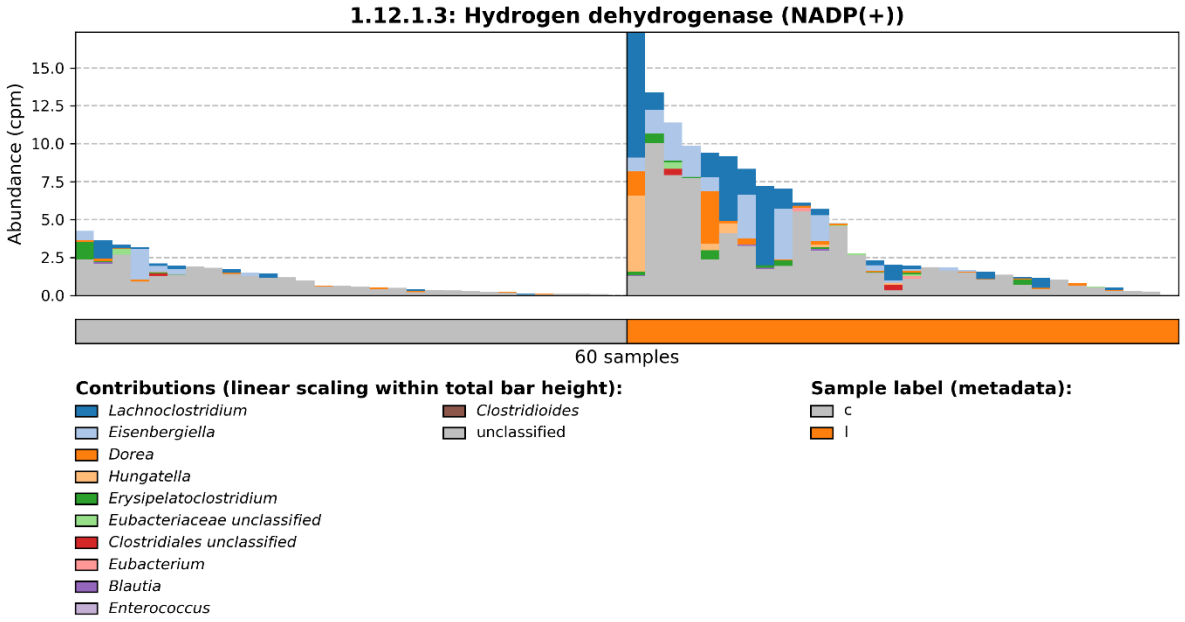
1.12.1.3: Hydrogen dehydrogenase (NADP(+))
Abundance (cpm)
15.0
12.5
10.0
7.5
5.0
2.5
0.0
60 samples
Contributions (linear scaling within total bar height):
Lachnoclostridium
Eisenbergiella
Dorea
Hungatella
Erysipelatoclostridium
Eubacteriaceae unclassified
Clostridiales unclassified
Eubacterium
Blautia
Enterococcus
Clostridioides
unclassified
Sample label (metadata):
c
l

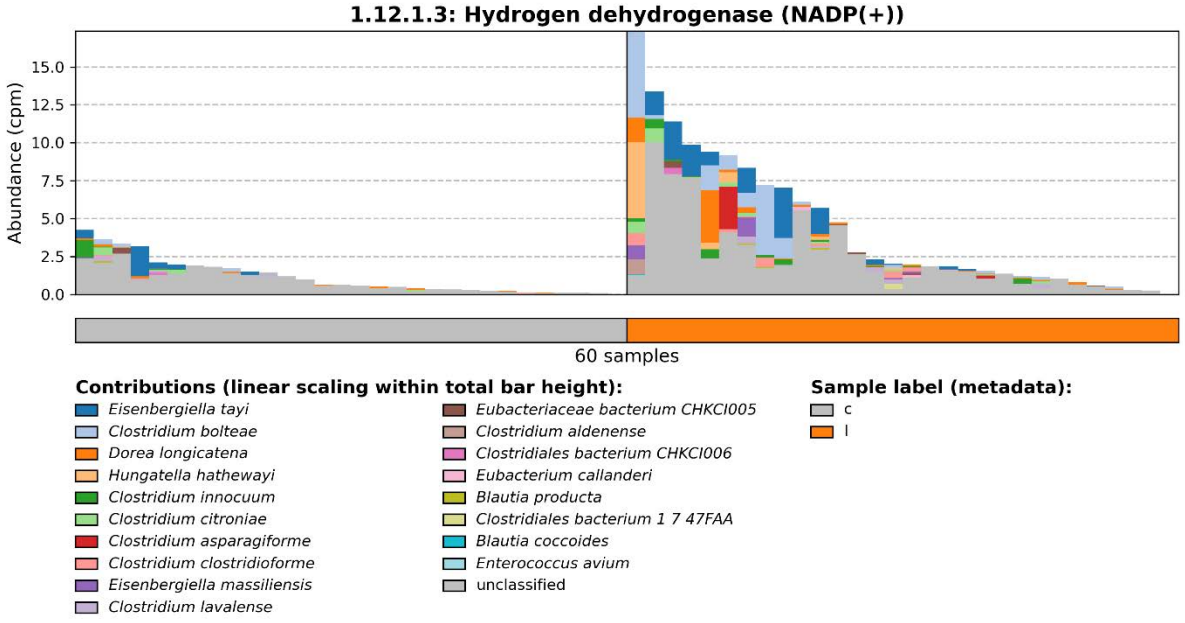
1.12.1.3: Hydrogen dehydrogenase (NADP(+))
Abundance (cpm)
15.0
12.5
10.0
7.5
5.0
2.5
0.0
60 samples
Contributions (linear scaling within total bar height):
Eisenbergiella tayi
Clostridium bolteae
Dorea longicatena
Hungatella hathewayi
Clostridium innocuum
Clostridium citroniae
Clostridium asparagiforme
Clostridium clostridioforme
Eisenbergiella massiliensis
Clostridium lavalense
Eubacteriaceae bacterium CHKCI005
Clostridium aldenense
Clostridiales bacterium CHKCI006
Eubacterium callanderi
Blautia producta
Clostridiales bacterium 1 7 47FAA
Blautia coccoides
Enterococcus avium
unclassified
Sample label (metadata):
c
l

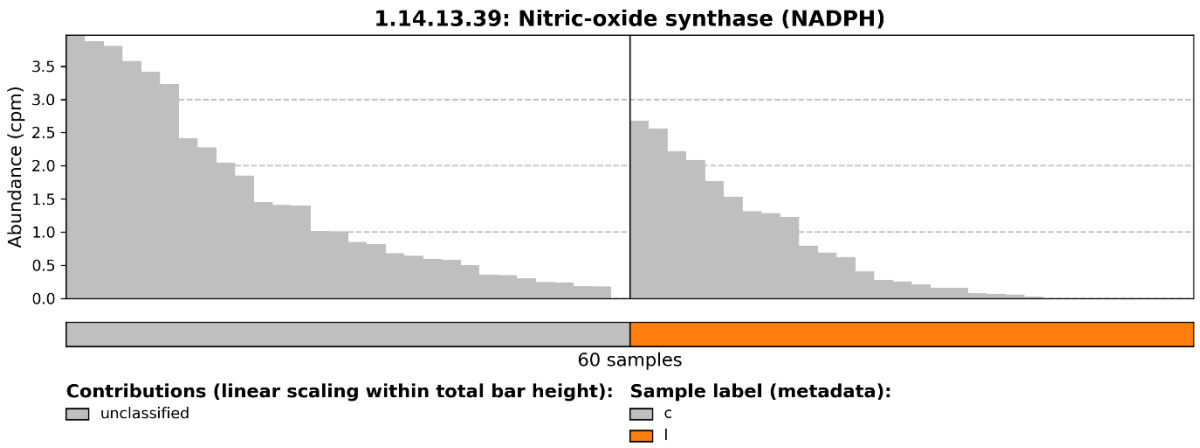
1.14.13.39: Nitric-oxide synthase (NADPH)
Abundance (cpm)
3.5
3.0
2.5
2.0
1.5
1.0
0.5
0.0
60 samples
Contributions (linear scaling within total bar height):
unclassified
Sample label (metadata):
c
l

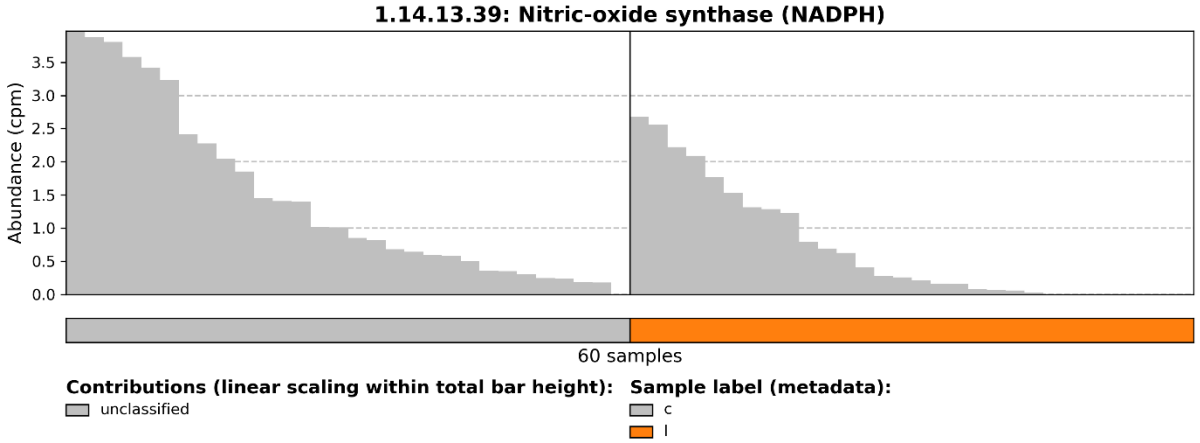
1.14.13.39: Nitric-oxide synthase (NADPH)
Abundance (cpm)
3.5
3.0
2.5
2.0
1.5
1.0
0.5
0.0
60 samples
Contributions (linear scaling within total bar height):
unclassified
Sample label (metadata):
c
l

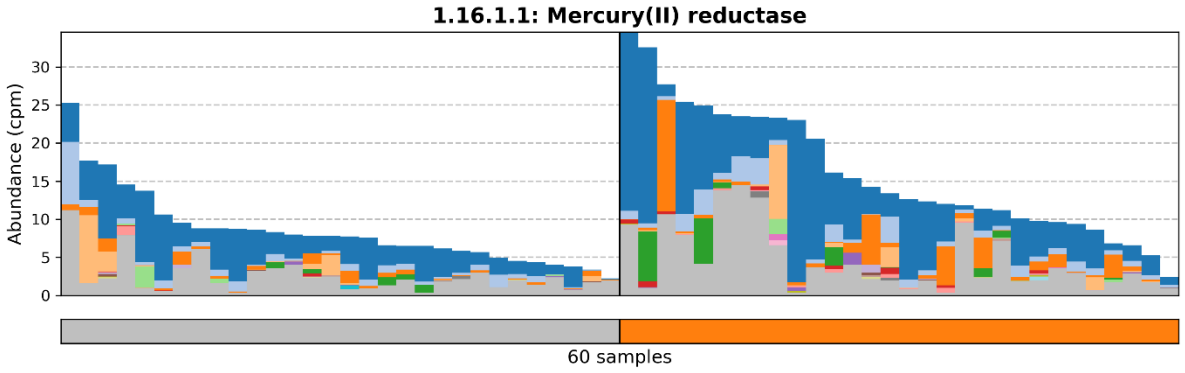

Contributions (linear scaling within total bar height):

- *Bacteroides*
- *Parabacteroides*
- *Streptococcus*
- *Escherichia*
- *Catenibacterium*
- *Lactobacillus*
- *Eisenbergiella*
- *Erysipelatoclostridium*
- *Lactococcus*
- *Rothia*
- *Haemophilus*
- *Actinomyces*
- *Clostridium*
- *Bifidobacterium*
- *Lachnoclostridium*
- *Veillonella*
- *Enterococcus*
- *Anaeromassilibacillus*
- other
- unclassified

Sample label (metadata):

- c
- l

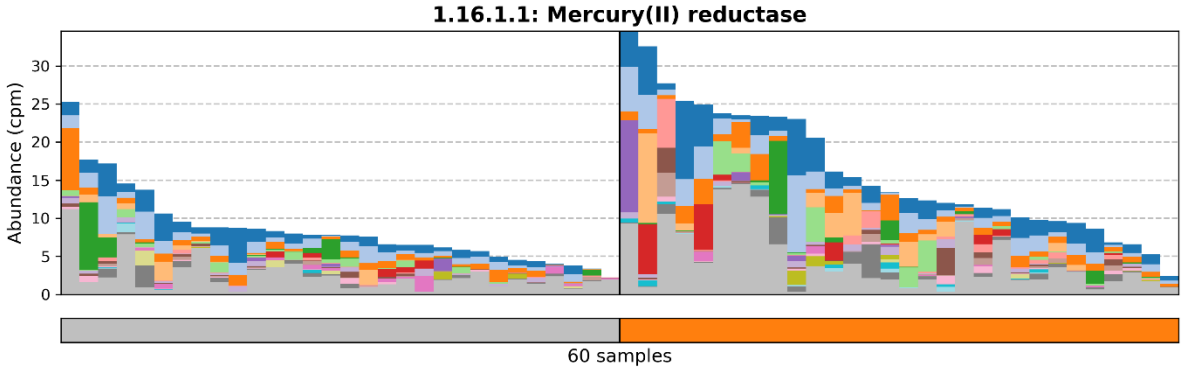

Contributions (linear scaling within total bar height):

- *Bacteroides uniformis CAG 3*
- *Bacteroides uniformis*
- *Parabacteroides distasonis*
- *Bacteroides cellulosilyticus*
- *Escherichia coli*
- *Bacteroides stercoris*
- *Catenibacterium mitsuokai*
- *Streptococcus salivarius*
- *Bacteroides intestinalis*
- *Bacteroides thetaiotaomicron*
- *Streptococcus thermophilus CAG 236*
- *Streptococcus salivarius CAG 79*
- *Bacteroides finegoldii*
- *Streptococcus thermophilus*
- *Bacteroides clarus*
- *Bacteroides faecis*
- *Eisenbergiella tayi*
- *Clostridium innocuum*
- other
- unclassified

Sample label (metadata):

- c
- l

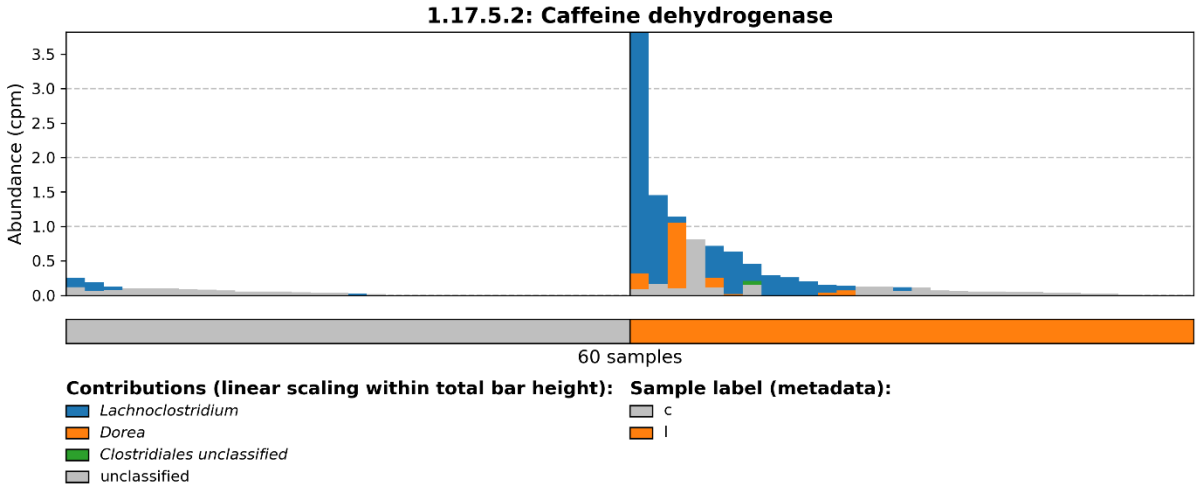
1.17.5.2: Caffeine dehydrogenase
Abundance (cpm)
3.5
3.0
2.5
2.0
1.5
1.0
0.5
0.0
60 samples
Contributions (linear scaling within total bar height):
Lachnoclostridium
Dorea
Clostridiales unclassified
unclassified
Sample label (metadata):
c
l

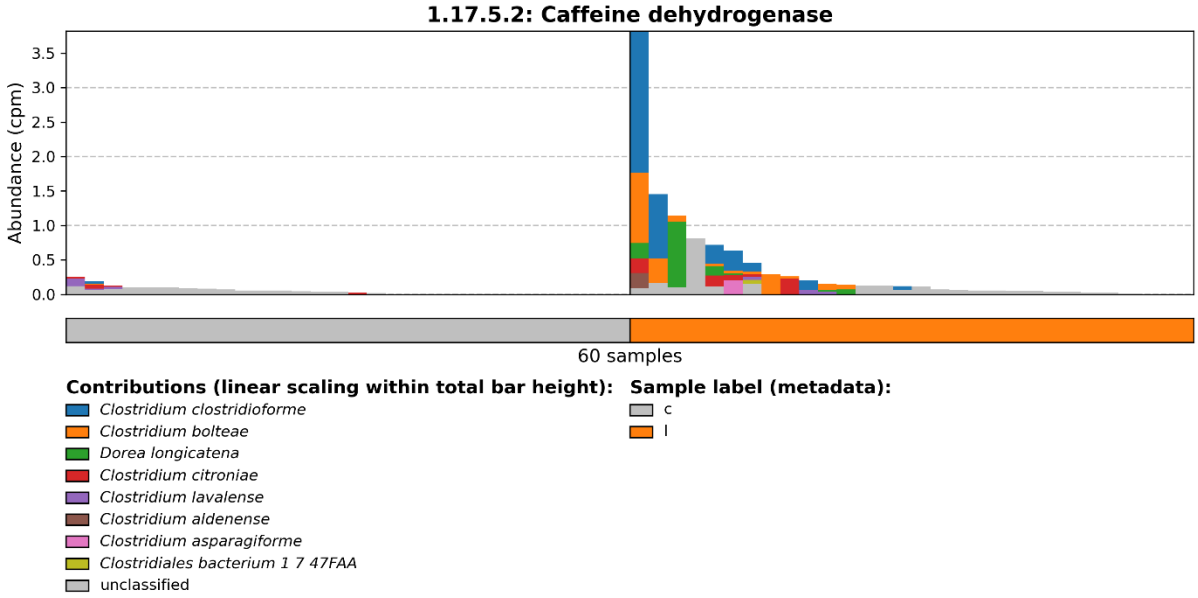
1.17.5.2: Caffeine dehydrogenase
Abundance (cpm)
3.5
3.0
2.5
2.0
1.5
1.0
0.5
0.0
60 samples
Contributions (linear scaling within total bar height):
Clostridium clostridioforme
Clostridium bolteae
Dorea longicatena
Clostridium citroniae
Clostridium lavalense
Clostridium aldenense
Clostridium asparagiforme
Clostridiales bacterium 1 7 47FAA
unclassified
Sample label (metadata):
c
l

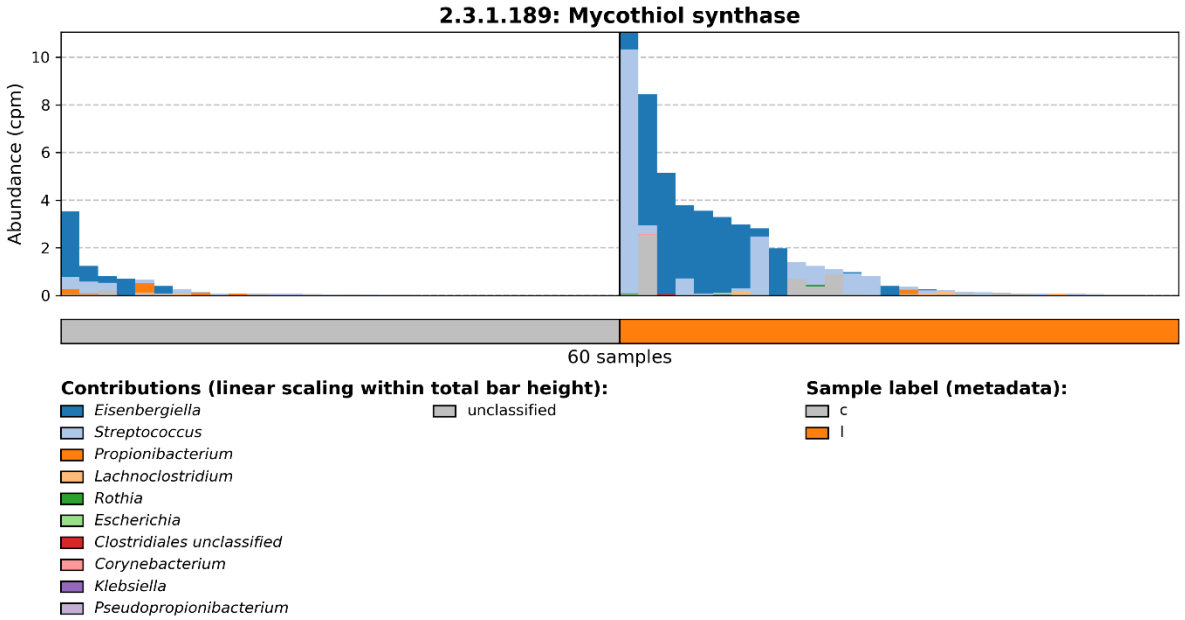
2.3.1.189: Mycothiol synthase
Abundance (cpm)
0
2
4
6
8
10
60 samples
Contributions (linear scaling within total bar height):
Eisenbergiella
Streptococcus
Propionibacterium
Lachnoclostridium
Rothia
Escherichia
Clostridiales unclassified
Corynebacterium
Klebsiella
Pseudopropionibacterium
unclassified
Sample label (metadata):
c
l

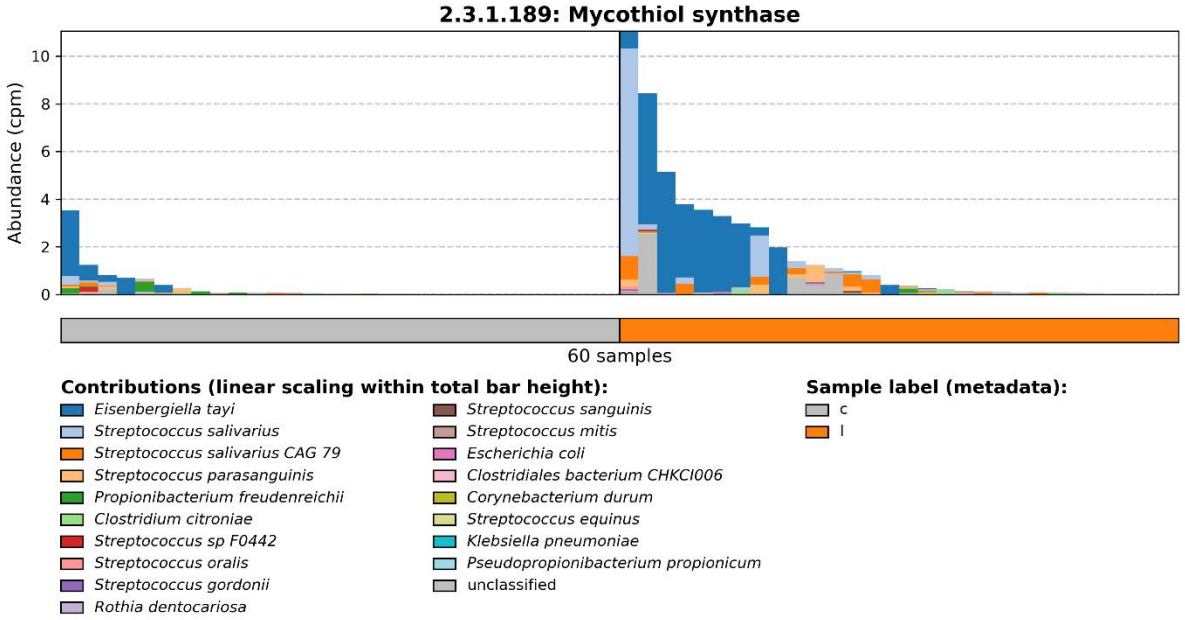
2.3.1.189: Mycothiol synthase
Abundance (cpm)
0
2
4
6
8
10
60 samples
Contributions (linear scaling within total bar height):
Eisenbergiella tayi
Streptococcus salivarius
Streptococcus salivarius CAG 79
Streptococcus parasanguinis
Propionibacterium freudenreichii
Clostridium citroniae
Streptococcus sp F0442
Streptococcus oralis
Streptococcus gordonii
Rothia dentocariosa
Streptococcus sanguinis
Streptococcus mitis
Escherichia coli
Clostridiales bacterium CHKCI006
Corynebacterium durum
Streptococcus equinus
Klebsiella pneumoniae
Pseudopropionibacterium propionicum
unclassified
Sample label (metadata):
c
l

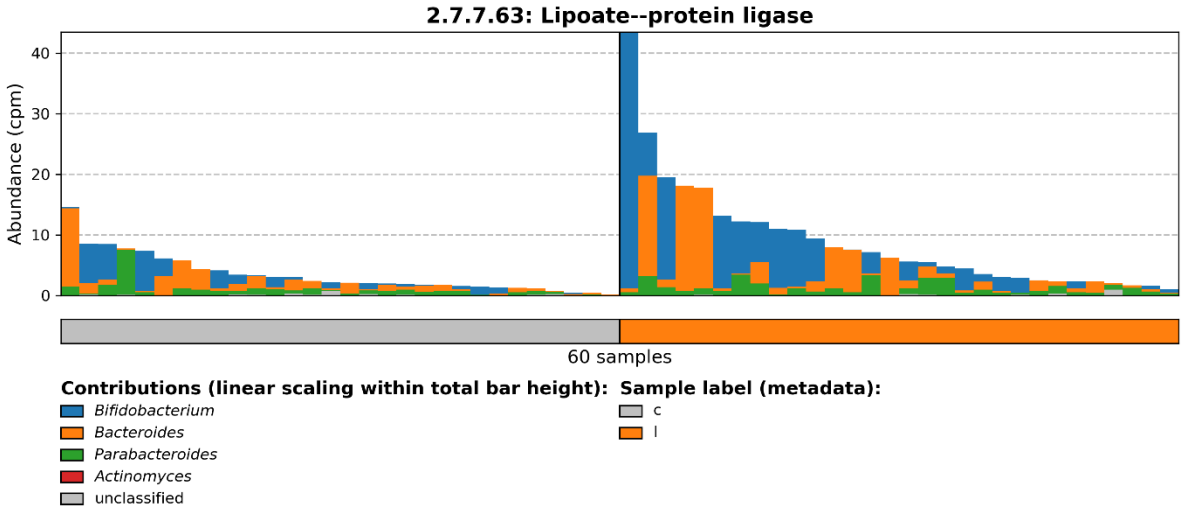
2.7.7.63: Lipoate--protein ligase
Abundance (cpm)
0
10
20
30
40
60 samples
Contributions (linear scaling within total bar height):
Bifidobacterium
Bacteroides
Parabacteroides
Actinomyces
unclassified
Sample label (metadata):
c
l

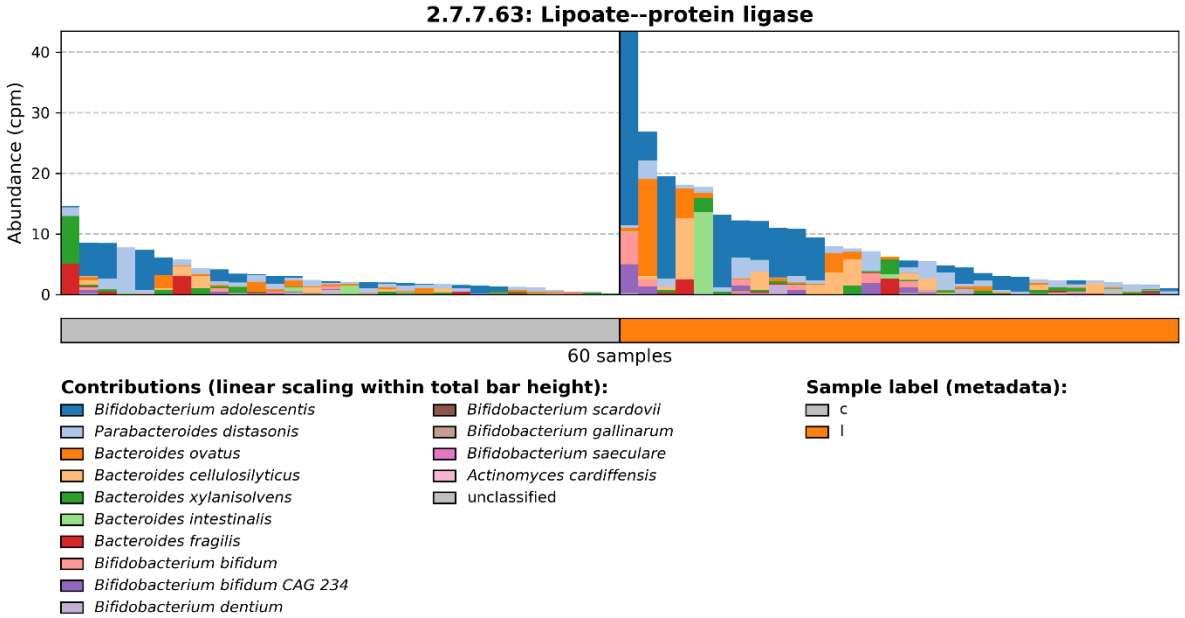
2.7.7.63: Lipoate--protein ligase
Abundance (cpm)
0
10
20
30
40
60 samples
Contributions (linear scaling within total bar height):
Bifidobacterium adolescentis
Parabacteroides distasonis
Bacteroides ovatus
Bacteroides cellulosilyticus
Bacteroides xylanisolvens
Bacteroides intestinalis
Bacteroides fragilis
Bifidobacterium bifidum
Bifidobacterium bifidum CAG 234
Bifidobacterium dentium
Bifidobacterium scardovii
Bifidobacterium gallinarum
Bifidobacterium saeculare
Actinomyces cardiffensis
unclassified
Sample label (metadata):
c
l

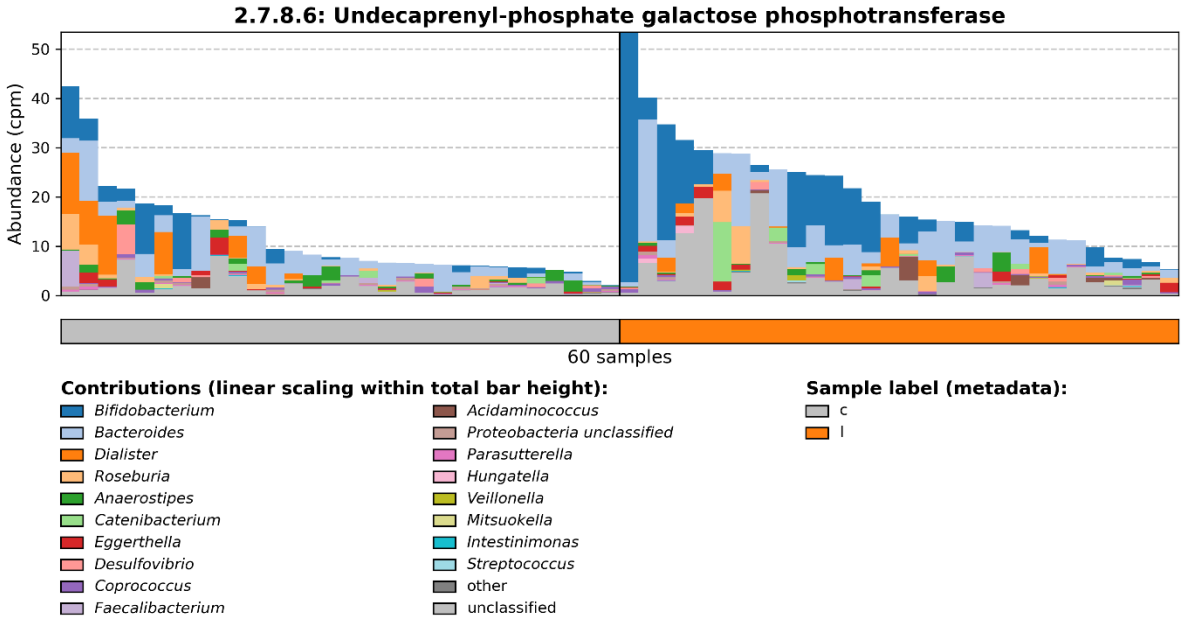
2.7.8.6: Undecaprenyl-phosphate galactose phosphotransferase
Abundance (cpm)
50
40
30
20
10
0
60 samples
Contributions (linear scaling within total bar height):
Bifidobacterium
Bacteroides
Dialister
Roseburia
Anaerostipes
Catenibacterium
Eggerthella
Desulfovibrio
Coprococcus
Faecalibacterium
Acidaminococcus
Proteobacteria unclassified
Parasutterella
Hungatella
Veillonella
Mitsuokella
Intestinimonas
Streptococcus
other
unclassified
Sample label (metadata):
c
l

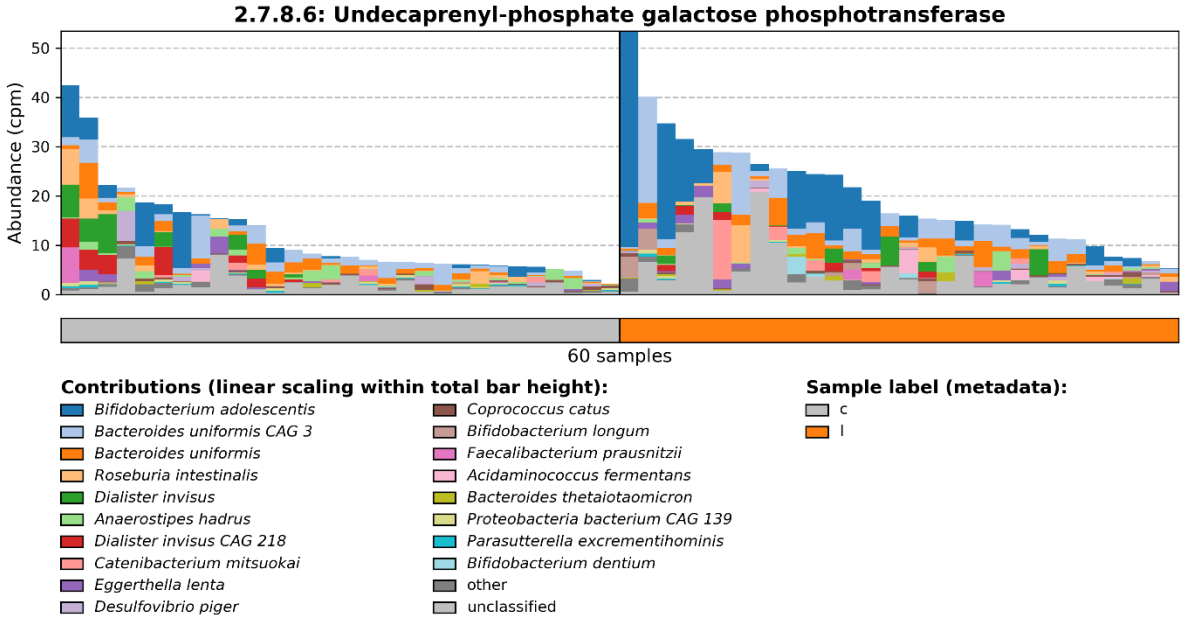
2.7.8.6: Undecaprenyl-phosphate galactose phosphotransferase
Abundance (cpm)
50
40
30
20
10
0
60 samples
Contributions (linear scaling within total bar height):
Bifidobacterium adolescentis
Bacteroides uniformis CAG 3
Bacteroides uniformis
Roseburia intestinalis
Dialister invisus
Anaerostipes hadrus
Dialister invisus CAG 218
Catenibacterium mitsuokai
Eggerthella lenta
Desulfovibrio piger
Coprococcus catus
Bifidobacterium longum
Faecalibacterium prausnitzii
Acidaminococcus fermentans
Bacteroides thetaiotaomicron
Proteobacteria bacterium CAG 139
Parasutterella excrementihominis
Bifidobacterium dentium
other
unclassified
Sample label (metadata):
c
l

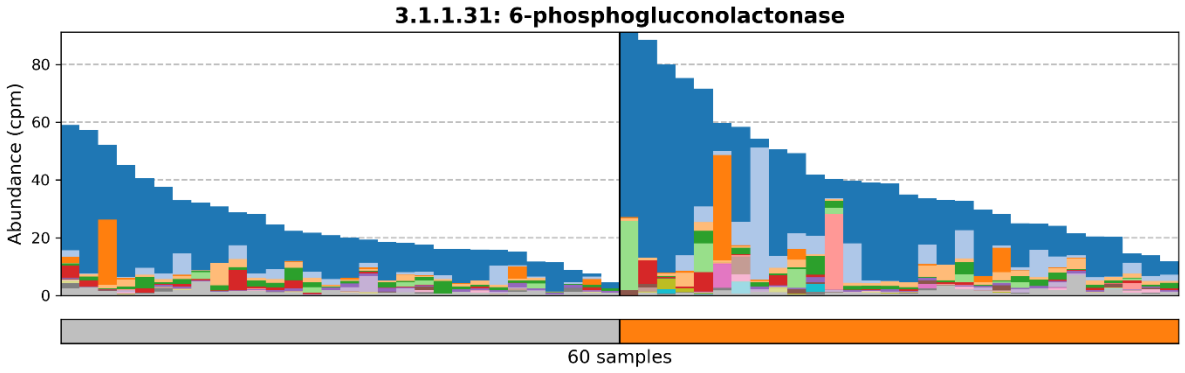

Contributions (linear scaling within total bar height):

- *Bacteroides*
- *Bifidobacterium*
- *Escherichia*
- *Parabacteroides*
- *Blautia*
- *Catenibacterium*
- *Roseburia*
- *Lactobacillus*
- *Coprococcus*
- *Desulfovibrio*
- *Eisenbergiella*
- *Veillonella*
- *Klebsiella*
- *Streptococcus*
- *Lachnoclostridium*
- *Haemophilus*
- *Hungatella*
- *Pediococcus*
- other
- unclassified

Sample label (metadata):

- c
- l

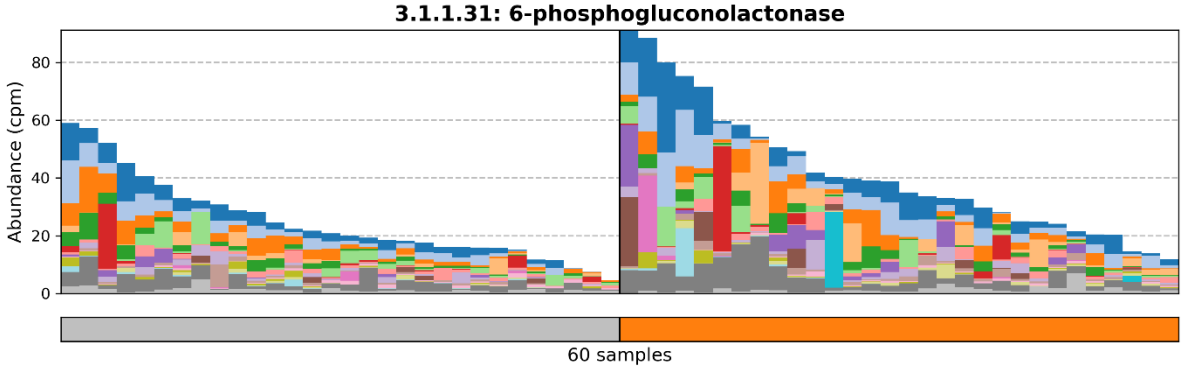

Contributions (linear scaling within total bar height):

- *Bacteroides uniformis*
- *Bacteroides uniformis CAG 3*
- *Bacteroides vulgatus CAG 6*
- *Bifidobacterium adolescentis*
- *Bacteroides vulgatus*
- *Bacteroides dorei*
- *Escherichia coli*
- *Blautia obeum*
- *Bacteroides cellulosilyticus*
- *Bacteroides thetaiotaomicron*
- *Catenibacterium mitsuokai*
- *Parabacteroides distasonis*
- *Bacteroides intestinalis*
- *Coprococcus catus*
- *Roseburia intestinalis*
- *Parabacteroides merdae*
- *Lactobacillus reuteri*
- *Bacteroides ovatus*
- other
- unclassified

Sample label (metadata):

- c
- l

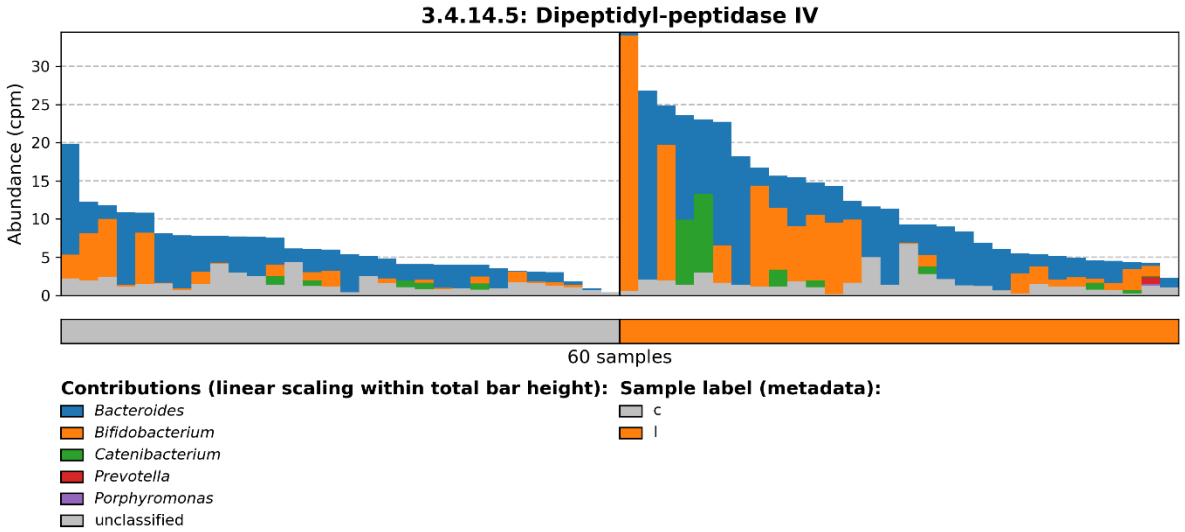
3.4.14.5: Dipeptidyl-peptidase IV
Abundance (cpm)
0
5
10
15
20
25
30
60 samples
Contributions (linear scaling within total bar height):
Bacteroides
Bifidobacterium
Catenibacterium
Prevotella
Porphyromonas
unclassified
Sample label (metadata):
c
l

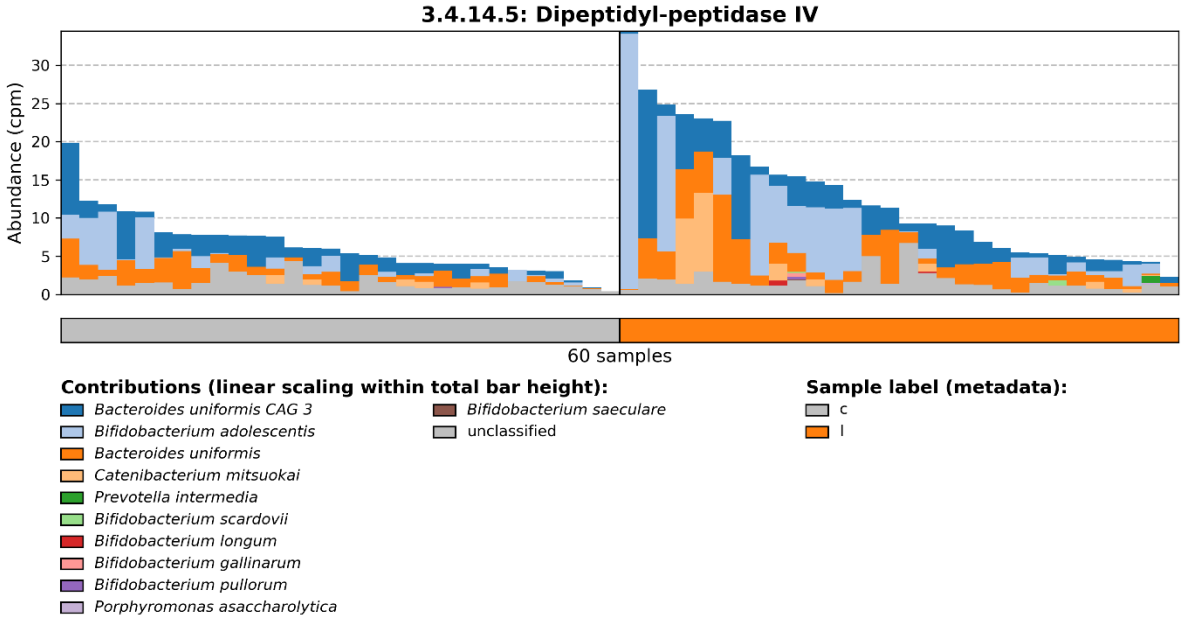
3.4.14.5: Dipeptidyl-peptidase IV
Abundance (cpm)
0
5
10
15
20
25
30
60 samples
Contributions (linear scaling within total bar height):
Bacteroides uniformis CAG 3
Bifidobacterium adolescentis
Bacteroides uniformis
Catenibacterium mitsuokai
Prevotella intermedia
Bifidobacterium scardovii
Bifidobacterium longum
Bifidobacterium gallinarum
Bifidobacterium pullorum
Porphyromonas asaccharolytica
Bifidobacterium saeculare
unclassified
Sample label (metadata):
c
l

3.5.1.18: Succinyl-diaminopimelate desuccinylase

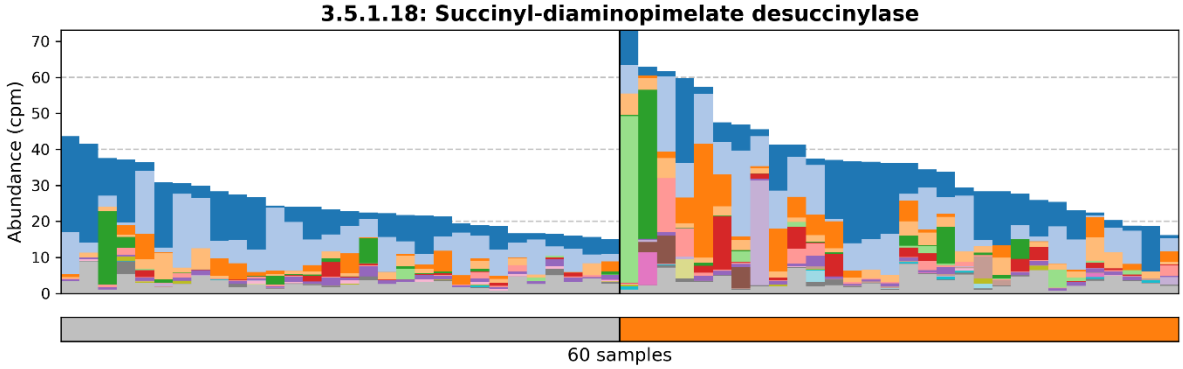

Contributions (linear scaling within total bar height):

- *Bacteroides*
- *Blautia*
- *Bifidobacterium*
- *Flavonifractor*
- *Escherichia*
- *Faecalitalea*
- *Ruminococcaceae unclassified*
- *Streptococcus*
- *Coprococcus*
- *Lactobacillus*
- *Pseudoflavonifractor*
- *Lachnoclostridium*
- *Klebsiella*
- *Parasutterella*
- *Proteobacteria unclassified*
- *Pediococcus*
- *Eisenbergiella*
- *Hungatella*
- other
- unclassified

Sample label (metadata):

- c
- l

3.5.1.18: Succinyl-diaminopimelate desuccinylase

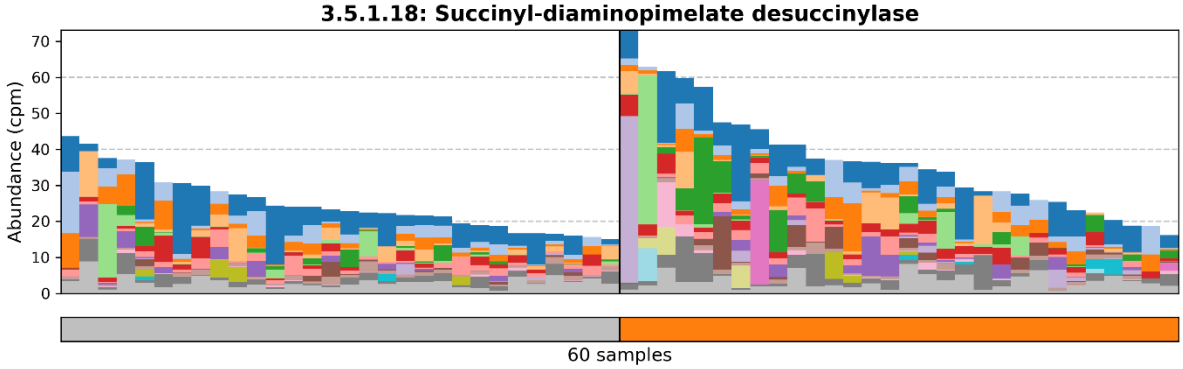

Contributions (linear scaling within total bar height):

- *Ruminococcus torques*
- *Bacteroides vulgatus CAG 6*
- *Bacteroides vulgatus*
- *Bacteroides dorei*
- *Bifidobacterium adolescentis*
- *Escherichia coli*
- *Flavonifractor plautii*
- *Blautia obeum*
- *Bacteroides massiliensis*
- *Faecalitalea cylindroides*
- *Eubacterium siraeum*
- *Coprococcus catus*
- *Lactobacillus reuteri*
- *Streptococcus salivarius*
- *Bifidobacterium pseudocatenulatum*
- *Pseudoflavonifractor capillosus*
- *Flavonifractor sp An10*
- *Klebsiella pneumoniae*
- other
- unclassified

Sample label (metadata):

- c
- l

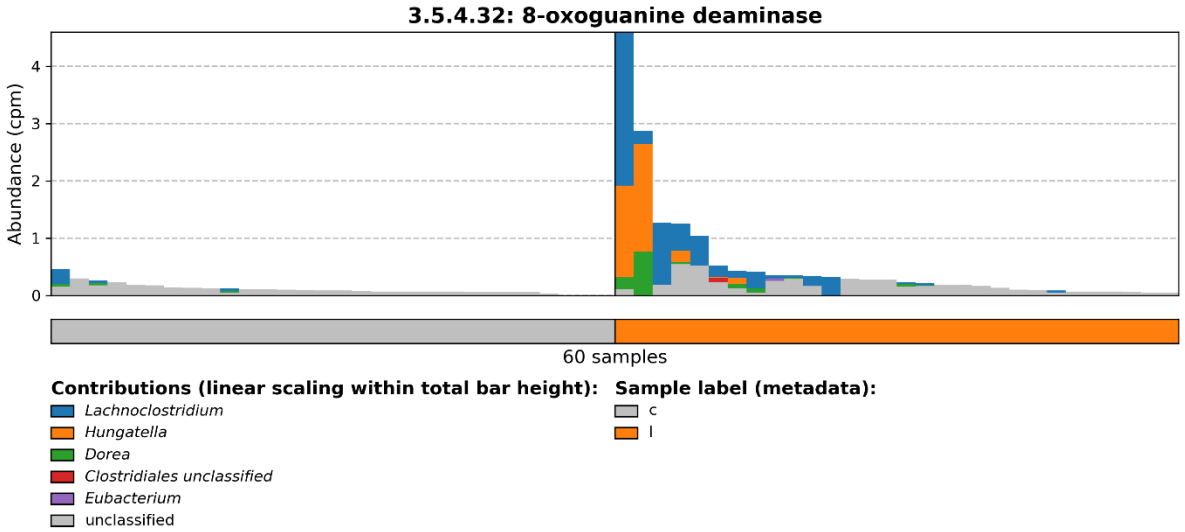
3.5.4.32: 8-oxoguanine deaminase
Abundance (cpm)
0
1
2
3
4
60 samples
Contributions (linear scaling within total bar height):
Lachnoclostridium
Hungatella
Dorea
Clostridiales unclassified
Eubacterium
unclassified
Sample label (metadata):
c
l

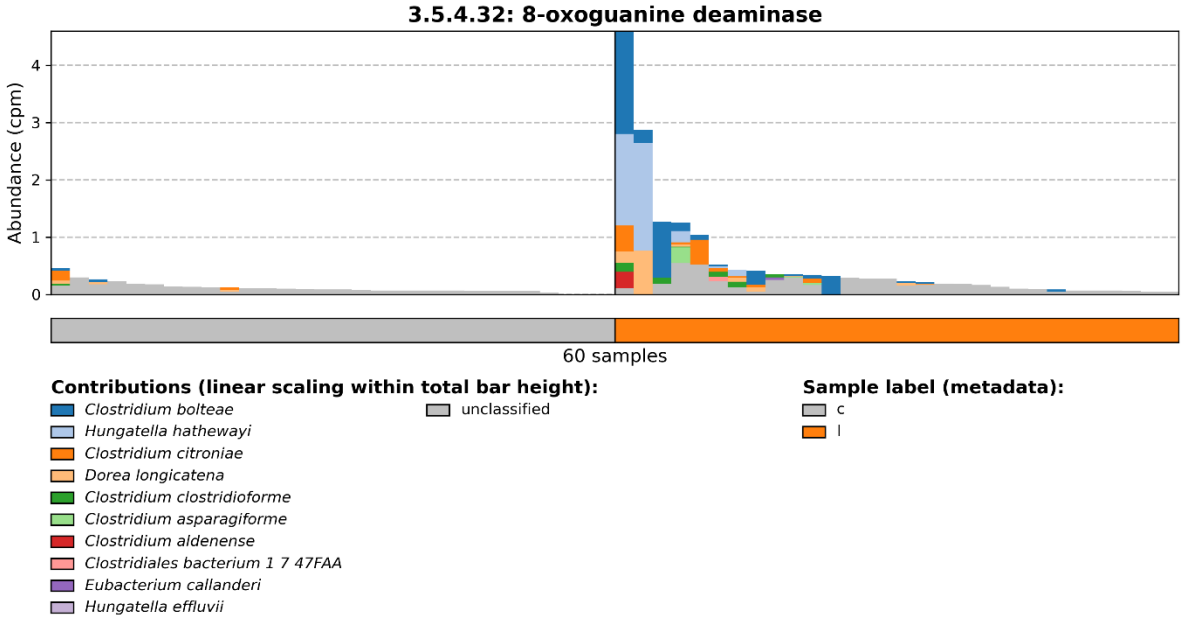
3.5.4.32: 8-oxoguanine deaminase
Abundance (cpm)
0
1
2
3
4
60 samples
Contributions (linear scaling within total bar height):
Clostridium bolteae
Hungatella hathewayi
Clostridium citroniae
Dorea longicatena
Clostridium clostridioforme
Clostridium asparagiforme
Clostridium aldenense
Clostridiales bacterium 1 7 47FAA
Eubacterium callanderi
Hungatella effluvii
unclassified
Sample label (metadata):
c
l

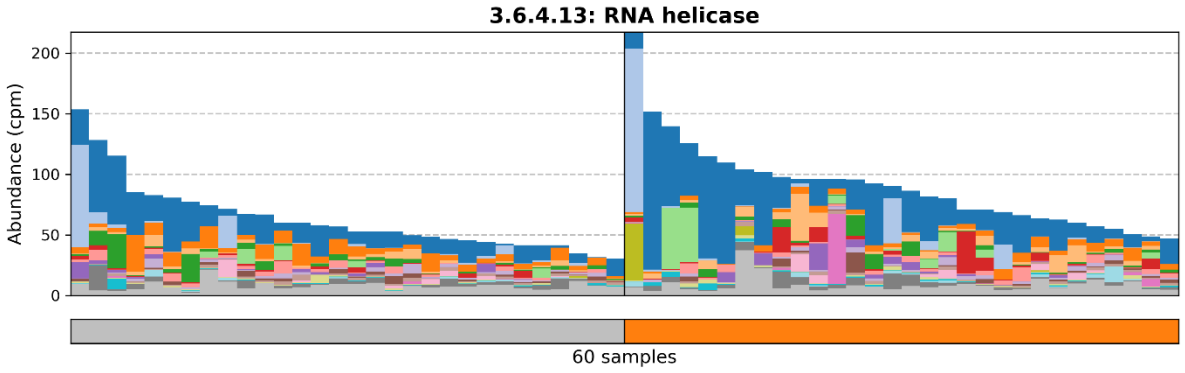

Contributions (linear scaling within total bar height):

- *Bacteroides*
- *Escherichia*
- *Eubacterium*
- *Bifidobacterium*
- *Lachnospiraceae unclassified*
- *Catenibacterium*
- *Streptococcus*
- *Roseburia*
- *Alistipes*
- *Dorea*
- *Blautia*
- *Coprococcus*
- *Lactobacillus*
- *Romboutsia*
- *Klebsiella*
- *Parabacteroides*
- *Flavonifractor*
- *Clostridium*
- other
- unclassified

Sample label (metadata):

- c
- l

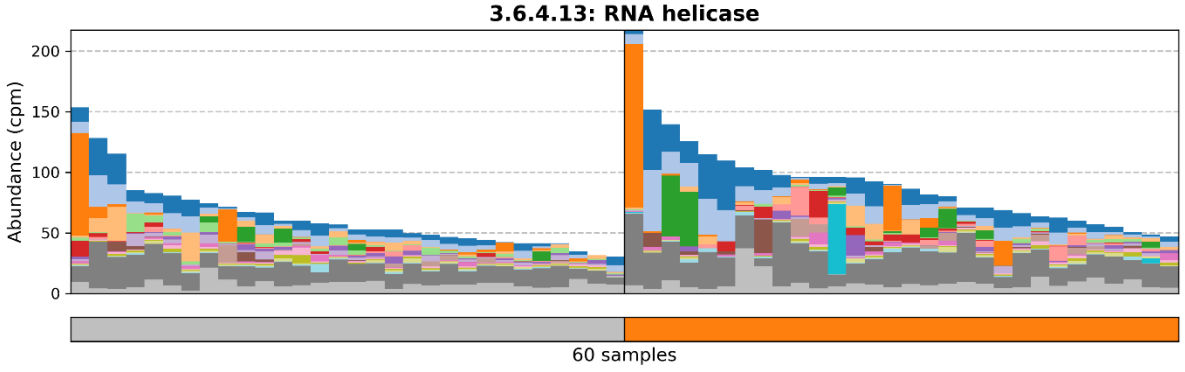

Contributions (linear scaling within total bar height):

- *Bacteroides uniformis*
- *Bacteroides uniformis CAG 3*
- *Escherichia coli*
- *Eubacterium rectale*
- *Catenibacterium mitsuokai*
- *Eubacterium eligens CAG 72*
- *Alistipes finegoldii*
- *Bifidobacterium adolescentis*
- *Ruminococcus torques*
- *Eubacterium eligens*
- *Bacteroides eggerthii*
- *Romboutsia ilealis*
- *Bacteroides thetaiotaomicron*
- *Eubacterium hallii*
- *Eubacterium hallii CAG 12*
- *Dorea longicatena CAG 42*
- *Lactobacillus reuteri*
- *Parabacteroides distasonis*
- other
- unclassified

Sample label (metadata):

- c
- l

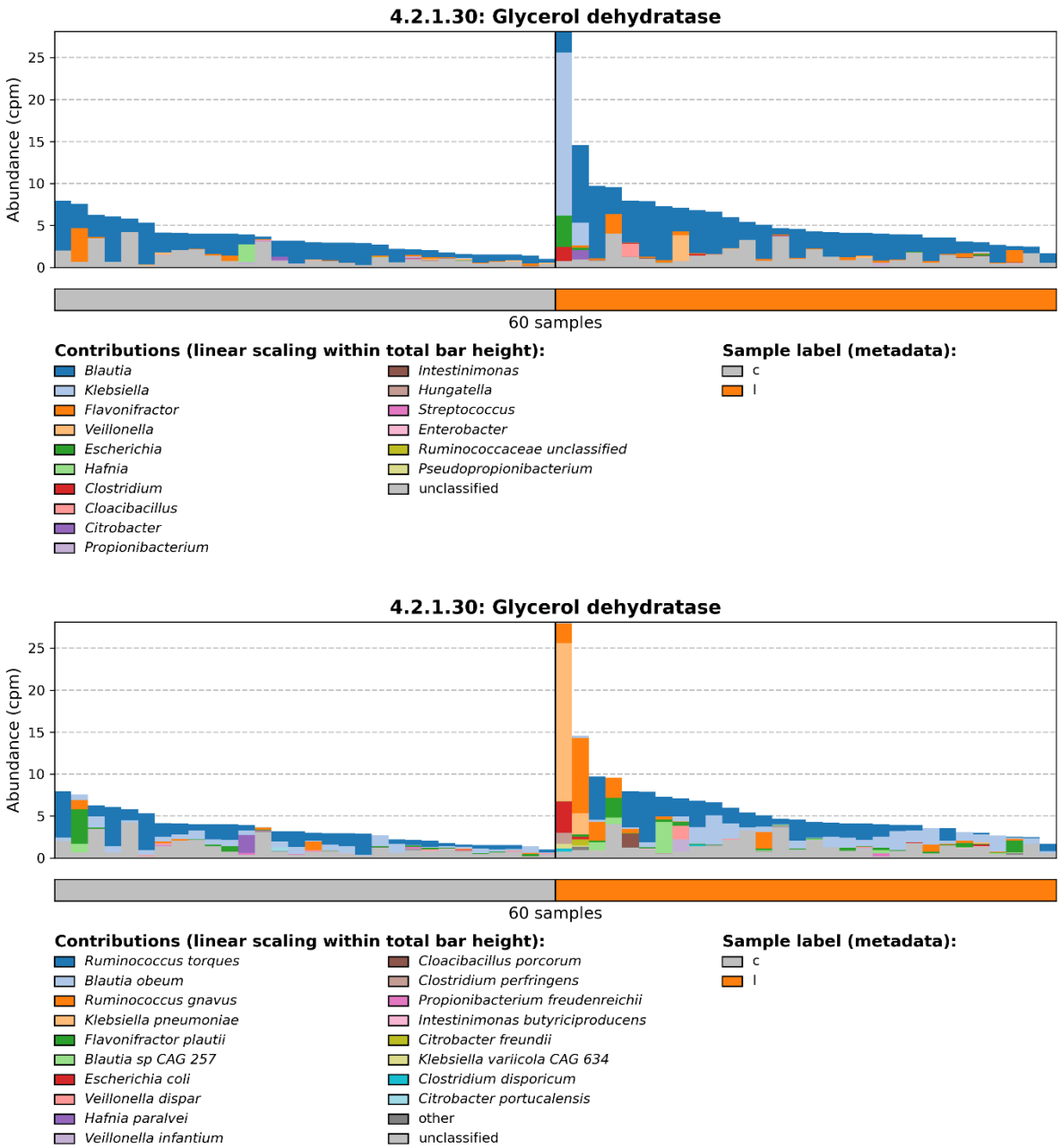
4.2.1.30: Glycerol dehydratase
Abundance (cpm)
25
20
15
10
5
0
60 samples
Contributions (linear scaling within total bar height):
Blautia
Klebsiella
Flavonifractor
Veillonella
Escherichia
Hafnia
Clostridium
Cloacibacillus
Citrobacter
Propionibacterium
Intestinimonas
Hungatella
Streptococcus
Enterobacter
Ruminococcaceae unclassified
Pseudopropionibacterium
unclassified
Sample label (metadata):
c
l

4.2.1.30: Glycerol dehydratase
Abundance (cpm)
25
20
15
10
5
0
60 samples
Contributions (linear scaling within total bar height):
Ruminococcus torques
Blautia obeum
Ruminococcus gnavus
Klebsiella pneumoniae
Flavonifractor plautii
Blautia sp CAG 257
Escherichia coli
Veillonella dispar
Hafnia paralvei
Veillonella infantium
Cloacibacillus porcorum
Clostridium perfringens
Propionibacterium freudenreichii
Intestinimonas butyriciproducens
Citrobacter freundii
Klebsiella variicola CAG 634
Clostridium disporicum
Citrobacter portucalensis
other
unclassified
Sample label (metadata):
c
l

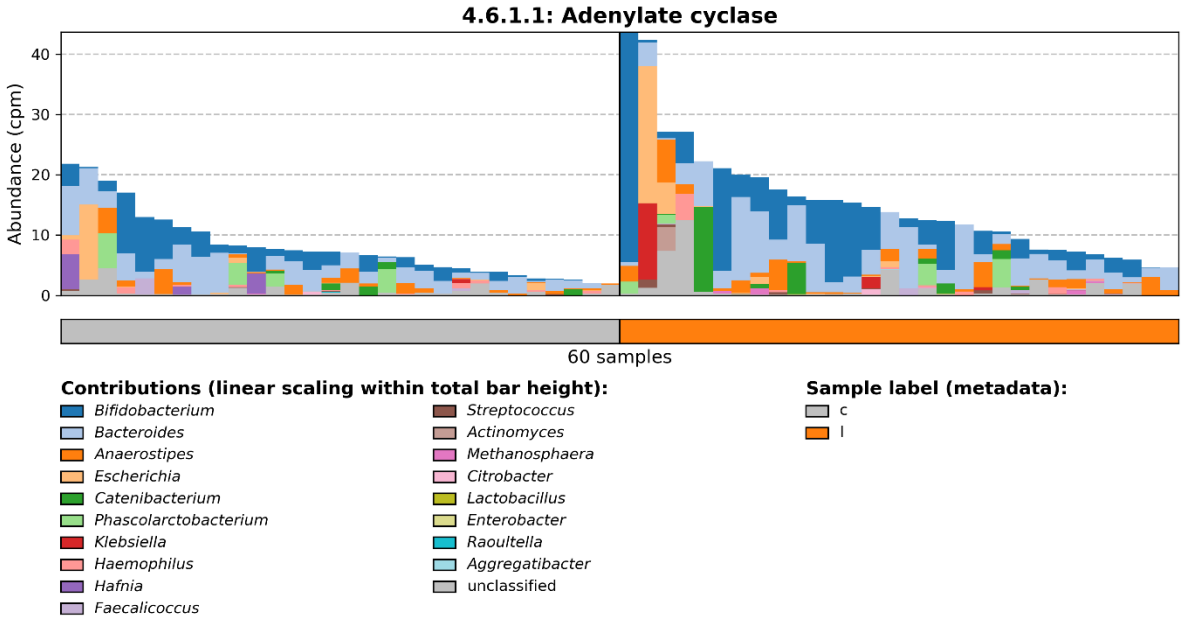
4.6.1.1: Adenylate cyclase
Abundance (cpm)
0
10
20
30
40
60 samples
Contributions (linear scaling within total bar height):
Bifidobacterium
Bacteroides
Anaerostipes
Escherichia
Catenibacterium
Phascolarctobacterium
Klebsiella
Haemophilus
Hafnia
Faecalicoccus
Streptococcus
Actinomyces
Methanosphaera
Citrobacter
Lactobacillus
Enterobacter
Raoultella
Aggregatibacter
unclassified
Sample label (metadata):
c
l

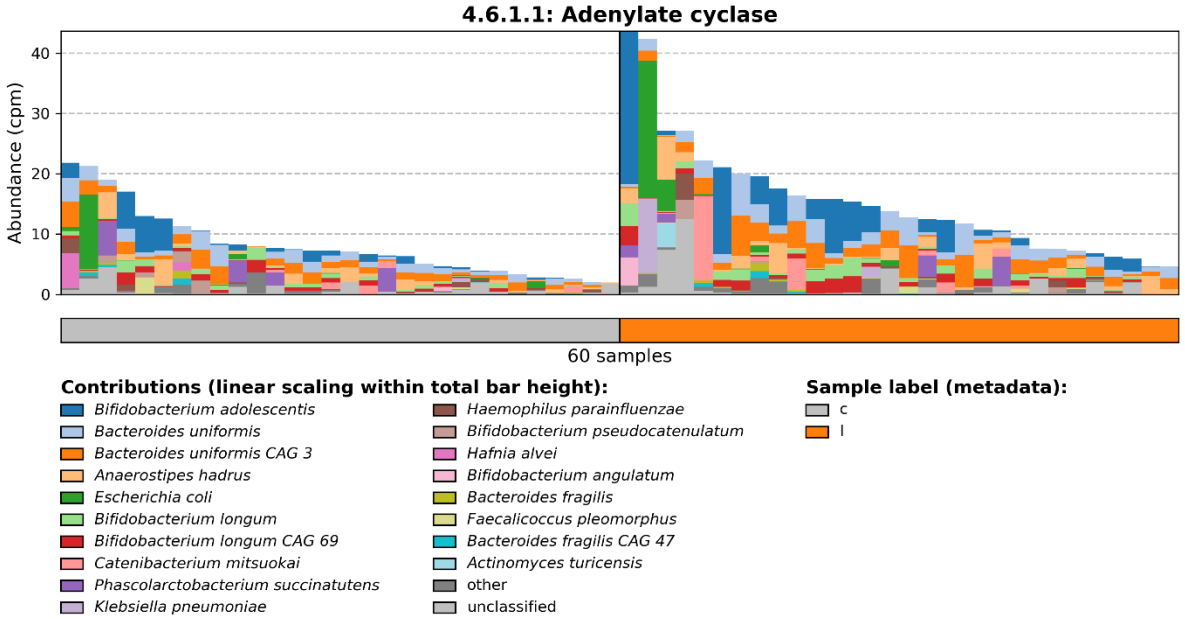
4.6.1.1: Adenylate cyclase
Abundance (cpm)
0
10
20
30
40
60 samples
Contributions (linear scaling within total bar height):
Bifidobacterium adolescentis
Bacteroides uniformis
Bacteroides uniformis CAG 3
Anaerostipes hadrus
Escherichia coli
Bifidobacterium longum
Bifidobacterium longum CAG 69
Catenibacterium mitsuokai
Phascolarctobacterium succinatutens
Klebsiella pneumoniae
Haemophilus parainfluenzae
Bifidobacterium pseudocatenulatum
Hafnia alvei
Bifidobacterium angulatum
Bacteroides fragilis
Faecalicoccus pleomorphus
Bacteroides fragilis CAG 47
Actinomyces turicensis
other
unclassified
Sample label (metadata):
c
l

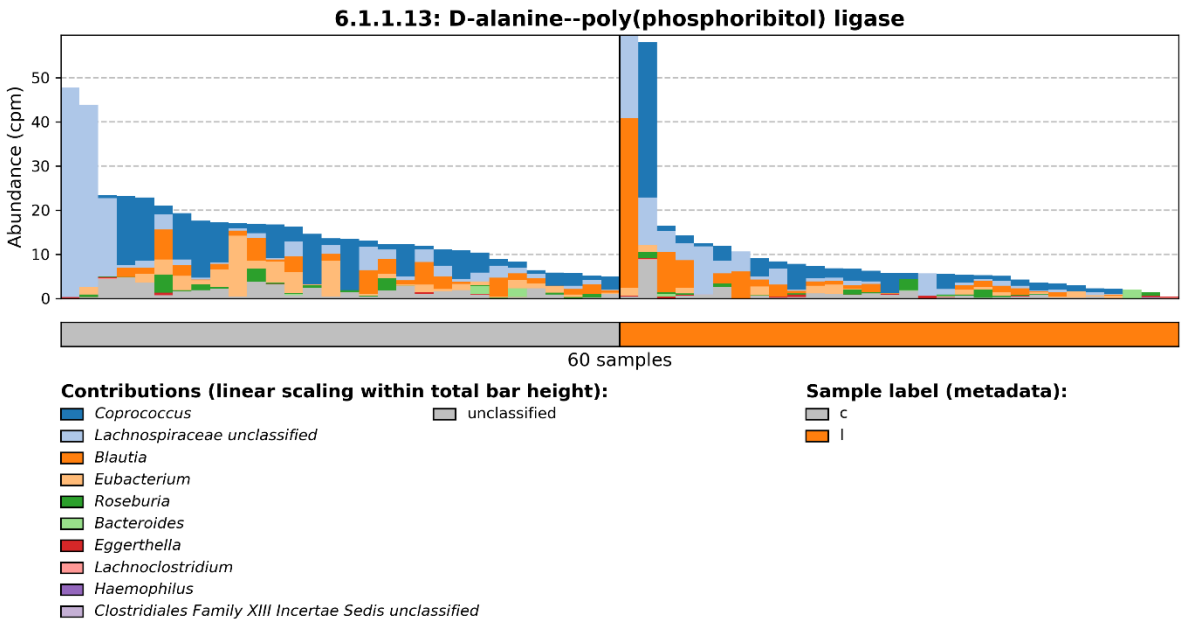
6.1.1.13: D-alanine--poly(phosphoribitol) ligase
Abundance (cpm)
0
10
20
30
40
50
60 samples
Contributions (linear scaling within total bar height):
Coprococcus
Lachnospiraceae unclassified
Blautia
Eubacterium
Roseburia
Bacteroides
Eggerthella
Lachnoclostridium
Haemophilus
Clostridiales Family XIII Incertae Sedis unclassified
unclassified
Sample label (metadata):
c
l

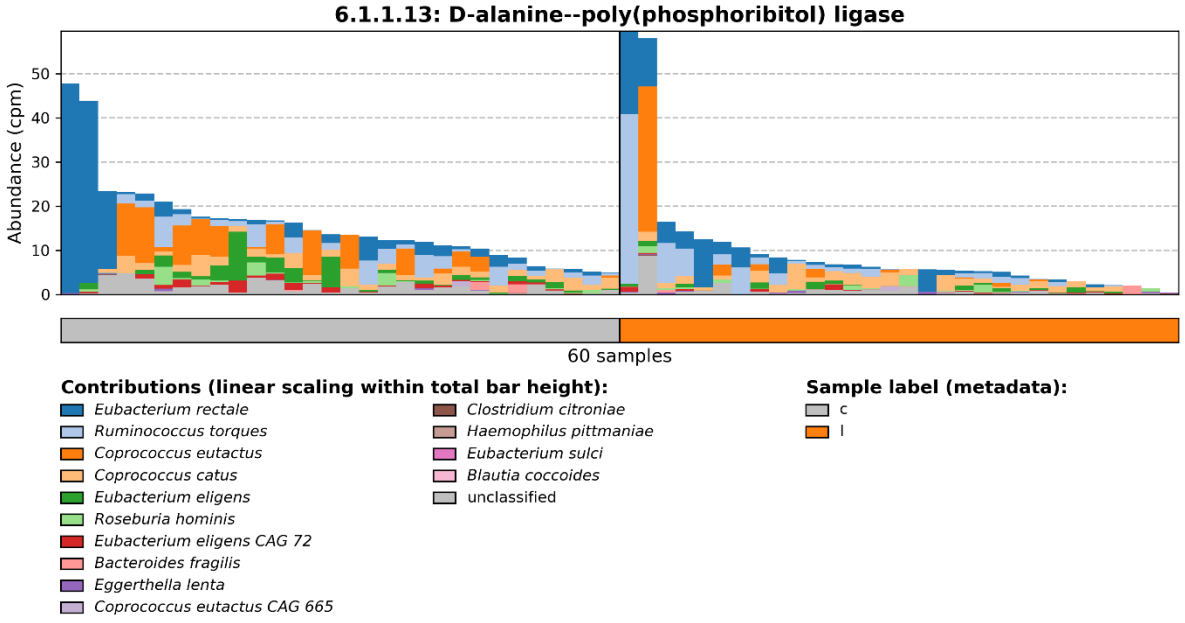
6.1.1.13: D-alanine--poly(phosphoribitol) ligase
Abundance (cpm)
0
10
20
30
40
50
60 samples
Contributions (linear scaling within total bar height):
Eubacterium rectale
Ruminococcus torques
Coprococcus eutactus
Coprococcus catus
Eubacterium eligens
Roseburia hominis
Eubacterium eligens CAG 72
Bacteroides fragilis
Eggerthella lenta
Coprococcus eutactus CAG 665
Clostridium citroniae
Haemophilus pittmaniae
Eubacterium sulci
Blautia coccoides
unclassified
Sample label (metadata):
c
l

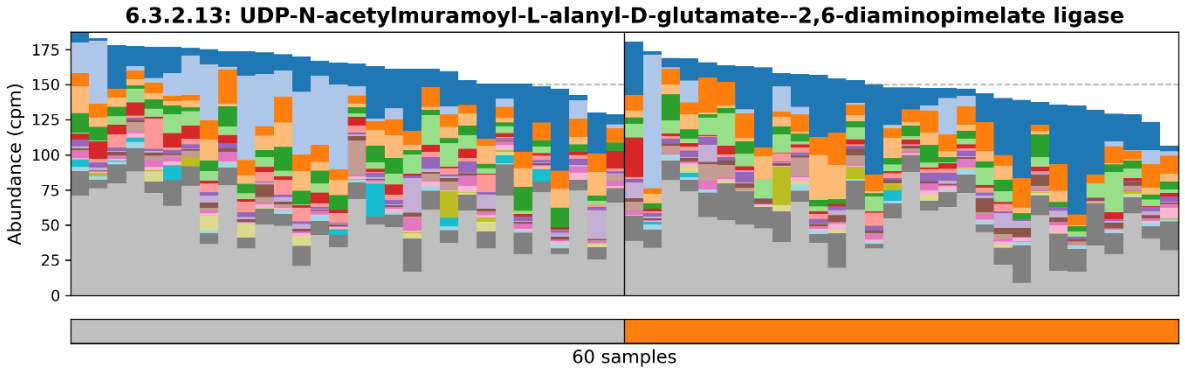

Contributions (linear scaling within total bar height):

- *Bacteroides*
- *Prevotella*
- *Blautia*
- *Roseburia*
- *Eubacterium*
- *Alistipes*
- *Coprococcus*
- *Ruminococcus*
- *Dorea*
- *Lachnospiraceae unclassified*
- *Parabacteroides*
- *Akkermansia*
- *Anaerostipes*
- *Fusicatenibacter*
- *Escherichia*
- *Dialister*
- *Butyrivibrio*
- *Phascolarctobacterium*
- other
- unclassified

Sample label (metadata):

- c
- l

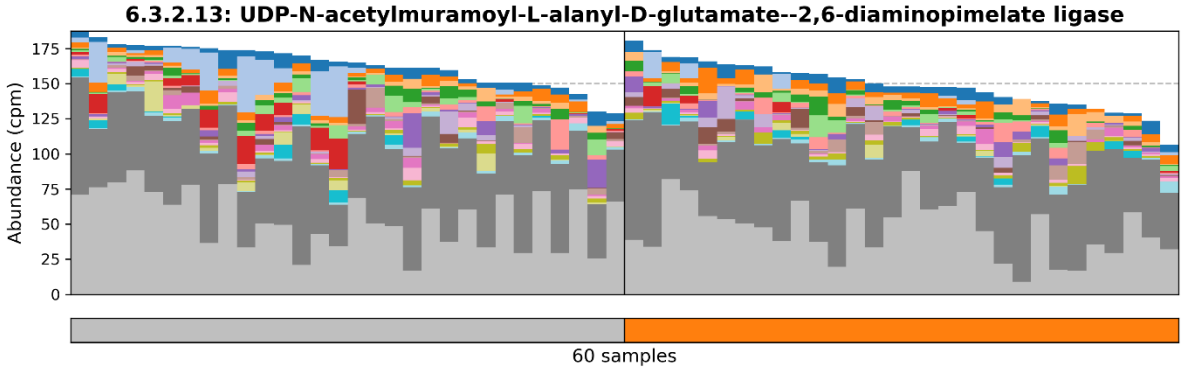

Contributions (linear scaling within total bar height):

- *Blautia obeum*
- *Prevotella copri CAG 164*
- *Ruminococcus torques*
- *Bacteroides uniformis*
- *Bacteroides vulgatus CAG 6*
- *Roseburia faecis*
- *Prevotella copri*
- *Bacteroides vulgatus*
- *Eubacterium rectale*
- *Alistipes finegoldii*
- *Akkermansia muciniphila*
- *Bacteroides dorei*
- *Alistipes putredinis*
- *Anaerostipes hadrus*
- *Bacteroides uniformis CAG 3*
- *Ruminococcus bicirculans*
- *Eubacterium sp CAG 180*
- *Fusicatenibacter saccharivorans*
- other
- unclassified

Sample label (metadata):

- c
- l

A

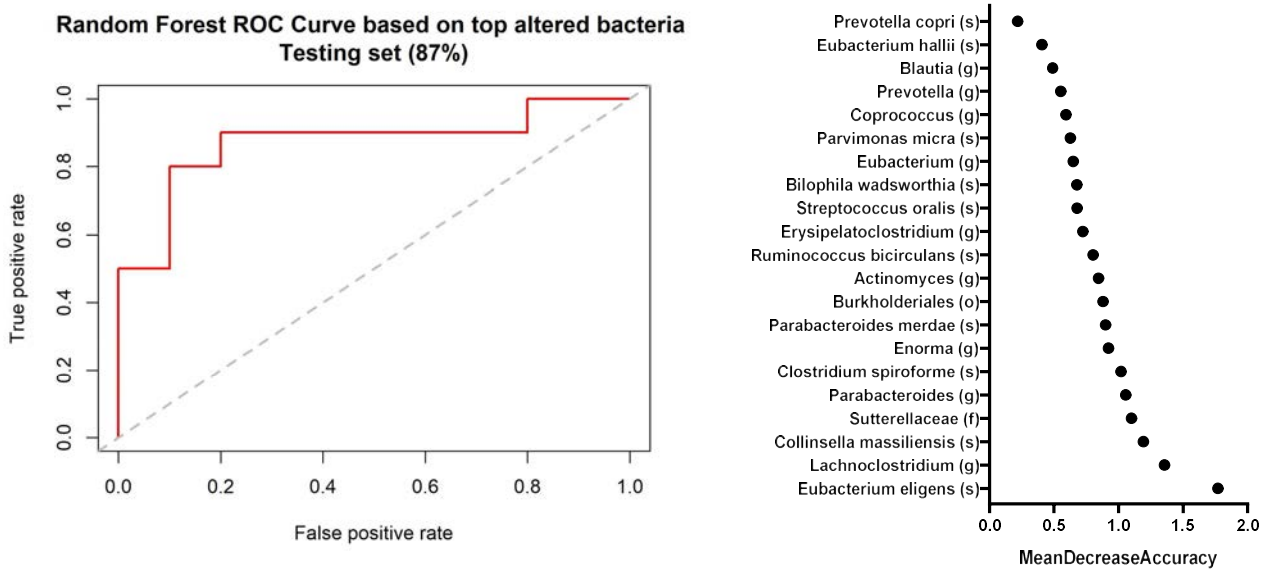

B

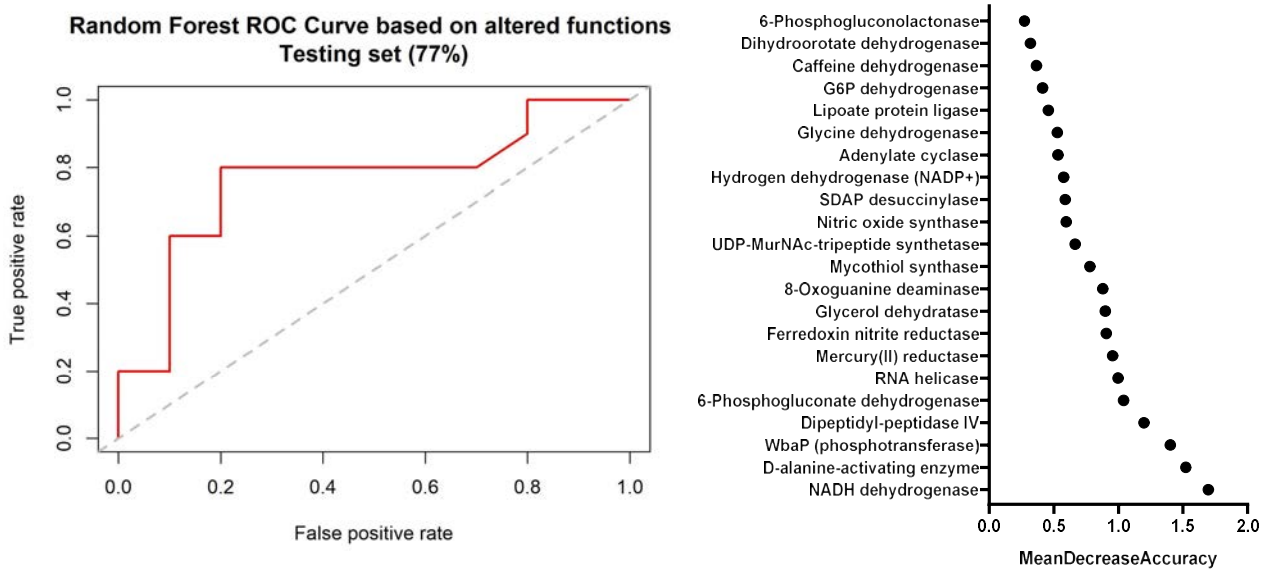

Figure S5. Bacterial taxa and functional signatures identified in AML patients.

A) RandomForest model ROC curve based on the top altered bacteria to predict AML status.

B) RandomForest model ROC curve based on altered EC enzyme functions to predict AML status.

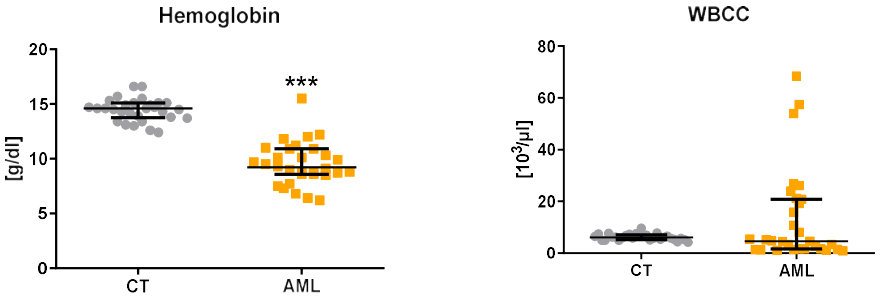

Figure S6. Confirmation of hemoglobin and white blood cell count alteration in AML patients.
Hemoglobin and WBCC (white blood cell count).
Variables are non-normally distributed and are expressed as median (interquartile range) and are tested by a Mann-Whitney U-test. AML in orange *vs.* CT in grey.
*** : p-value < 0.001

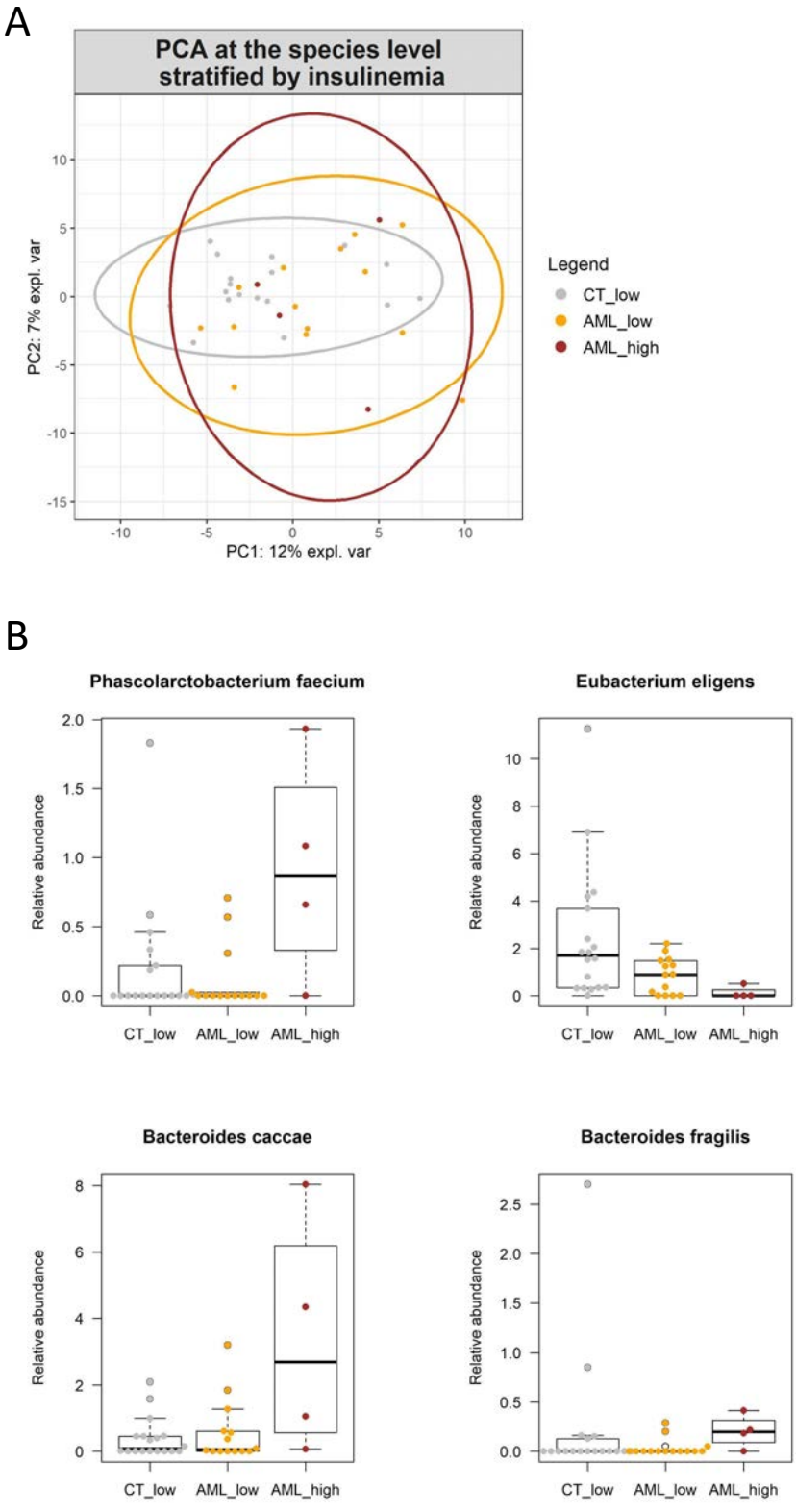

Figure S7. Alterations in the gut microbiota composition in AML patients with high insulinemia (results of metagenomics sequencing).

A) PCA analyses on CLR-transformed data at the species level, stratified by insulinemia and disease (CT low/AML low/ AML high). Insulinemia class does not explain a significant part of the variance in the dataset (PERMANOVA ns). B) 4 species were significantly different between individuals with low versus high insulinemia levels (pvalue<0.05, qvalue ns).

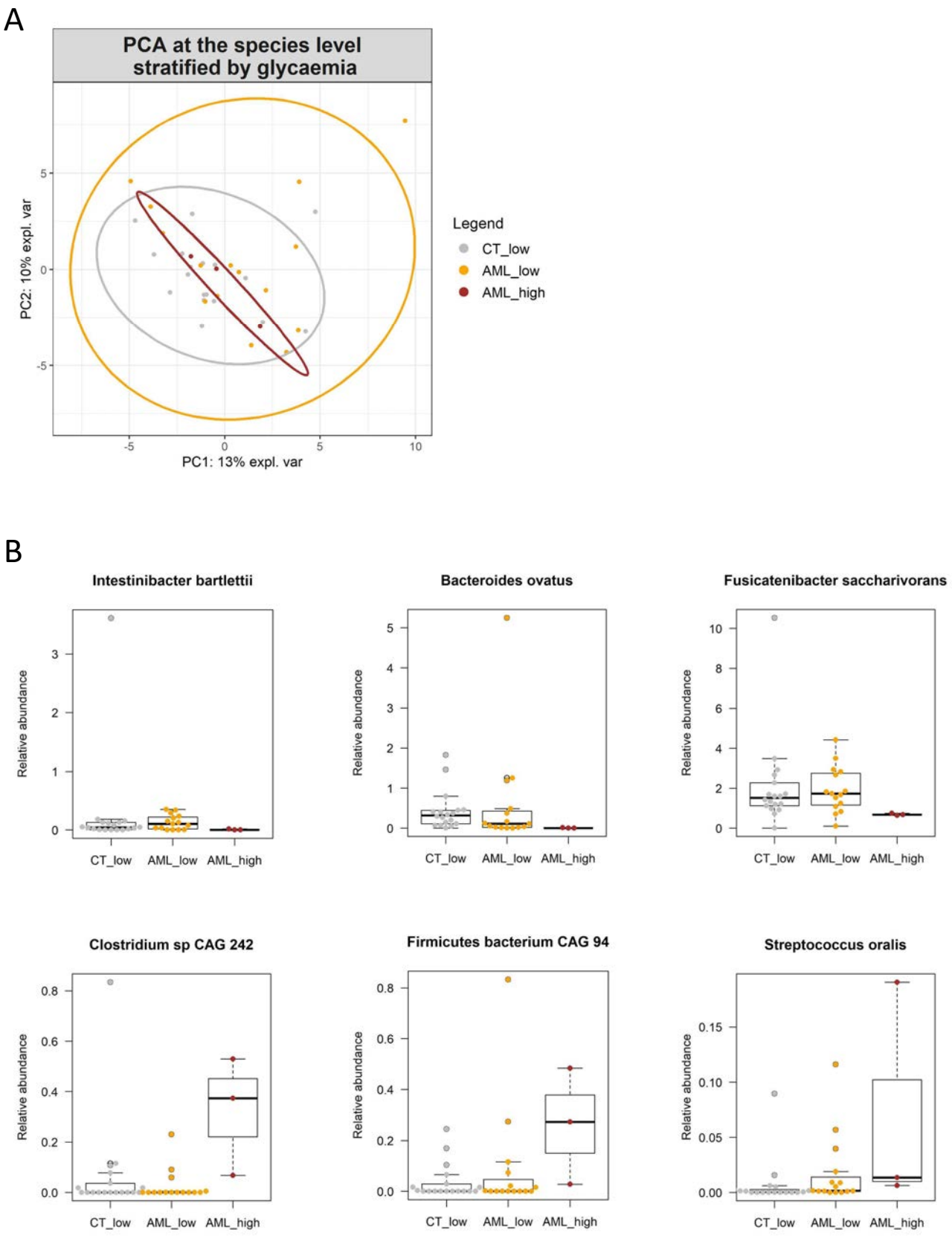

Figure S8. Alterations in the gut microbiota composition in AML patients with high glycaemia (results of metagenomics sequencing).

A) PCA analyses on CLR-transformed data at the species level, stratified by glycaemia and disease (CT low/AML low/ AML high). Glycaemia class does not explain a significant part of the variance in the dataset (PERMANOVA ns). B) 6 species were significantly different between individuals with low versus high glycemia levels (pvalue<0.05, qvalue ns).

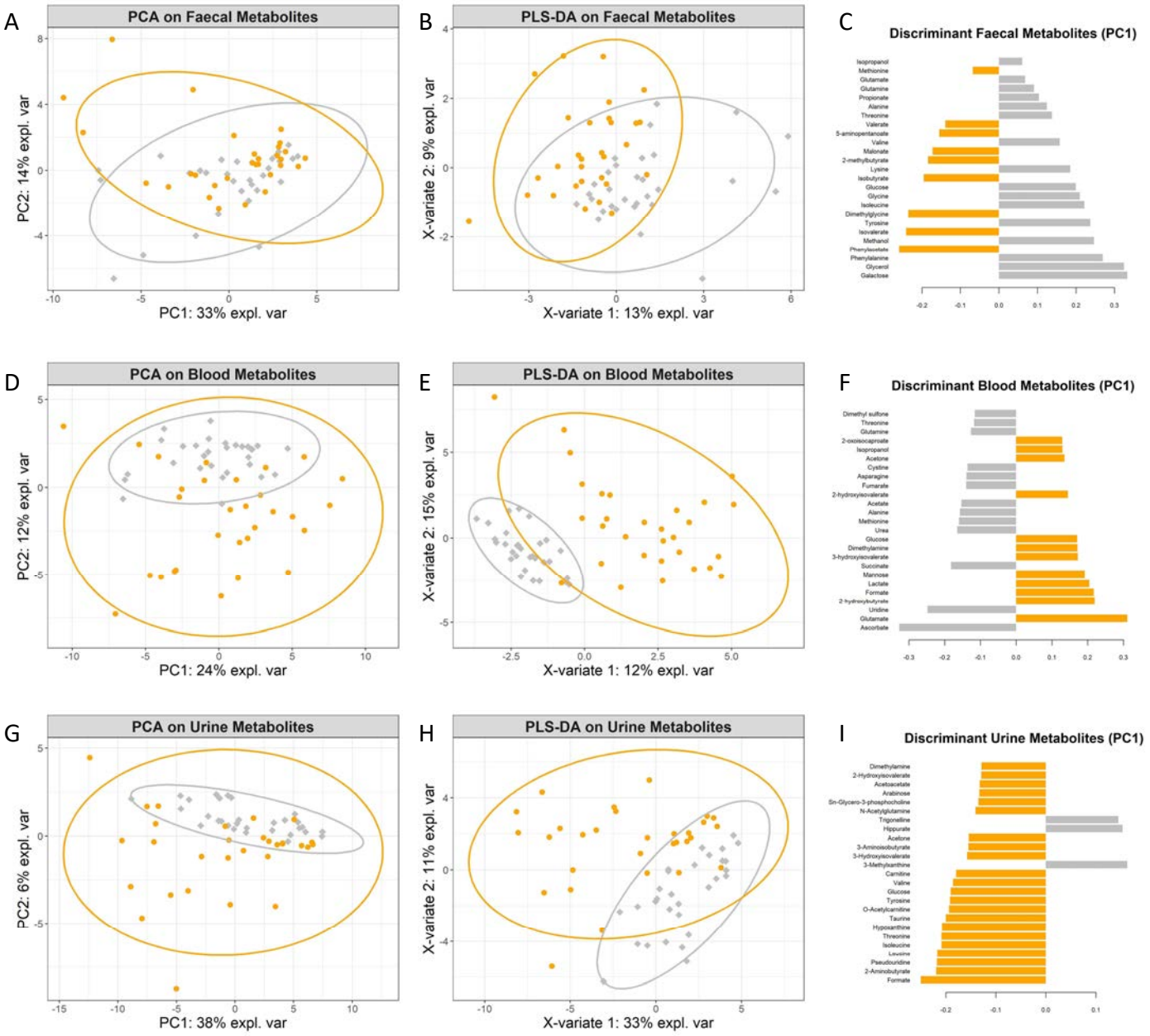

Figure S9. Multivariate analyses on faecal, blood and urine metabolites pinpoint differences between AML and CT subjects.

Principal component analyses (PCA), partial least square discriminant analyses (PLS-DA) and first 25 loadings of the PLS-DA for faecal (A-C), blood (D-F) and urine (G-I) metabolites (first principal component). A) PERMANOVA: R2 = 0.2% ns. D) PERMANOVA: R2 = 11.2% ** G) PERMANOVA R2 = 2.9% *. AML in orange vs. CT in grey. *p-value < 0.05; **p-value < 0.01.

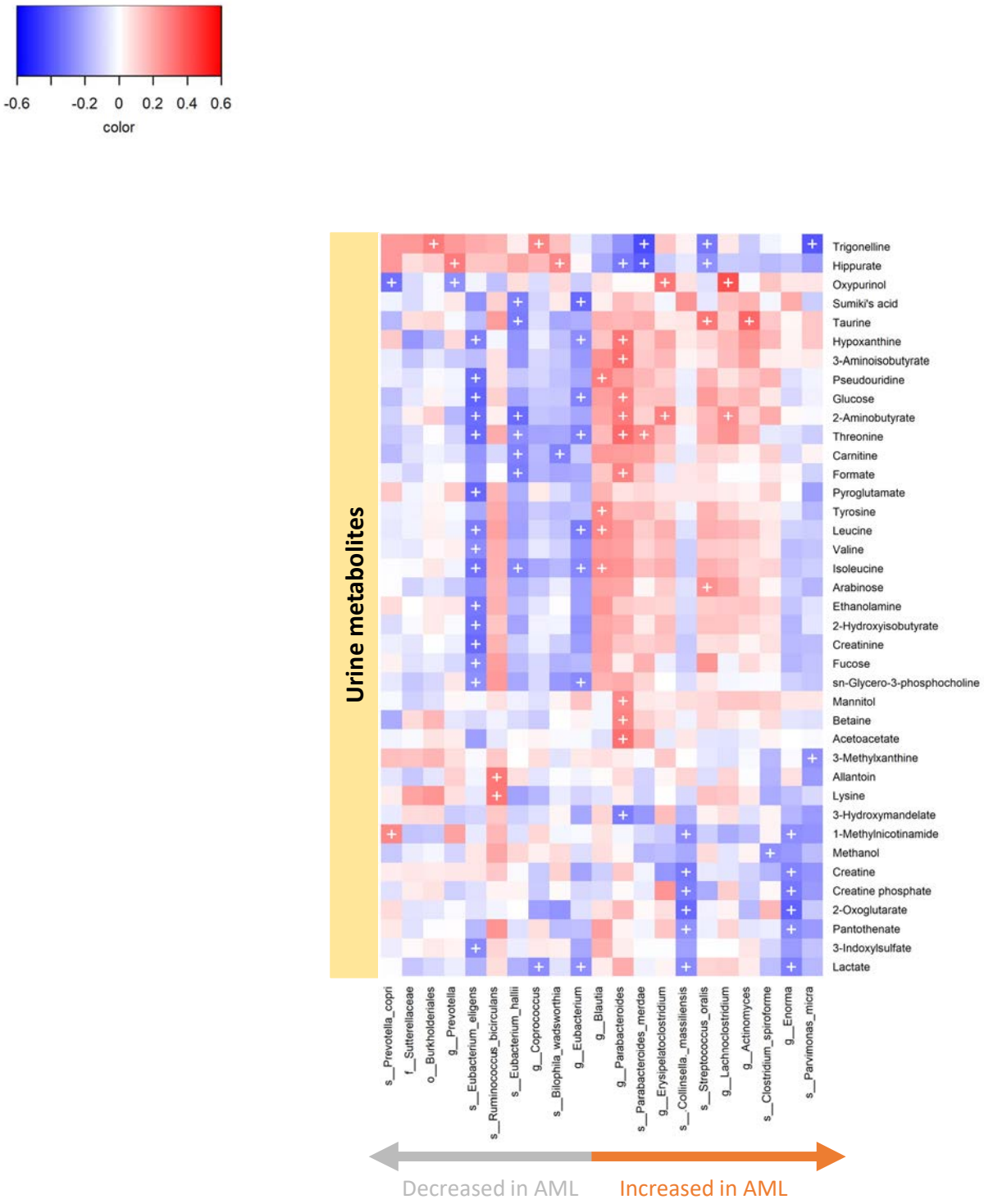

Figure S10. Correlations between urine metabolites and the top altered bacteria.
Spearman correlations. Metabolites with at least one correlation with an altered taxon are present. Microbial taxa are ordered by fold change. '+' symbolizes a p-value < 0.05 and '*' symbolizes an FDR-corrected q-value < 0.1.

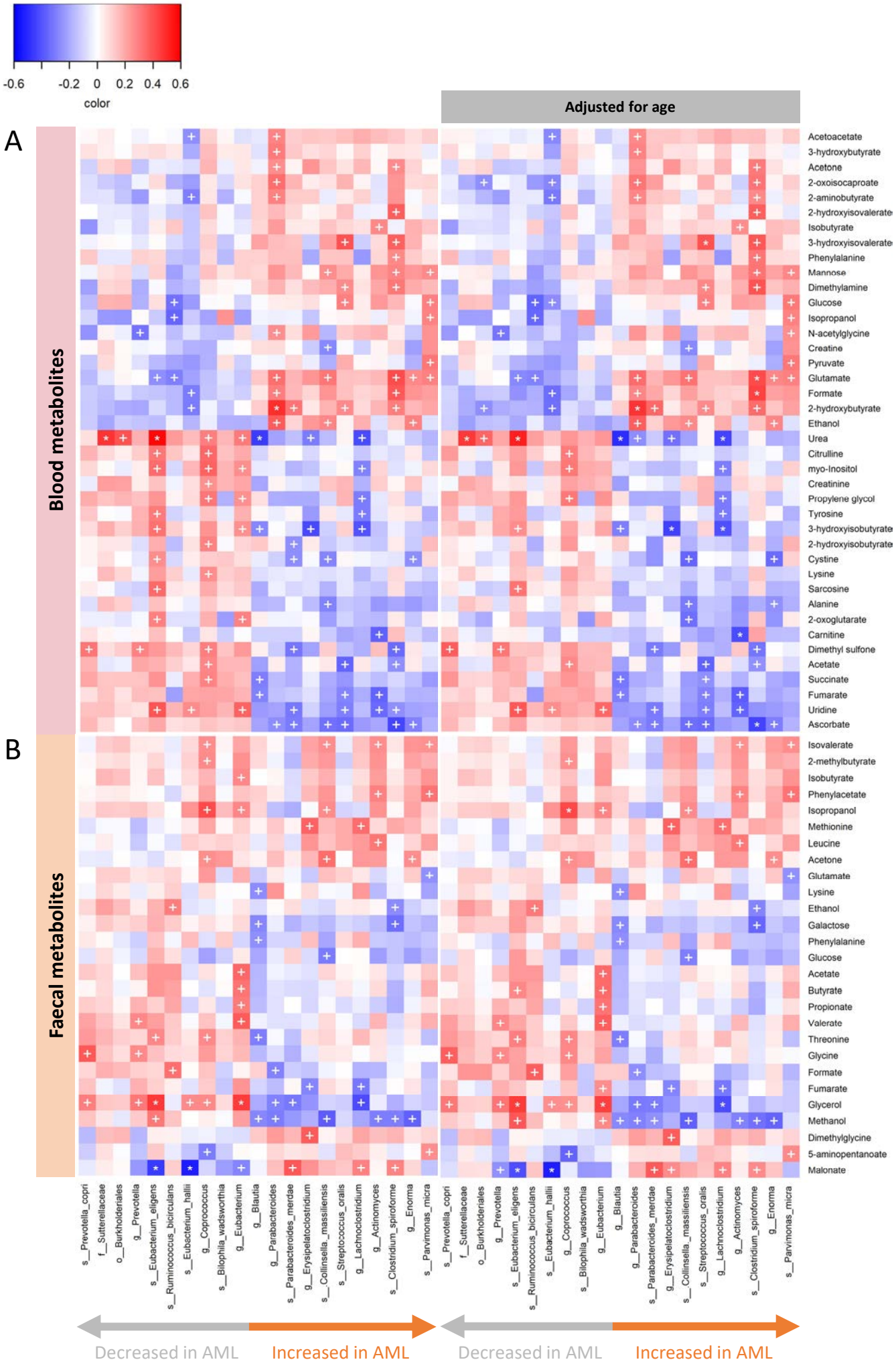
-0.6
-0.2
0
0.2
0.4
0.6
color
Adjusted for age
A
Blood metabolites
Acetoacetate
3-hydroxybutyrate
Acetone
2-oxoisocaproate
2-aminobutyrate
2-hydroxyisovalerate
Isobutyrate
3-hydroxyisovalerate
Phenylalanine
Mannose
Dimethylamine
Glucose
Isopropanol
N-acetylglycine
Creatine
Pyruvate
Glutamate
Formate
2-hydroxybutyrate
Ethanol
Urea
Citrulline
myo-Inositol
Creatinine
Propylene glycol
Tyrosine
3-hydroxyisobutyrate
2-hydroxyisobutyrate
Cystine
Lysine
Sarcosine
Alanine
2-oxoglutarate
Carnitine
Dimethyl sulfone
Acetate
Succinate
Fumarate
Uridine
Ascorbate
B
Faecal metabolites
Isovalerate
2-methylbutyrate
Isobutyrate
Phenylacetate
Isopropanol
Methionine
Leucine
Acetone
Glutamate
Lysine
Ethanol
Galactose
Phenylalanine
Glucose
Acetate
Butyrate
Propionate
Valerate
Threonine
Glycine
Formate
Fumarate
Glycerol
Methanol
Dimethylglycine
5-aminopentanoate
Malonate
s__Prevotella_copri
f__Sutterellaceae
o__Burkholderiales
g__Prevotella
s__Eubacterium_eligens
s__Ruminococcus_bicirculans
s__Eubacterium_hallii
g__Coprococcus
s__Bilophila_wadsworthia
g__Eubacterium
g__Blautia
g__Parabacteroides
s__Parabacteroides_merdae
g__Erysipelatoclostridium
s__Collinsella_massiliensis
s__Streptococcus_oralis
g__Lachnoclostridium
g__Actinomyces
s__Clostridium_spiroforme
g__Enorma
s__Parvimonas_micra
Decreased in AML
Increased in AML
Decreased in AML
Increased in AML

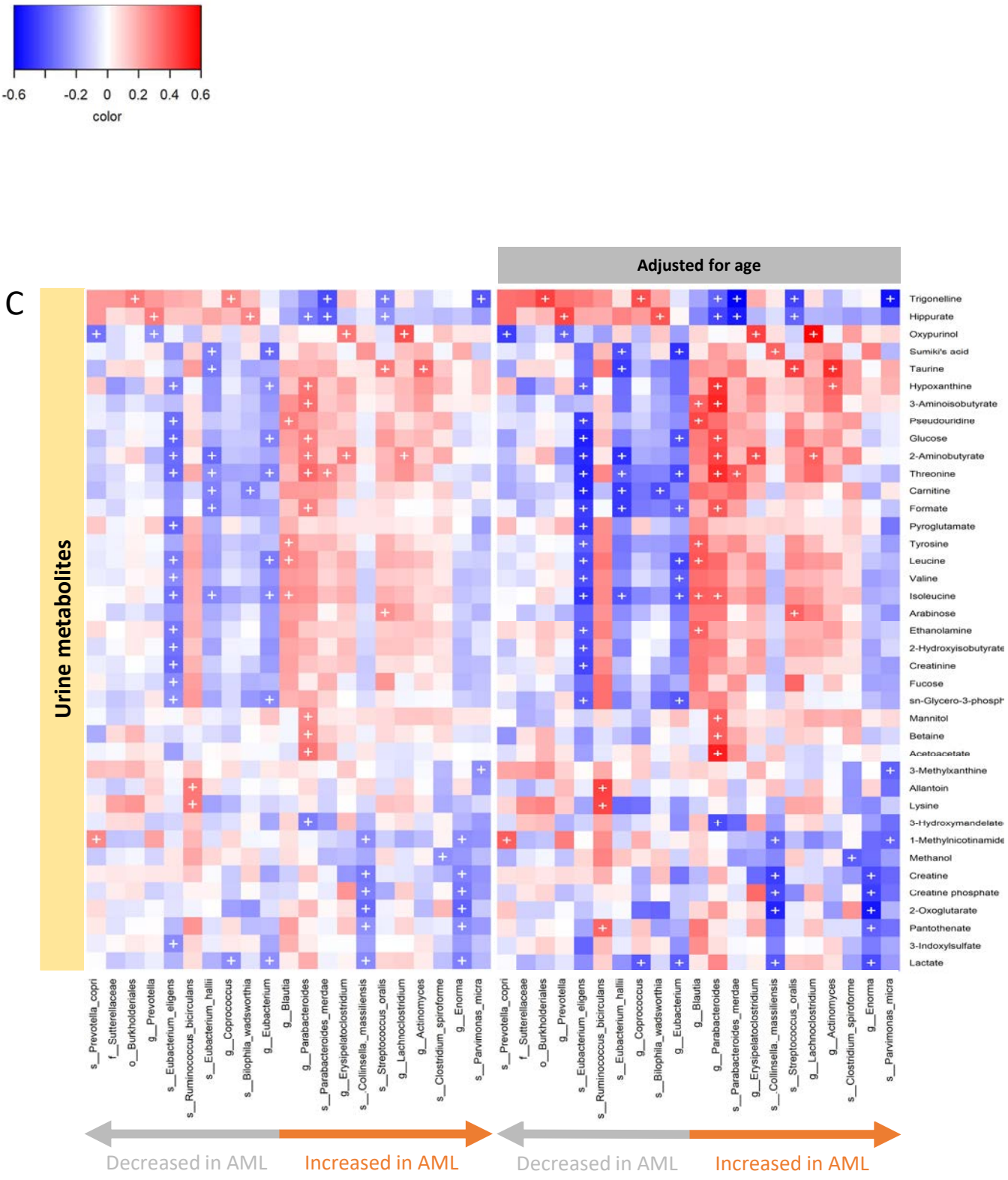

Figure S11. Correlations between blood, faecal and urine metabolites and the top altered bacteria. Spearman correlations (left) and partial Spearman rank-based correlations (pSRBC) adjusted for age (right) for the whole cohort (AML group and CT group). Metabolites with at least one correlation with an altered taxon are present. '+' symbolizes a p-value < 0.05 and '*' symbolizes an FDR-corrected q-value < 0.1. A) Correlations between blood metabolites and top altered bacteria. B) Correlations between faecal metabolites and top altered bacteria. C) Correlations between urine metabolites and top altered bacteria.

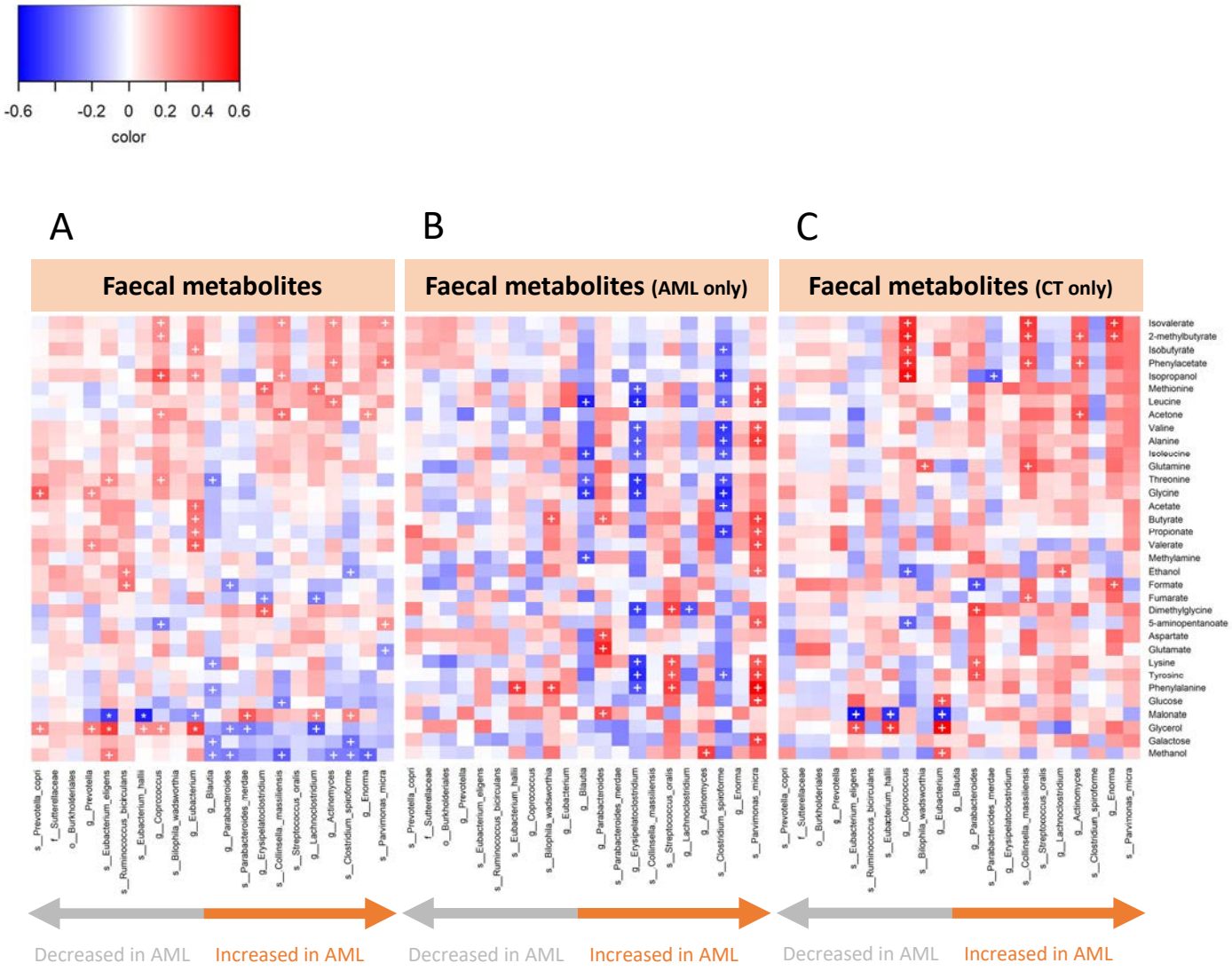

Figure S12. Correlations between faecal metabolites and the top altered bacteria.
Spearman correlations. All identified metabolites are present. Microbial taxa are ordered by fold change in the whole dataset. '+' symbolizes a p-value < 0.05 and '*' symbolizes an FDR-corrected q-value < 0.1. A) Spearman correlations within the whole cohort, both acute myeloid leukaemia group (AML group) and the healthy control group (CT group). B) Spearman correlations within the acute myeloid leukaemia group (AML group). C) Spearman correlations within the healthy control group (CT group).

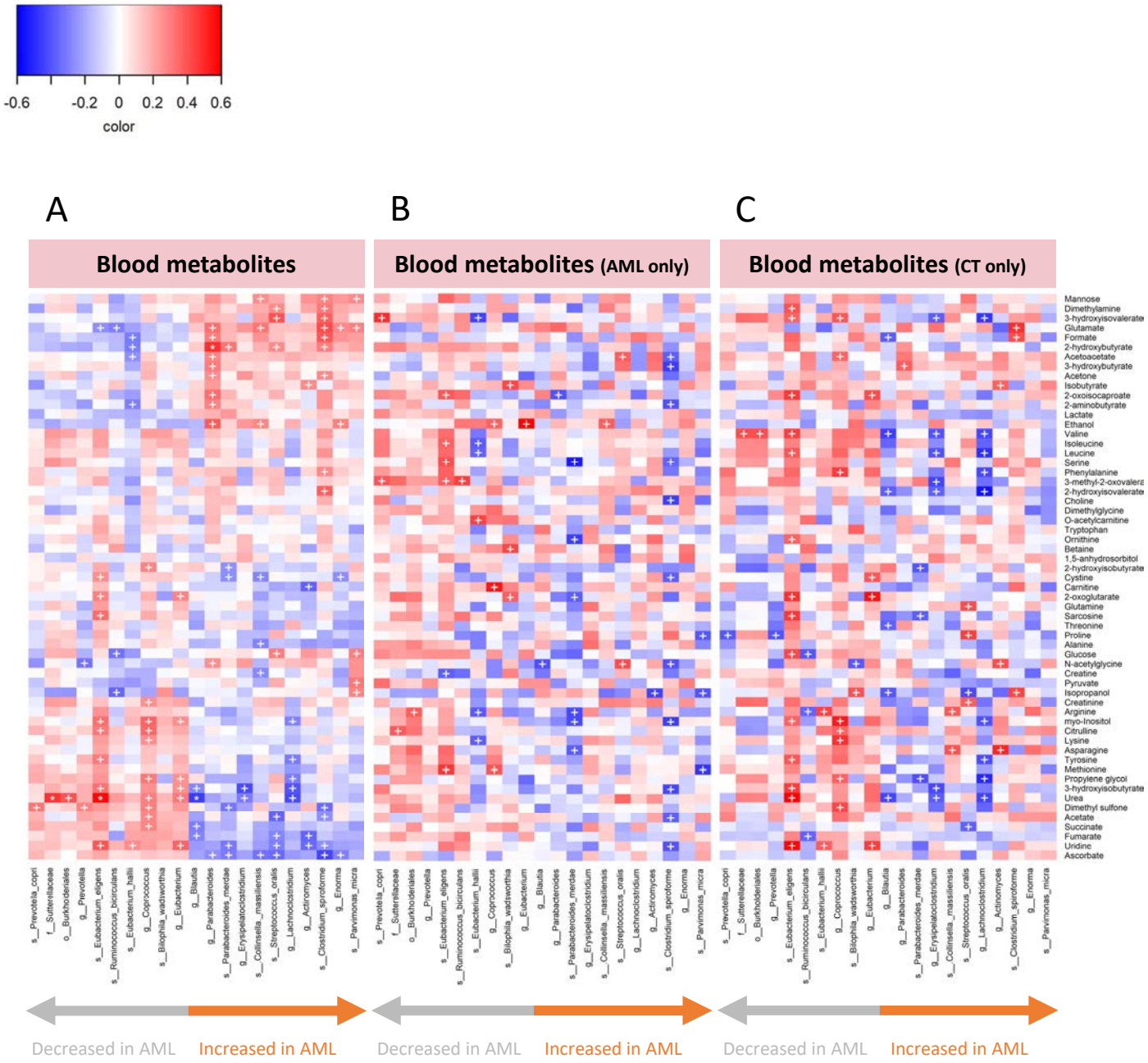

Figure S13. Correlations between blood metabolites and the top altered bacteria.
Spearman correlations. All identified metabolites are present. Microbial taxa are ordered by fold change in the whole dataset. '+' symbolizes a p-value < 0.05 and '*' symbolizes an FDR-corrected q-value < 0.1. A) Spearman correlations within the whole cohort, both acute myeloid leukaemia group (AML group) and the healthy control group (CT group). B) Spearman correlations within the acute myeloid leukaemia group (AML group). C) Spearman correlations within the healthy control group (CT group).

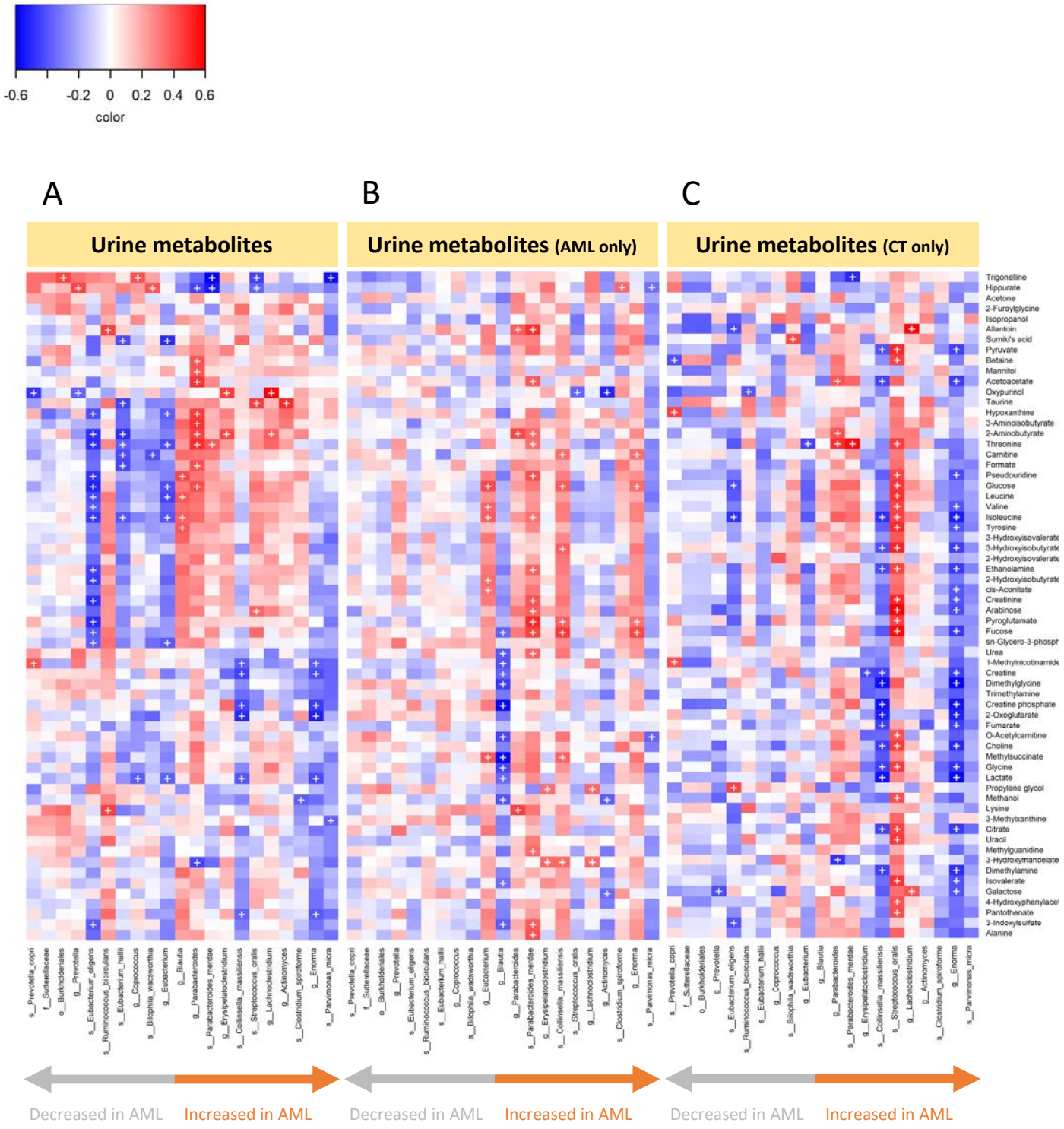

Figure S14. Correlations between urine metabolites and the top altered bacteria.
Spearman correlations. All identified metabolites are present. Microbial taxa are ordered by fold change in the whole dataset. '+' symbolizes a p-value < 0.05 and '*' symbolizes an FDR-corrected q-value < 0.1. A) Spearman correlations within the whole cohort, both acute myeloid leukaemia group (AML group) and the healthy control group (CT group). B) Spearman correlations within the acute myeloid leukaemia group (AML group). C) Spearman correlations within the healthy control group (CT group).

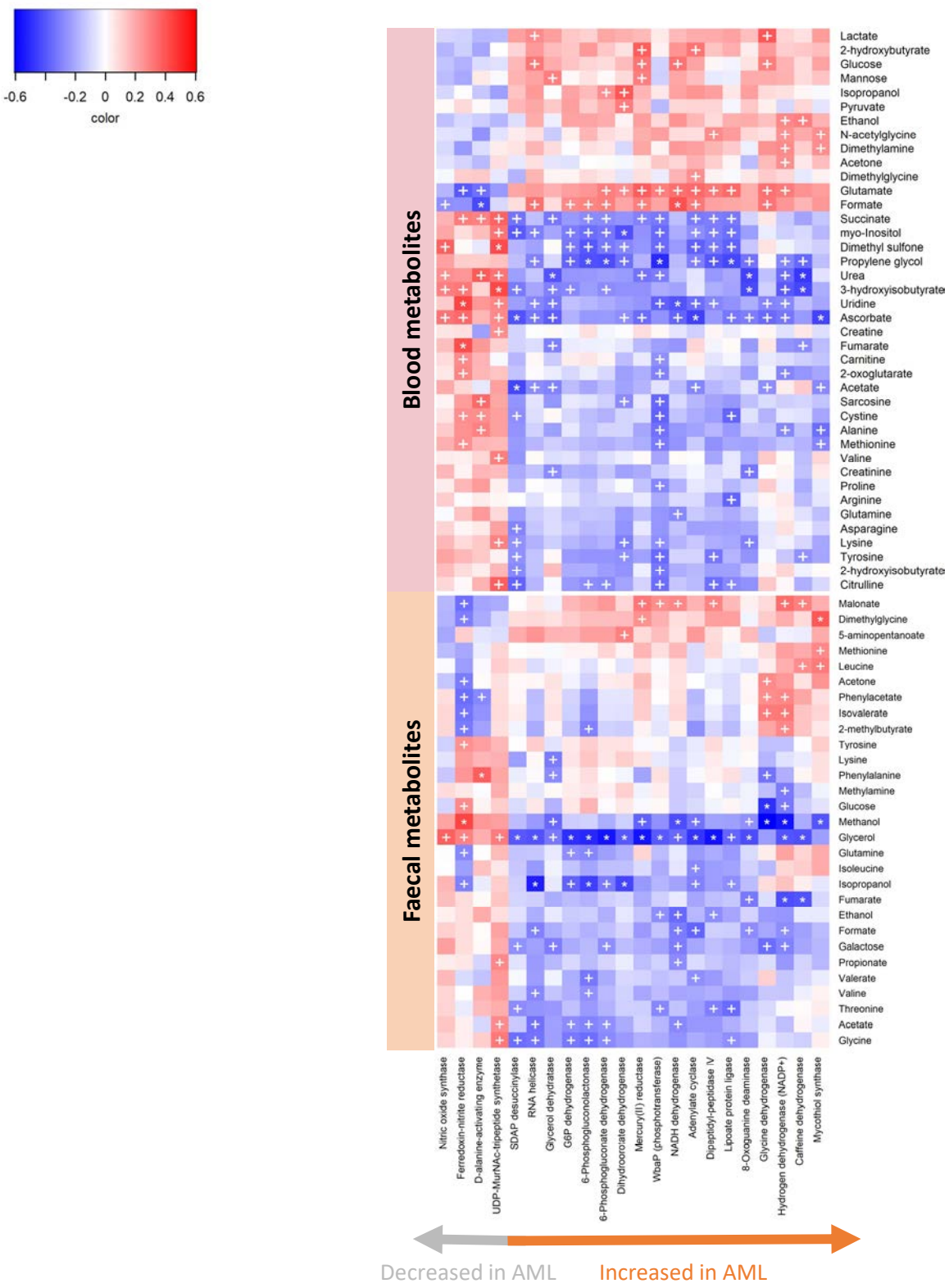

Figure S15. Correlations between blood and faecal metabolites and altered EC enzyme functions. Spearman correlations. Metabolites with at least one correlation with an EC enzyme function are present. Microbial functions are ordered by fold change. '+' symbolizes a p-value < 0.05 and '*' symbolizes an FDR-corrected q-value < 0.1.

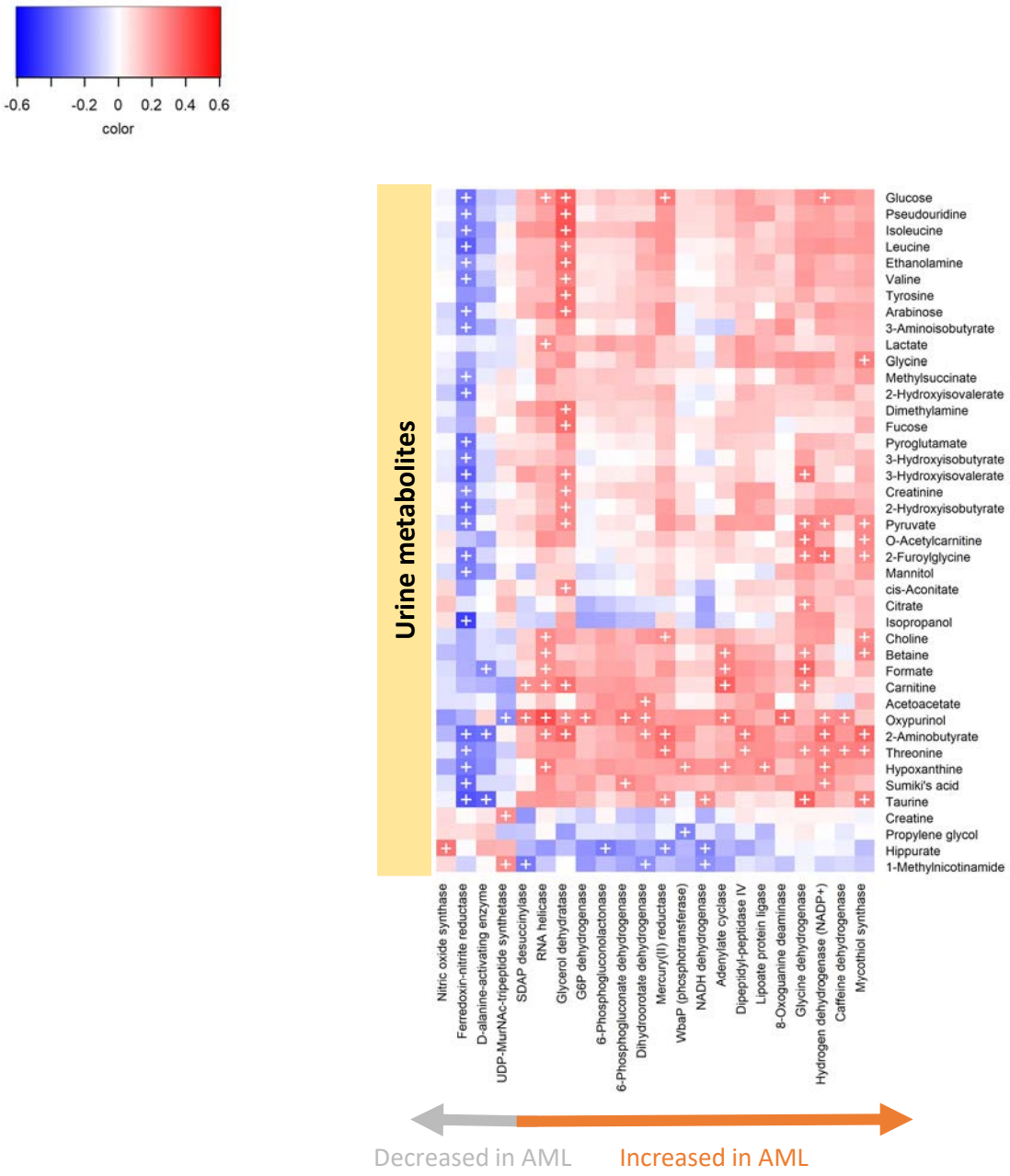

Figure S16. Correlations between urine metabolites and altered EC enzyme functions.
Spearman correlations. Metabolites with at least one correlation with an EC enzyme function are present. Microbial functions are ordered by fold change. '+' symbolizes a p-value < 0.05 and '*' symbolizes an FDR-corrected q-value < 0.1.

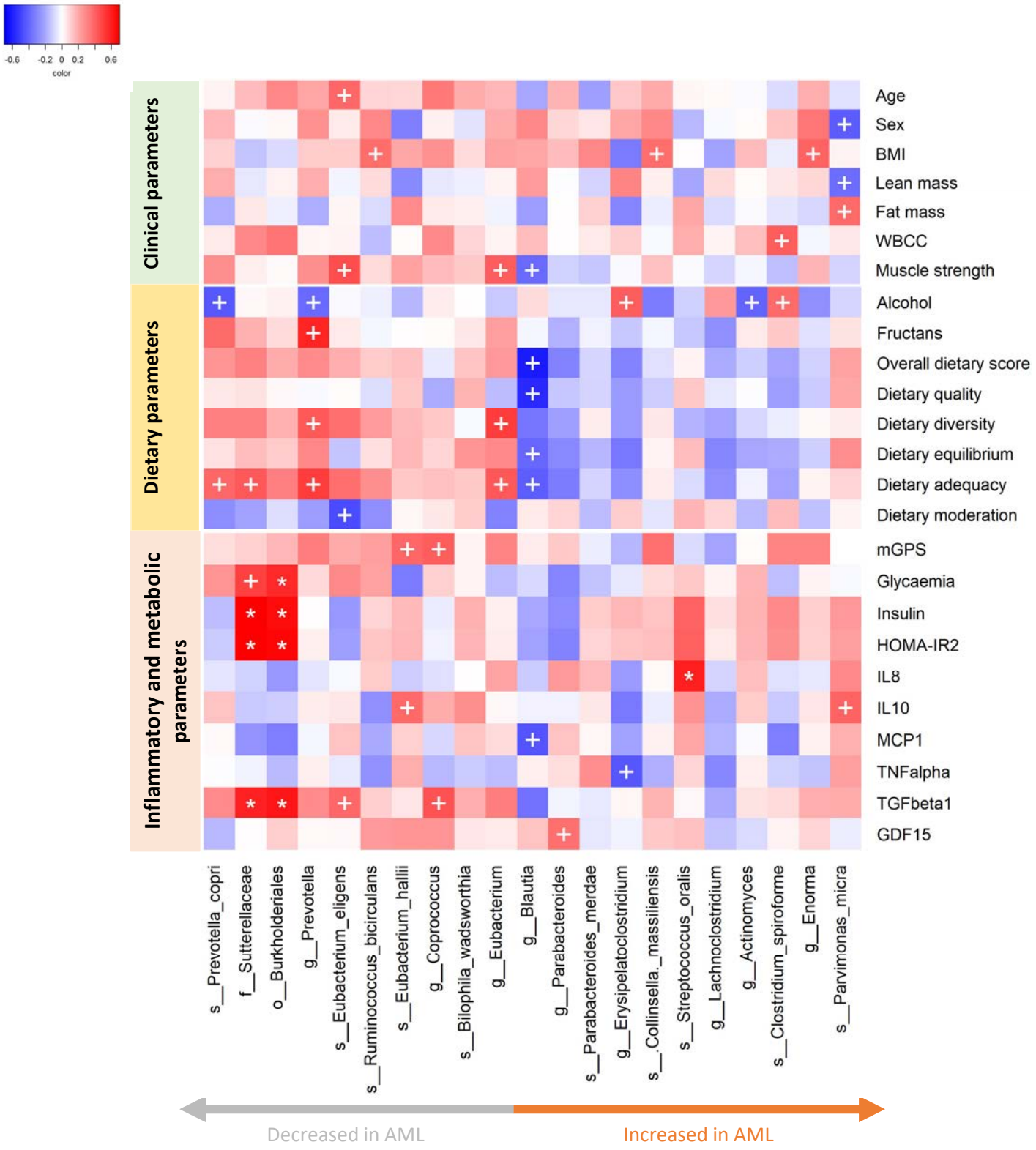

Figure S17. Correlations between clinical, dietary, inflammatory and metabolic parameters and the top altered bacteria in AML patients exclusively.

Spearman correlations. Microbial taxa are ordered by fold change. '+' symbolizes a p-value < 0.05 and '*' symbolizes an FDR-corrected q-value < 0.1. Parameters with at least one correlation with an altered taxon are present. BMI: body mass index; WBCC: white blood cell count; mGPS: modified Glasgow prognostic score; HOMA-IR2: second homeostatic model assessment for insulin resistance; IL8: interleukin-8; IL10: interleukin-10; MCP1: monocyte chemoattractant protein 1; TNFα: tumor necrosis factor alpha-1; TGFβ1: transforming growth factor beta-1; GDF15: growth differentiation factor 15.

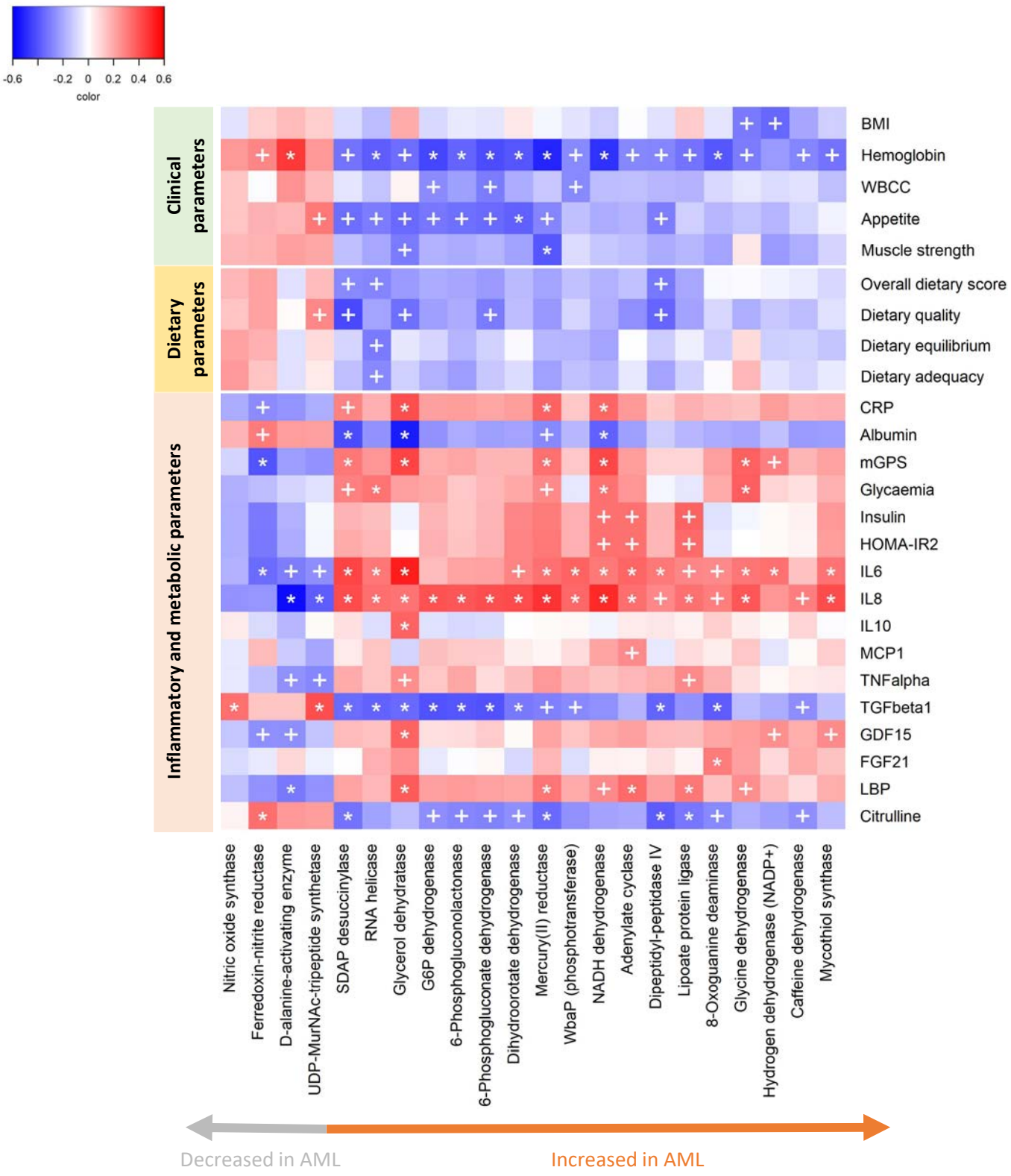

Figure S18. Correlations between clinical, dietary, inflammatory and metabolic parameters and altered EC enzyme functions in CT subjects and AML patients.

Spearman correlations. Microbial functions are ordered by fold change. '+' symbolizes a p-value < 0.05 and '*' symbolizes an FDR-corrected q-value < 0.1. Parameters with at least one correlation with an altered taxon are present. BMI: body mass index; WBCC: white blood cell count; appetite (SNAQ score); CRP: C-reactive protein; mGPS: modified Glasgow prognostic score; HOMA-IR2: second homeostatic model assessment for insulin resistance; IL6: interleukin-6; IL8: interleukin-8; IL10: interleukin-10; MCP1: monocyte chemoattractant protein 1; TNFα: tumor necrosis factor alpha-1; TGFβ1: transforming growth factor beta-1; GDF15: growth differentiation factor 15; FGF21: fibroblast growth factor 21; LBP: lipopolysaccharide binding protein.

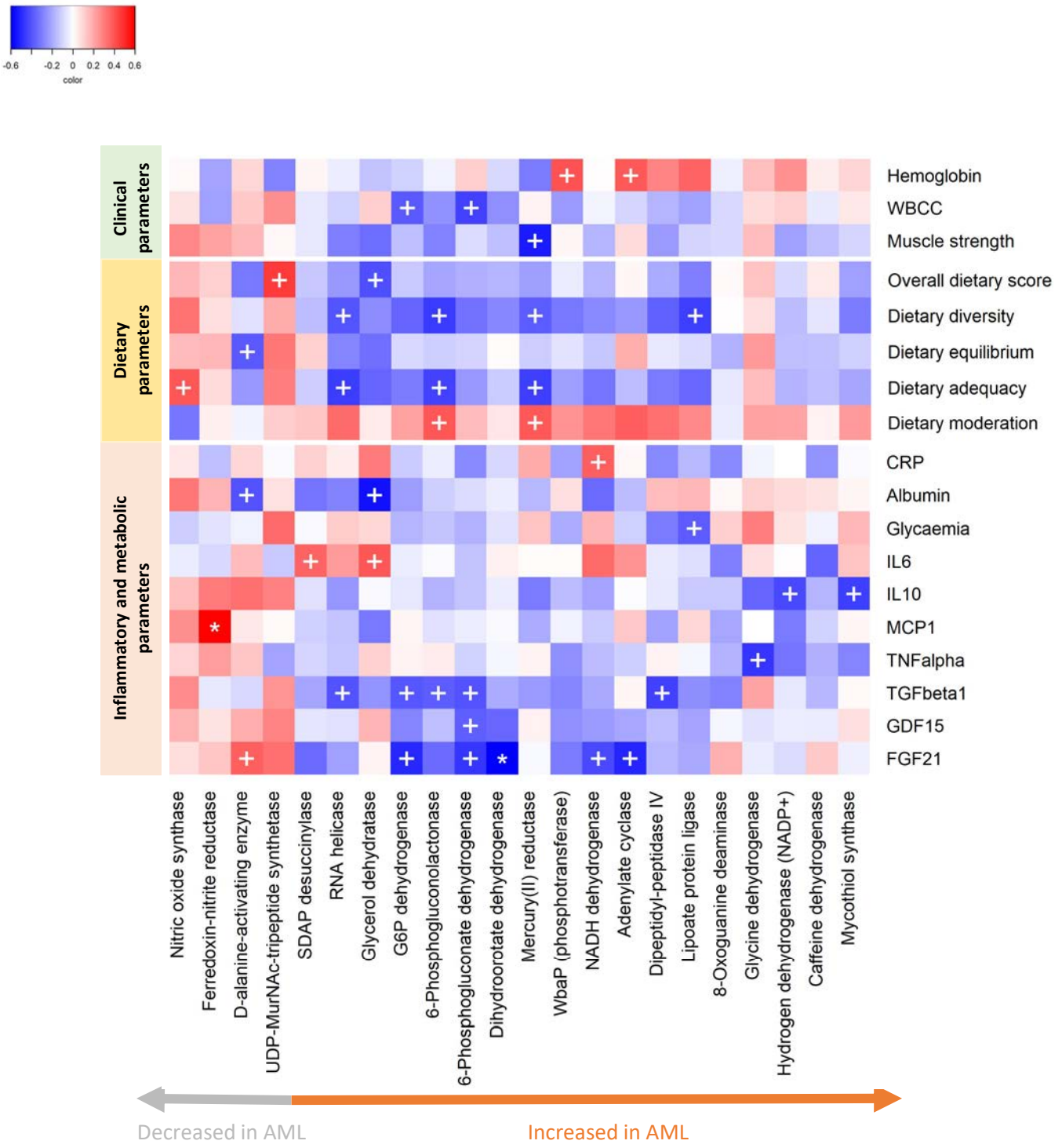

Figure S19. Correlations between clinical, dietary, inflammatory and metabolic parameters and altered EC enzyme functions in AML patients exclusively.

Spearman correlations. Microbial functions are ordered by fold change. '+' symbolizes a p-value < 0.05 and '*' symbolizes an FDR-corrected q-value < 0.1. Parameters with at least one correlation with an altered taxon are present. WBCC: white blood cell count; CRP: C-reactive protein; IL6: interleukin-6; IL10: interleukin-10; MCP1: monocyte chemoattractant protein 1; TNFα: tumor necrosis factor alpha-1; TGFβ1: transforming growth factor beta-1; GDF15: growth differentiation factor 15; FGF21: fibroblast growth factor 21.

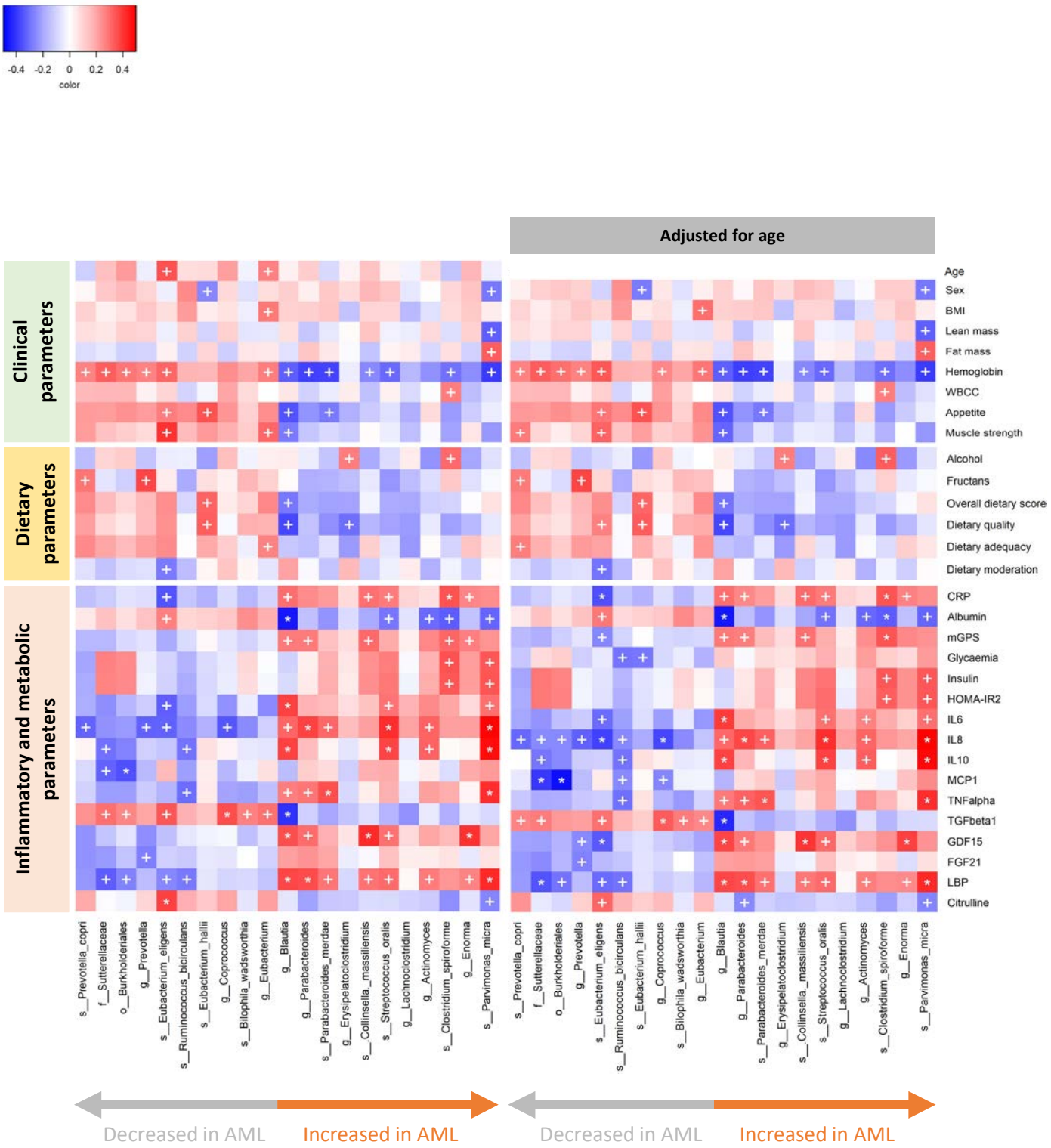

Figure S20. Correlations between clinical, dietary, inflammatory and metabolic parameters and the top altered bacteria. Spearman correlations (left) and partial Spearman rank-based correlations (pSRBC) adjusted for age (right) for the whole cohort (AML group and CT group). Metabolites with at least one correlation with an altered taxon are present. '+' symbolizes a p-value < 0.05 and '*' symbolizes an FDR-corrected q-value < 0.1.

BMI: body mass index; WBCC: white blood cell count; appetite (SNAQ score); CRP: C-reactive protein; mGPS: modified Glasgow prognostic score; HOMA-IR2: second homeostatic model assessment for insulin resistance; IL6: interleukin-6; IL8: interleukin-8; IL10: interleukin-10; MCP1: monocyte chemoattractant protein 1; TNFα: tumor necrosis factor alpha-1; TGFβ1: transforming growth factor beta-1; GDF15: growth differentiation factor 15; FGF21: fibroblast growth factor 21; LBP: lipopolysaccharide binding protein.

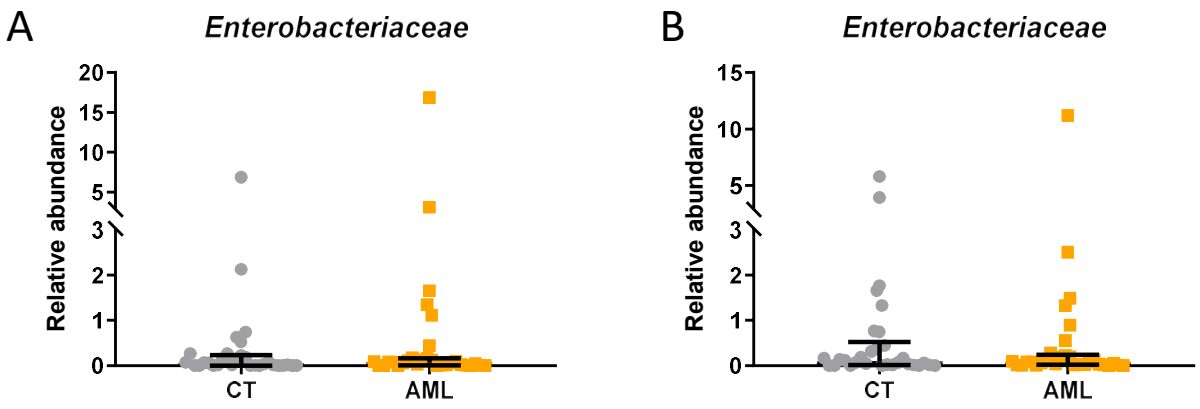

Figure S21. *Enterobacteriaceae* family levels are not different in AML patients compared to CT subjects. A) Results obtained using shotgun metagenomics. B) Results obtained using 16S rRNA gene sequencing. Mann-Whitney U-tests with an FDR correction were applied. AML in orange *vs.* CT in grey.

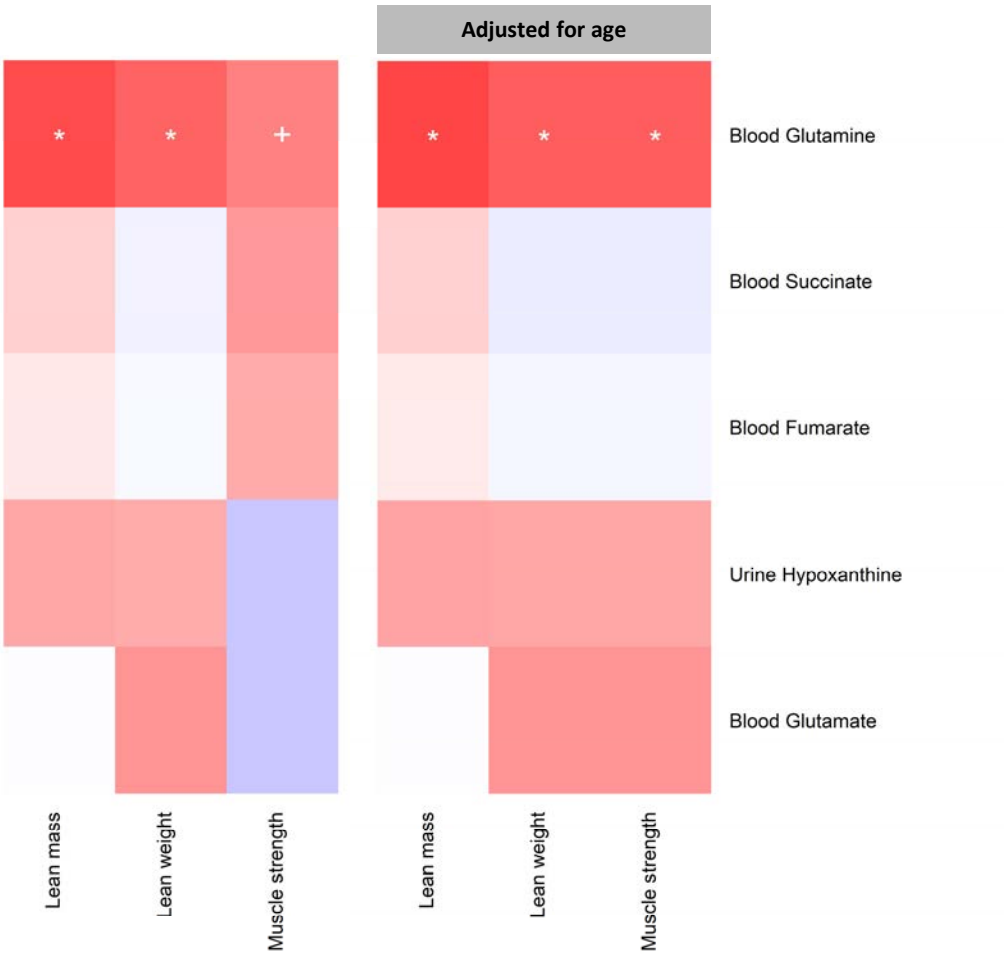

Figure S22. Correlations between lean mass, lean weight, muscle strength and significantly changed metabolites between AML and CT individuals involved in purine nucleotide metabolism and intense metabolic stress.

Spearman correlations (left) and partial Spearman rank-based correlations (pSRBC) adjusted for age (right). '+' symbolizes a p-value < 0.05 and '*' symbolizes an FDR-corrected q-value < 0.1.

Table S1. Drugs and Food Supplements.

Drugs are grouped by category according to the Belgian classification (CBIP: *Centre Belge d'Information Pharmacothérapeutique*). Only drug categories taken regularly by more than 3 patients in the whole cohort are listed. Less than 3 patients report to take supplementation of amino acids, plants and probiotics. Significance was tested using Fisher's exact test.

Drug category	CT (n = 30)	AML (n = 30)	Significance
Hypertension (CBIP 1.1)	8	6	*ns*
Adrenergic beta-antagonists (CBIP 1.5)	5	3	*ns*
Calcium channel clockers (CBIP 1.6)	4	3	*ns*
Drugs acting on the renin-angiotensin system (CBIP 1.7)	5	4	*ns*
Hypolipidemic agents (CBIP 1.12)	6	4	*ns*
Antithrombotic agents(CBIP 2.1)	3	8	*ns*
Gastric and duodenal pathologies (CBIP 3.1)	2	5	*ns*
Laxatives (CBIP 3.5)	1	3	*ns*
Contraception (CBIP 6.2)	2	3	*ns*
Prostate benign hypertrophy (CBIP 7.2)	1	3	*ns*
Gout (CBIP 9.3)	1	4	*ns*
Osteoporosis and Paget disease (CBIP 9.5)	4	2	*ns*
Hypnotics, sedatives, anxiolytics (CBIP 10.1)	2	2	*ns*
Antidepressants (CBIP 10.3)	5	4	*ns*
Allergies (CBIP 12.4)	2	2	*ns*
Minerals (CBIP 14.1)	2	2	*ns*
Vitamins (CBIP 14.1)	7	4	*ns*
Rhinitis and sinusitis (CBIP 17.3)	3	2	*ns*

NB: Anti-Bacterial agents were taken by 2 CT subjects and 1 AML patient between day -30 and day -90 before inclusion.

Table S2. Top altered bacteria in AML patients.

Top 21 bacteria selected based on top bacteria from untargeted metagenomics analyses. Bacteria were selected based on p-values from Mann-Whitney U-test on raw data (MW), Mann-Whitney U-test on centered log-ratio data (MW-CLR), and ALDEx2. Results of targeted metagenomics (16S rRNA gene sequencing, Mann-Whitney U-test, MW) are also mentioned (p-value). IQR: interquartile range.

	Shotgun metagenomics								**16S rRNA gene sequencing**	
	Median		IQR		MW		MW-CLR	ALDEx2	MW	
	CT	AML	CT	AML	p-value	q-value	p-value	p-value	p-value	q-value
s__Parvimonas_micra	0.000	0.000	0.000	0.001	0.000	0.067	0.004	0.395	ND	ND
s__Eubacterium_eligens	1.363	0.364	2.370	1.276	0.001	0.074	0.000	0.000	ND	ND
g__Parabacteroides	1.235	2.137	1.011	1.716	0.002	0.075	0.061	0.020	0.006	0.112
g__Actinomyces	0.022	0.052	0.028	0.099	0.003	0.076	0.001	0.009	0.001	0.046
g__Blautia	1.918	3.144	1.602	1.772	0.004	0.094	0.063	0.032	0.723	0.952
s__Streptococcus_oralis	0.000	0.006	0.002	0.018	0.005	0.106	0.012	0.104	ND	ND
s__Clostridium_spiroforme	0.000	0.008	0.003	0.085	0.005	0.106	0.007	0.045	ND	ND
g__Prevotella	3.388	0.224	19.569	2.856	0.006	0.109	0.005	0.007	0.004	0.100
g__Coprococcus	2.371	1.223	2.598	1.796	0.006	0.109	0.000	0.001	0.001	0.046
s__Prevotella_copri	0.030	0.000	10.689	0.011	0.008	0.131	0.024	0.027	ND	ND
s__Parabacteroides_merdae	0.340	0.700	0.659	0.937	0.010	0.163	0.010	0.011	ND	ND
s__Eubacterium_hallii	1.461	0.955	1.295	1.387	0.015	0.186	0.013	0.011	ND	ND
g__Lachnoclostridium	0.010	0.090	0.055	0.215	0.016	0.186	0.051	0.020	ND	ND
f__Sutterellaceae	0.059	0.020	0.530	0.114	0.016	0.186	0.004	0.013	0.030	0.236
g__Eubacterium	6.290	4.124	6.168	2.901	0.019	0.201	0.027	0.032	ND	ND
s__.Collinsella._massiliensis	0.000	0.005	0.001	0.041	0.019	0.201	0.008	0.069	ND	ND
g__Erysipelatoclostridium	0.013	0.105	0.046	0.357	0.021	0.206	0.032	0.035	ND	ND
g__Enorma	0.000	0.016	0.002	0.056	0.028	0.227	0.010	0.089	ND	ND
s__Ruminococcus_bicirculans	0.416	0.041	1.780	0.392	0.033	0.227	0.026	0.034	ND	ND
s__Bilophila_wadsworthia	0.053	0.024	0.071	0.064	0.036	0.227	0.007	0.056	ND	ND
o__Burkholderiales	0.059	0.031	0.534	0.144	0.064	0.301	0.014	0.042	0.011	0.134

Table S3. List of the 22 EC enzyme functions altered in AML patients compared to CT, as assessed using MaAsLin2.

For sake of clarity, abbreviated names are used throughout the paper. Correspondence between EC nomenclature, full function names and abbreviated names are included here.

EC function	Full name	Abbreviated name
EC 1.14.13.39	Nitric-oxide synthase (NADPH)	Nitric oxide synthase
EC 1.7.7.1	Ferredoxin-nitrite reductase	Ferredoxin nitrite reductase
EC 6.1.1.13	D-alanine-poly(phosphoribitol) ligase	D-alanine-activating enzyme
EC 6.3.2.13	UDP-N-acetylmuramoyl-L-alanyl-D-glutamate-2,6-diaminopimelate ligase	UDP-MurNAc-tripeptide synthetase
EC 3.5.1.18	Succinyl-diaminopimelate desuccinylase	SDAP desuccinylase
EC 3.6.4.13	RNA helicase	RNA helicase
EC 4.2.1.30	Glycerol dehydratase	Glycerol dehydratase
EC 1.1.1.49	Glucose-6-phosphate dehydrogenase (NADP+)	G6P dehydrogenase
EC 3.1.1.31	6-Phosphogluconolactonase	6-Phosphogluconolactonase
EC 1.1.1.44	Phosphogluconate dehydrogenase (NADP dependent, decarboxylating)	6-Phosphogluconate dehydrogenase
EC 1.3.98.1	Dihydroorotate dehydrogenase (fumarate)	Dihydroorotate dehydrogenase
EC 1.16.1.1	Mercury(II) reductase	Mercury(II) reductase
EC 2.7.8.6	Undecaprenyl-phosphate galactose phosphotransferase	WbaP (phosphotransferase)
EC 1.6.99.3	NADH dehydrogenase	NADH dehydrogenase
EC 4.6.1.1	Adenylate cyclase	Adenylate cyclase
EC 3.4.14.5	Dipeptidyl-peptidase IV	Dipeptidyl-peptidase IV
EC 2.7.7.63	Lipoate protein ligase	Lipoate protein ligase
EC 3.5.4.32	8-Oxoguanine deaminase	8-Oxoguanine deaminase
EC 1.4.99.5	Glycine dehydrogenase (cyanide-forming)	Glycine dehydrogenase
EC 1.12.1.3	Hydrogen dehydrogenase (NADP+)	Hydrogen dehydrogenase (NADP+)
EC 1.17.5.2	Caffeine dehydrogenase	Caffeine dehydrogenase
EC 2.3.1.189	Mycothiol synthase	Mycothiol synthase

Table S4. Median, interquartile range (IQR), p-value of Mann-Whitney U-test and q-value after false discovery rate correction for all metabolites in the three compartments. Imputation was not performed on maleate and 3-phenylpropionate due to more than 40% missing values in one group. For those metabolites, the differences between CT and AML was tested using a Fisher test. No q-value is therefore reported for those metabolites.

Metabolite	Faeces						Blood						Urine					
	Median		IQR		Mann-Whitney		Median		IQR		Mann-Whitney		Median		IQR		Mann-Whitney	
	CT	AML	CT	AML	p-value	q-value	CT	AML	CT	AML	p-value	q-value	CT	AML	CT	AML	p-value	q-value
Acetate	20.995	17.499	10.738	12.570	0.485	0.635	0.033	0.024	0.015	0.019	0.010	0.053	NA	NA	NA	NA	NA	NA
Acetoacetate	NA	NA	NA	NA	NA	NA	0.020	0.021	0.024	0.023	0.294	0.438	0.185	0.241	0.195	0.536	0.449	0.625
Acetone	0.030	0.024	0.022	0.027	0.888	0.888	0.008	0.011	0.004	0.013	0.240	0.382	0.112	0.116	0.047	0.130	0.663	0.772
Alanine	0.273	0.192	0.130	0.166	0.181	0.382	0.258	0.208	0.076	0.094	0.010	0.053	0.929	0.822	0.965	0.961	0.467	0.636
Allantoin	NA	NA	NA	NA	NA	NA	NA	NA	NA	NA	NA	NA	0.400	0.369	0.339	0.383	0.631	0.772
Arabinose	NA	NA	NA	NA	NA	NA	NA	NA	NA	NA	NA	NA	1.147	1.230	0.869	1.107	0.260	0.545
Arginine	NA	NA	NA	NA	NA	NA	0.051	0.042	0.018	0.020	0.171	0.307	NA	NA	NA	NA	NA	NA
Ascorbate	NA	NA	NA	NA	NA	NA	0.035	0.011	0.013	0.022	0.000	0.000	NA	NA	NA	NA	NA	NA
Asparagine	NA	NA	NA	NA	NA	NA	0.029	0.024	0.004	0.012	0.029	0.089	NA	NA	NA	NA	NA	NA
Aspartate	0.321	0.268	0.164	0.178	0.644	0.730	NA	NA	NA	NA	NA	NA	NA	NA	NA	NA	NA	NA
Betaine	NA	NA	NA	NA	NA	NA	0.023	0.024	0.011	0.012	1.000	1.000	0.283	0.400	0.484	0.589	0.209	0.545
Butyrate	4.785	3.568	2.982	3.237	0.374	0.578	NA	NA	NA	NA	NA	NA	NA	NA	NA	NA	NA	NA
Carnitine	NA	NA	NA	NA	NA	NA	0.027	0.025	0.008	0.012	0.395	0.507	0.138	0.477	0.491	0.656	0.003	0.069
Choline	NA	NA	NA	NA	NA	NA	0.005	0.005	0.002	0.003	0.668	0.730	0.165	0.210	0.138	0.168	0.301	0.545
cis-Aconitate	NA	NA	NA	NA	NA	NA	NA	NA	NA	NA	NA	NA	1.003	0.986	0.853	0.781	0.676	0.772
Citrate	NA	NA	NA	NA	NA	NA	NA	NA	NA	NA	NA	NA	11.271	10.451	9.905	10.020	0.423	0.616
Citrulline	NA	NA	NA	NA	NA	NA	0.020	0.016	0.008	0.008	0.019	0.073	NA	NA	NA	NA	NA	NA
Creatine	NA	NA	NA	NA	NA	NA	0.017	0.018	0.012	0.017	0.464	0.571	0.647	0.269	1.829	0.519	0.248	0.545
Creatine phosphate	NA	NA	NA	NA	NA	NA	NA	NA	NA	NA	NA	NA	0.329	0.284	0.405	0.324	0.242	0.545
Creatinine	NA	NA	NA	NA	NA	NA	0.055	0.051	0.014	0.014	0.188	0.327	48.632	46.992	37.005	46.704	0.562	0.709
Cystine	NA	NA	NA	NA	NA	NA	0.044	0.031	0.017	0.028	0.044	0.117	NA	NA	NA	NA	NA	NA
Dimethylglycine	0.005	0.004	0.005	0.013	0.183	0.382	0.002	0.002	0.001	0.001	0.141	0.267	0.206	0.196	0.146	0.232	0.654	0.772
Dimethyl sulfone	NA	NA	NA	NA	NA	NA	0.007	0.006	0.004	0.004	0.109	0.229	NA	NA	NA	NA	NA	NA
Dimethylamine	NA	NA	NA	NA	NA	NA	0.001	0.001	0.000	0.001	0.027	0.088	2.409	2.207	1.556	3.111	0.350	0.596
Ethanol	0.146	0.032	0.081	0.094	0.011	0.098	0.002	0.003	0.001	0.004	0.006	0.038	NA	NA	NA	NA	NA	NA
Ethanolamine	NA	NA	NA	NA	NA	NA	NA	NA	NA	NA	NA	NA	1.613	1.755	1.532	1.819	0.485	0.647
Formate	0.006	0.002	0.008	0.005	0.040	0.162	0.009	0.014	0.004	0.007	0.000	0.000	1.037	1.633	0.871	1.608	0.004	0.069
Fucose	NA	NA	NA	NA	NA	NA	NA	NA	NA	NA	NA	NA	0.578	0.622	0.540	0.542	0.382	0.596
Fumarate	0.035	0.023	0.035	0.031	0.363	0.578	0.000	0.000	0.000	0.000	0.034	0.101	0.015	0.023	0.028	0.021	0.404	0.615
Galactose	0.131	0.053	0.077	0.076	0.002	0.023	NA	NA	NA	NA	NA	NA	0.630	0.824	0.698	0.598	0.889	0.903
Glucose	0.694	0.257	0.523	0.308	0.043	0.162	4.018	4.323	0.621	1.785	0.020	0.073	1.419	1.897	1.189	1.848	0.028	0.172
Glutamate	1.451	1.039	0.574	0.911	0.542	0.658	0.015	0.032	0.011	0.013	0.000	0.000	NA	NA	NA	NA	NA	NA
Glutamine	0.264	0.223	0.163	0.193	0.485	0.635	0.355	0.318	0.052	0.090	0.022	0.075	NA	NA	NA	NA	NA	NA
Glycerol	0.927	0.087	1.120	0.215	0.000	0.003	NA	NA	NA	NA	NA	NA	NA	NA	NA	NA	NA	NA
Glycine	0.134	0.090	0.072	0.060	0.072	0.230	NA	NA	NA	NA	NA	NA	4.035	5.712	4.188	5.537	0.307	0.545
Hippurate	NA	NA	NA	NA	NA	NA	NA	NA	NA	NA	NA	NA	14.958	7.931	13.200	10.889	0.011	0.112
Hypoxanthine	NA	NA	NA	NA	NA	NA	NA	NA	NA	NA	NA	NA	0.144	0.269	0.208	0.380	0.004	0.069
Isobutyrate	0.829	0.728	0.566	0.920	0.213	0.382	0.000	0.000	0.000	0.000	0.056	0.136	NA	NA	NA	NA	NA	NA
Isoleucine	0.097	0.060	0.081	0.063	0.228	0.388	0.044	0.041	0.014	0.019	0.249	0.386	0.051	0.063	0.036	0.069	0.041	0.172
Isopropanol	0.029	0.014	0.033	0.021	0.756	0.829	0.000	0.001	0.000	0.001	0.085	0.186	0.033	0.035	0.030	0.036	0.701	0.787
Isovalerate	0.567	0.557	0.409	0.897	0.150	0.376	NA	NA	NA	NA	NA	NA	0.034	0.030	0.032	0.037	0.929	0.929
Lactate	NA	NA	NA	NA	NA	NA	0.761	1.108	0.380	0.425	0.000	0.003	0.301	0.318	0.292	0.258	0.423	0.616
Leucine	0.132	0.101	0.092	0.083	0.802	0.852	0.080	0.081	0.021	0.038	0.918	0.933	0.088	0.115	0.053	0.130	0.041	0.172
Lysine	0.130	0.079	0.102	0.071	0.081	0.230	0.115	0.101	0.033	0.046	0.075	0.170	0.317	0.311	0.382	0.860	0.665	0.772
Maleate	NA	NA	NA	NA	NA	NA	NA	NA	NA	NA	NA	NA	0.020	0.029	0.016	0.023	0.000	NA
Malonate	0.155	0.135	0.090	0.166	0.155	0.376	NA	NA	NA	NA	NA	NA	NA	NA	NA	NA	NA	NA
Mannitol	NA	NA	NA	NA	NA	NA	NA	NA	NA	NA	NA	NA	1.376	2.240	2.284	3.050	0.155	0.450
Mannose	NA	NA	NA	NA	NA	NA	0.043	0.059	0.012	0.036	0.012	0.053	NA	NA	NA	NA	NA	NA
Methanol	0.218	0.068	0.124	0.067	0.000	0.003	NA	NA	NA	NA	NA	NA	0.915	0.784	1.106	0.791	0.449	0.625
Methionine	0.067	0.062	0.039	0.056	0.595	0.697	0.018	0.016	0.005	0.006	0.018	0.073	NA	NA	NA	NA	NA	NA
Methylamine	0.059	0.044	0.036	0.043	0.520	0.655	NA	NA	NA	NA	NA	NA	NA	NA	NA	NA	NA	NA
Methylguanidine	NA	NA	NA	NA	NA	NA	NA	NA	NA	NA	NA	NA	0.153	0.102	0.265	0.163	0.300	0.545
Methylsuccinate	NA	NA	NA	NA	NA	NA	NA	NA	NA	NA	NA	NA	0.040	0.055	0.049	0.068	0.176	0.490
myo-Inositol	NA	NA	NA	NA	NA	NA	0.021	0.020	0.008	0.009	0.379	0.507	NA	NA	NA	NA	NA	NA
N-Acetylglycine	NA	NA	NA	NA	NA	NA	0.001	0.002	0.001	0.002	0.158	0.290	NA	NA	NA	NA	NA	NA
O-Acetylcarnitine	NA	NA	NA	NA	NA	NA	0.005	0.005	0.002	0.004	0.351	0.487	0.074	0.107	0.073	0.113	0.146	0.446
Ornithine	NA	NA	NA	NA	NA	NA	0.036	0.040	0.011	0.019	0.530	0.638	NA	NA	NA	NA	NA	NA
Oxypurinol	NA	NA	NA	NA	NA	NA	NA	NA	NA	NA	NA	NA	1.043	2.105	2.184	29.182	0.286	0.545
Pantothenate	NA	NA	NA	NA	NA	NA	NA	NA	NA	NA	NA	NA	0.073	0.076	0.056	0.106	0.819	0.873
Phenylacetate	0.231	0.224	0.134	0.265	0.040	0.162	NA	NA	NA	NA	NA	NA	NA	NA	NA	NA	NA	NA
Phenylalanine	0.060	0.034	0.044	0.038	0.020	0.135	0.036	0.042	0.009	0.013	0.057	0.136	NA	NA	NA	NA	NA	NA
Proline	NA	NA	NA	NA	NA	NA	0.130	0.109	0.060	0.039	0.198	0.334	NA	NA	NA	NA	NA	NA
Propionate	5.949	4.822	3.060	3.917	0.432	0.635	NA	NA	NA	NA	NA	NA	NA	NA	NA	NA	NA	NA
Propylene glycol	NA	NA	NA	NA	NA	NA	0.001	0.001	0.002	0.002	0.387	0.507	0.108	0.095	0.158	0.118	0.854	0.882
Pseudouridine	NA	NA	NA	NA	NA	NA	NA	NA	NA	NA	NA	NA	0.683	0.847	0.471	0.934	0.037	0.172
Pyroglutamate	NA	NA	NA	NA	NA	NA	NA	NA	NA	NA	NA	NA	1.088	1.239	0.610	1.083	0.382	0.596
Pyruvate	NA	NA	NA	NA	NA	NA	0.056	0.060	0.029	0.020	0.343	0.487	0.080	0.096	0.075	0.155	0.530	0.678
Sarcosine	NA	NA	NA	NA	NA	NA	0.001	0.001	0.001	0.001	0.049	0.127	NA	NA	NA	NA	NA	NA
Serine	NA	NA	NA	NA	NA	NA	0.079	0.083	0.016	0.028	0.762	0.803	NA	NA	NA	NA	NA	NA
sn-Glycero-3-phosphocholin	NA	NA	NA	NA	NA	NA	NA	NA	NA	NA	NA	NA	0.219	0.237	0.177	0.237	0.286	0.545
Succinate	NA	NA	NA	NA	NA	NA	0.003	0.002	0.001	0.001	0.001	0.007	NA	NA	NA	NA	NA	NA
Sumiki's acid	NA	NA	NA	NA	NA	NA	NA	NA	NA	NA	NA	NA	0.058	0.121	0.115	0.300	0.030	0.172
Taurine	NA	NA	NA	NA	NA	NA	NA	NA	NA	NA	NA	NA	1.479	5.266	3.995	8.152	0.001	0.037
Threonine	0.109	0.062	0.063	0.064	0.030	0.162	0.097	0.079	0.026	0.043	0.038	0.108	0.333	0.548	0.290	0.480	0.018	0.141
Trigonelline	NA	NA	NA	NA	NA	NA	NA	NA	NA	NA	NA	NA	1.309	0.692	2.321	1.814	0.014	0.125
Trimethylamine	NA	NA	NA	NA	NA	NA	NA	NA	NA	NA	NA	NA	0.078	0.069	0.096	0.073	0.523	0.678
Tryptophan	NA	NA	NA	NA	NA	NA	0.005	0.005	0.002	0.002	0.646	0.730	NA	NA	NA	NA	NA	NA
Tyrosine	0.072	0.051	0.053	0.036	0.196	0.382	0.052	0.052	0.015	0.025	0.564	0.666	0.388	0.663	0.345	0.682	0.028	0.172
Uracil	NA	NA	NA	NA	NA	NA	NA	NA	NA	NA	NA	NA	0.205	0.136	0.186	0.136	0.034	0.172
Urea	NA	NA	NA	NA	NA	NA	0.772	0.637	0.349	0.209	0.011	0.053	40.891	35.550	17.906	16.420	0.119	0.382
Uridine	NA	NA	NA	NA	NA	NA	0.003	0.002	0.001	0.001	0.000	0.000	NA	NA	NA	NA	NA	NA
Valerate	0.851	0.645	0.504	0.759	0.859	0.885	NA	NA	NA	NA	NA	NA	NA	NA	NA	NA	NA	NA
Valine	0.164	0.104	0.101	0.064	0.076	0.230	0.163	0.165	0.032	0.055	0.728	0.781	0.133	0.164	0.122	0.252	0.095	0.337
1,5-Anhydrosorbitol	NA	NA	NA	NA	NA	NA	0.085	0.070	0.043	0.030	0.654	0.730	NA	NA	NA	NA	NA	NA
1-Methylnicotinamide	NA	NA	NA	NA	NA	NA	NA	NA	NA	NA	NA	NA	0.187	0.141	0.174	0.185	0.236	0.545
2-Aminobutyrate	NA	NA	NA	NA	NA	NA	0.012	0.014	0.007	0.008	0.297	0.438	0.047	0.078	0.024	0.080	0.007	0.089
2-Furoylglycine	NA	NA	NA	NA	NA	NA	NA	NA	NA	NA	NA	NA	0.121	0.259	0.398	0.875	0.236	0.545
2-Hydroxybutyrate	NA	NA	NA	NA	NA	NA	0.023	0.030	0.010	0.020	0.001	0.007	NA	NA	NA	NA	NA	NA
2-Hydroxyisobutyrate	NA	NA	NA	NA	NA	NA	0.001	0.001	0.000	0.001	0.462	0.571	0.200	0.226	0.174	0.151	0.243	0.545
2-Hydroxyisovalerate	NA	NA	NA	NA	NA	NA	0.005	0.006	0.002	0.006	0.214	0.351	0.023	0.029	0.026	0.038	0.363	0.596
2-Methylbutyrate	0.919	0.783	0.628	1.367	0.449	0.635	NA	NA	NA	NA	NA	NA	NA	NA	NA	NA	NA	NA
2-Oxoglutarate	NA	NA	NA	NA	NA	NA	0.005	0.005	0.002	0.002	0.657	0.730	0.433	0.500	0.428	0.490	0.358	0.596
2-Oxoisocaproate	NA	NA	NA	NA	NA	NA	0.003	0.004	0.001	0.002	0.120	0.240	NA	NA	NA	NA	NA	NA
3-Aminoisobutyrate	NA	NA	NA	NA	NA	NA	NA	NA	NA	NA	NA	NA	0.346	0.501	0.402	1.809	0.049	0.187
3-Hydroxybutyrate	NA	NA	NA	NA	NA	NA	0.028	0.027	0.039	0.039	0.859	0.885	NA	NA	NA	NA	NA	NA
3-Hydroxyisobutyrate	NA	NA	NA	NA	NA	NA	0.012	0.009	0.004	0.005	0.122	0.240	0.301	0.328	0.321	0.382	0.307	0.545
3-Hydroxyisovalerate	NA	NA	NA	NA	NA	NA	0.001	0.001	0.000	0.001	0.006	0.038	0.229	0.275	0.199	0.310	0.107	0.361
3-Hydroxymandelate	NA	NA	NA	NA	NA	NA	NA	NA	NA	NA	NA	NA	0.324	0.285	0.320	0.634	0.741	0.818
3-Indoxylsulfate	NA	NA	NA	NA	NA	NA	NA	NA	NA	NA	NA	NA	0.995	0.937	1.212	1.173	0.854	0.882
3-Methyl-2-oxovalerate	NA	NA	NA	NA	NA	NA	0.003	0.003	0.001	0.001	0.355	0.487	NA	NA	NA	NA	NA	NA
3-Methylxanthine	NA	NA	NA	NA	NA	NA	NA	NA	NA	NA	NA	NA	0.196	0.099	0.280	0.132	0.043	0.172
3-Phenylpropionate	0.090	0.061	0.060	0.036	0.007	NA	NA	NA	NA	NA	NA	NA	NA	NA	NA	NA	NA	NA
4-Hydroxyphenylacetate	NA	NA	NA	NA	NA	NA	NA	NA	NA	NA	NA	NA	0.484	0.538	0.406	0.478	0.786	0.853
5-Aminopentanoate	0.051	0.040	0.045	0.079	0.208	0.382	NA	NA	NA	NA	NA	NA	NA	NA	NA	NA	NA	NA

Table S5. Significantly changed bacterial species in AML patients with high insulinemia and high glycaemia reported in diseases and syndromes characterized by high insulinemia and glycaemia

Bacteria names	Results of this study	Diseases and syndromes characterized by high insulinemia and glycaemia
Significantly different bacteria between individuals with low versus high insulin levels		
Phascolarctobacterium faecium	↑	↑ Hypertension patient with and without type II diabetes[9]
Eubacterium eligens	↓	↓ Type I diabetes[1], Gestational diabetes[2], Metabolic syndrome in HIV patients[3]
Bacteroides caccae	↑	↑ Type II diabetes[4]
Bacteroides fragilis	↑	↓ Type I diabetes in children[1], ↑ Type I diabetes in children[5], ↑ Obesity in children[6]
Significantly different bacteria between individuals with low versus high glycaemia levels		
Intestinibacter bartlettii	↓	↓ Overweight and obese children[10]
Bacteroides ovatus	↓	↑ Type I diabetes[1], ↑ Type I diabetes in children[5], ↓ Obesity in children[7]
Fusicatenibacter saccharivorans	↓	-
Clostridium sp CAG 242	↑	-
Firmicutes bacterium CAG 94	↑	-
Streptococcus oralis	↑	↑ Type I diabetes[8]

1. Giongo A, Gano KA, Crabb DB, et al. Toward defining the autoimmune microbiome for type 1 diabetes. ISME J 2011;5(1):82–91.
2. Ma S, You Y, Huang L, et al. Alterations in Gut Microbiota of Gestational Diabetes Patients During the First Trimester of Pregnancy. Frontiers in Cellular and Infection Microbiology 2020;10(58):1–19.
3. Villanueva-Millán MJ, Pérez-Matute P, Recio-Fernández E, Lezana Rosales J-M, Oteo J-A. Characterization of gut microbiota composition in HIV-infected patients with metabolic syndrome. J Physiol Biochem 2019;75(3):299–309.
4. Zhong H, Ren H, Lu Y, et al. Distinct gut metagenomics and metaproteomics signatures in prediabetics and treatment-naïve type 2 diabetics. EBioMedicine 2019;47373–383.
5. de Goffau MC, Luopajärvi K, Knip M, et al. Fecal Microbiota Composition Differs Between Children With β-Cell Autoimmunity and Those Without. Diabetes 2013;62(4):1238–1244.
6. Ignacio A, Fernandes MR, Rodrigues VAA, et al. Correlation between body mass index and faecal microbiota from children. Clinical Microbiology and Infection 2016;22(3):258.e1-258.e8.
7. Maya-Lucas O, Murugesan S, Nirmalkar K, et al. The gut microbiome of Mexican children affected by obesity. Anaerobe 2019;5511–23.
8. Vatanen T, Franzosa EA, Schwager R, et al. The human gut microbiome in early-onset type 1 diabetes from the TEDDY study. Nature 2018;562(7728):589–594.
9. Ding H, Xu Y, Cheng Y, et al. Gut microbiome profile of Chinese hypertension patients with and without type 2 diabetes mellitus. BMC Microbiol 2023;23(1):254.
10. Murga-Garrido SM, Ulloa-Pérez EJ, Díaz-Benítez CE, et al. Virulence Factors of the Gut Microbiome Are Associated with BMI and Metabolic Blood Parameters in Children with Obesity. Microbiology Spectrum 2023;11(2):e03382-22.